CELLULAR PLASTICITY IN LIVER INJURY:

on the origin of bipotential adult liver progenitor cells

By

Branden D. Tarlow

A DISSERTATION

Presented to the Department of Cell, Developmental & Cancer Biology
and Oregon Health & Science University
School of Medicine
in partial fulfillment of
the requirements for the degree of

Doctor of Philosophy

August 2014

School of Medicine

Oregon Health & Science University

CERTIFICATE OF APPROVAL

This is to certify that the PhD dissertation of

Branden D. Tarlow

has been approved

Cary Harding, MD (Chair)

Markus Grompe, MD (Advisor)

Melissa Wong, PhD

William Fleming, MD, PhD

Gail Mandel, PhD

TABLE OF CONTENTS

ACKNOWLEDGEMENTS

The modern complexities of a biomedical research project have essentially made science a team sport. I am indebted to many people who have provided essential contributions to the scientific work presented here. I received technical training and advice from several post-doctoral fellows and assistant professors that took an interest in my work and me. Craig Dorrell, Qingshuo Zhang, Bin Li, Devorah Goldman, Carl Pelz, Andrew Duncan, Matthew Taylor and Scott Naugler were particularly helpful. Sean Nygaard, our laboratory manager, deserves special note for enacting processes and procedures to make the lab run smoothly which freed up time to think about experimental designs and data interpretation.

At OHSU I was fortunate to have access to several excellent collaborating groups that I utilized extensively to generate nearly every major figure in this thesis. Many people of the Flow Cytometry Core, Massively Parallel Sequencing Shared Resource, and Advanced Microscopy Imaging Core laboratories provided this support. Milton Finegold at Texas Children's Hospital also provided pathology support and experimental suggestions.

I am grateful to my mentor and laboratory advisor, Markus Grompe, for sharing his passion for science with me. His creativity, enthusiasm for science, and gift for identifying the important questions have left their mark. Dr. Grompe pushed me to do better work, to repeat experiments until they were well done, and challenged me

to think more clearly. I hope to replicate many aspects of his approach to science in my own career.

Additionally, I would like to acknowledge and thank members of my dissertation committee, the MD/PhD program, and my teachers in the graduate and medical school for their support, guidance, and unique perspectives. Drs. David Jacoby and Lynn Loriaux deserve special mention for their encouragement and career advice.

This work simply would not have been completed without the support and encouragement of my family. My wife, Kathleen, helped me work through difficult problems and encouraged me when the path forward was bleak or uncertain. I also want to thank my family for their support through this long program. Ramona and Benjamin, in particular, motivated me to do my best.

Finally, biomedical science is expensive. I am grateful to have received financial support from a federal training grant (through the National Institutes of Health) that supports the training of young scientists in MD/PhD programs. This grant provided considerable academic freedom that allowed me to pursue smaller side projects that matured into the major piece of my thesis work.

LIST OF FIGURES

LIST OF TABLES

LIST OF ABBREVIATIONS

AAV8	Adeno-Associated Virus Serotype 8
Ad-uPA	Adenoviral Urokinase plasminogen activator
APOLT	auxiliary partial orthotopic liver transplant
BDL	Bile duct ligation
BrdU	Bromo-Deoxyuridine
CCl4	Carbon Tetrachloride
CDE	Choline-Deficient Ethionine-Supplemented Diet
CLD	Chronic Liver Disease
cLPC	Cholangiocyte-Derived Liver Progenitor Cell;
CreERT2	Cre recombinase-Estrogen receptor ligand binding fusion protein
CV	Central Vein
DDC	3,5-Diethoxycarbonyl-1, 4-Dihydrocollidine
E	Embryonic Day
EdU	5-Ethynyl-2'-Deoxyuridine
EMT	Epithelial-To-Mesenchymal Transition
FACS	Fluorescence Activated Cell Sorting
FACS	Fluorescence Activated Cell Sorting;
FRG	*Fah*$^{-/-}$ *Rag2*$^{-/-}$ *Il2rg*$^{-/-}$
GSEA	Gene Set Enrichment Analysis
H&E	Hematoxylin And Eosin
hLPC	Hepatocyte-Derived Liver Progenitor Cell
Hnf4α	Hepatocyte Nuclear Factor 4α
HSA	Human Serum Albumin
IACUC	Institutional Animal Care And Use Committees.
IF	Immunofluorescence
IP	Intraperitoneal
iPS	induced pluripotent stem (cell)
Krt19	Cytokeratin 19
LSC	Liver Stem Cell

MET	Mesenchymal-To-Epithelial Transition
mTmG	Membranous-Tomato/Membranous-Gfp Dual Fluorescent Reporter
NAFLD	non-alcoholic fatty liver disease
NASH	non-alcoholic steatohepatitis
NPC	Non-Parenchymal Cell
NTBC	2-(2- Nitro-4-Trifluoromethylbenzoyl)-1,3-Cyclohexanedione
Opn	Osteopontin (Same As Secreted Phosphoprotein 1 Or Spp1)
PBS	Phosphate-Buffered Saline
PV	Portal Vein
RFP	Red Fluorescent Protein
RPKM	Reads Per Kilobase Per Million
Sox9	Sex-Determining Region Y–Box (Sry-Box) Containing Gene 9
WT	Wild Type
YFP	Yellow Fluorescent Protein

ABSTRACT

Adult liver progenitor cells are biliary-like epithelial cells that emerge only under injury conditions in the periportal region of the liver. They exhibit phenotypes of both hepatocytes and cholangiocytes. Experimental injury models in rodents designed to model this biliary progenitor proliferation have demonstrated that duct-like "oval cells" act as progenitor cells and can differentiate into both hepatocytes and cholangiocytes. This finding suggested that the progenitor compartment represents a clinically important cell population that could be pharmacologically manipulated to improve liver function in advanced liver disease where mortality is high and few treatment options currently exist. Historically, bipotential oval cells were proposed to originate from a quiescent, reserve stem cell located at the interface between the bile ducts and hepatocytes in "the canal of Hering". Nevertheless, the precise origin of liver progenitors has continued to be a matter of controversy and debate in the field for over 50 years.

The goal of this thesis is to understand the cellular mechanisms of liver regeneration in models of chronic liver injury. Specifically, I focus on the origin and function of putative liver stem/progenitor, a cell type whose function is disputed but tightly associated with chronic liver disease. I begin by reviewing the liver architecture, embryology of the liver, and histologic observations in human liver injury that have guided experimental efforts. Next, I explore the experimental systems used to look for the presence of liver stem/progenitors cells and the conclusions drawn from

chronic injury models in rodents. I focus on the experimental evidence used to justify the liver stem cell hypothesis, a controversial but predominant theory in the field. The next three chapters focus on independent research I performed under the supervision of Dr. Markus Grompe. The first chapter of original research encompasses over 2 years of unpublished work developing *in vitro* systems to identify liver progenitor cells in mice and humans. The next chapter is adapted from an article published in the journal *Hepatology*. We utilize clonal lineage tracing to test the hypothesis that biliary duct derived liver progenitor cells are an important source of new hepatocytes in the injured mouse liver. The final research chapter (manuscript in peer review/revision at the time of this writing) explores the opposite hypothesis through lineage tracing techniques—namely, that hepatocytes themselves are the source of progenitor-like ductal cells. The chapter leads to a unifying hypothesis for the thesis as a whole—that hepatocyte metaplasia mimics liver stem cell activation. We also propose a new hypothesis to explain observations of cellular plasticity in experimental rodent injury models and human disease called the decoy metaplasia hypothesis. With the decoy metaplasia hypothesis in mind, I use the final chapter to discuss how several fast moving areas of liver biology may provide new therapeutic strategies for improving liver regeneration and liver function in patients with liver disease.

CHAPTER 1: LIVER REGENERATION IN CHRONIC INJURY

Liver disease is a major unmet medical need

Liver disease accounts for over 44,000 deaths per year in the United States (1.9% of all deaths). In particular, chronic liver disease or cirrhosis is the 12th leading cause of death for the total population in the United States and accounted for 31,903 deaths in 2010 according to the United States Center for Disease Control(1). It is estimated that up to 1% of the population in the United States is afflicted with some degree of histologic cirrhosis(2). Liver disease has many causes including infectious, autoimmune, environmental and genetic etiologies. In the United States, alcoholic liver disease accounts for 40% of deaths due to cirrhosis. Hepatitis C-virus, non-alcoholic fatty liver disease (NAFLD), biliary cirrhosis, and hematochromatosis significantly contribute to overall disease burden(3,4). Regardless of etiology, untreated chronic liver disease can progress to a common end-stage disease called cirrhosis.

Cirrhosis is defined histologically as the development of regenerative nodules encased in fibrotic bands of extracellular matrix. Fibrosis is associated with a decrease in the hepatocellular mass, impaired liver function, and a series of complications that arise regardless of the underlying cause of liver disease. Patients with decompensated cirrhosis, characterized by jaundice, ascites, and/or esophageal varices have a 20-57% one-year mortality rate without transplantation (Figure 1-1)(5). Five-year survival rates once cirrhosis has progressed are as low as 15% in patients who do not receive a liver transplant(2).

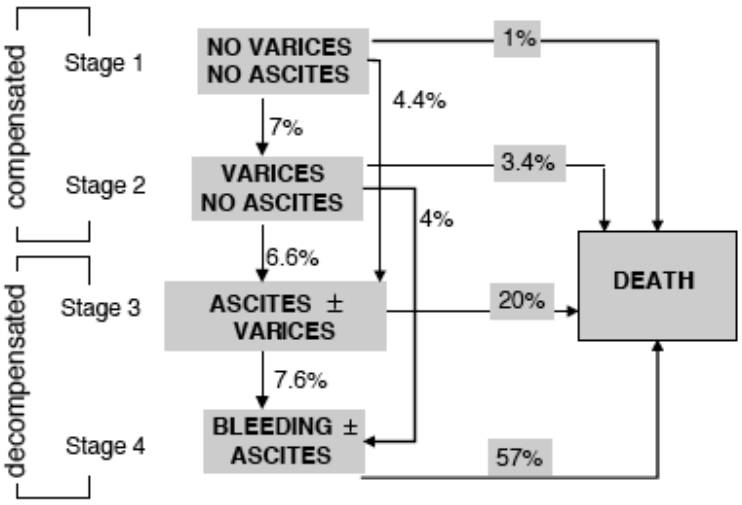

Figure 1-1: One-year outcome probabilities in cirrhosis according to clinical stage. Cirrhosis is a progressive disease. The probability of progressing to each stage is listed next to the arrow. One-year mortality rates vary by stage. Stage 1 is characterized by the absence of esophageal varices and of ascites. Stage 2 is characterized by the presence of esophageal varices without ascites and without bleeding. Stage 3 is characterized by ascites with or without esophageal varices in a patient that has never bled. Stage 4 is characterized by GI bleeding with or without ascites. *Figure adapted from D'Amico 2006.*

Orthotopic liver transplantation significantly improves the survival and quality of life of patients who receive new livers. One and five year survival rates following transplantation are 83% and 70%, respectively(2). But a large proportion of cirrhotic patients die on the transplantation list due to a severe shortage of donor livers. Additional patients are never added to the transplantation list due to substance problems, the lack of insurance, or a lack of social support.

Medical management and supportive care have produced impressive improvements in both the survival and quality of life of patients with cirrhosis in the last few decades. The death rate for all patients with cirrhosis has dropped from 40 per 100,000 people in 1975 to less than 15 per 100,000 in 2000, largely as a function of improved management of complications like bleeding, infection, and renal complications(6). Yet, few treatments exist for patients to improve liver

regeneration and function; no alternative to liver transplant currently exists. The challenge in the next 10 years is to capitalize upon recent basic science discoveries that have improved our mechanistic understanding of liver regeneration, hepatocyte biology, and the pathophysiology of cirrhosis.

Liver anatomy, cell composition, and functions

An understanding of liver function begins with the anatomy. The liver is located in the right upper quadrant of the abdomen inferior to the diaphragm. It is positioned between the digestive tract and the rest of the body. The liver receives blood from two sources: a portal and arterial circulation. Deoxygenated portal blood comprises 70% of afferent blood and comes from the spleen, pancreas, stomach and intestines. The other 30% of the blood supply is well-oxygenated arterial blood from the hepatic artery. Efferent blood exits the liver into the superior vena cava. A 4th connection, the umbilical vein, allows for well-oxygenated blood to pass from the placenta to the fetus in utero. The vein remains patent in infants but becomes obliterated and is renamed the *round ligament* in adults. In infants and children, the umbilical vein can provide minimally invasive vascular access to the liver for cell transplantation (see Chapter 6) (7).

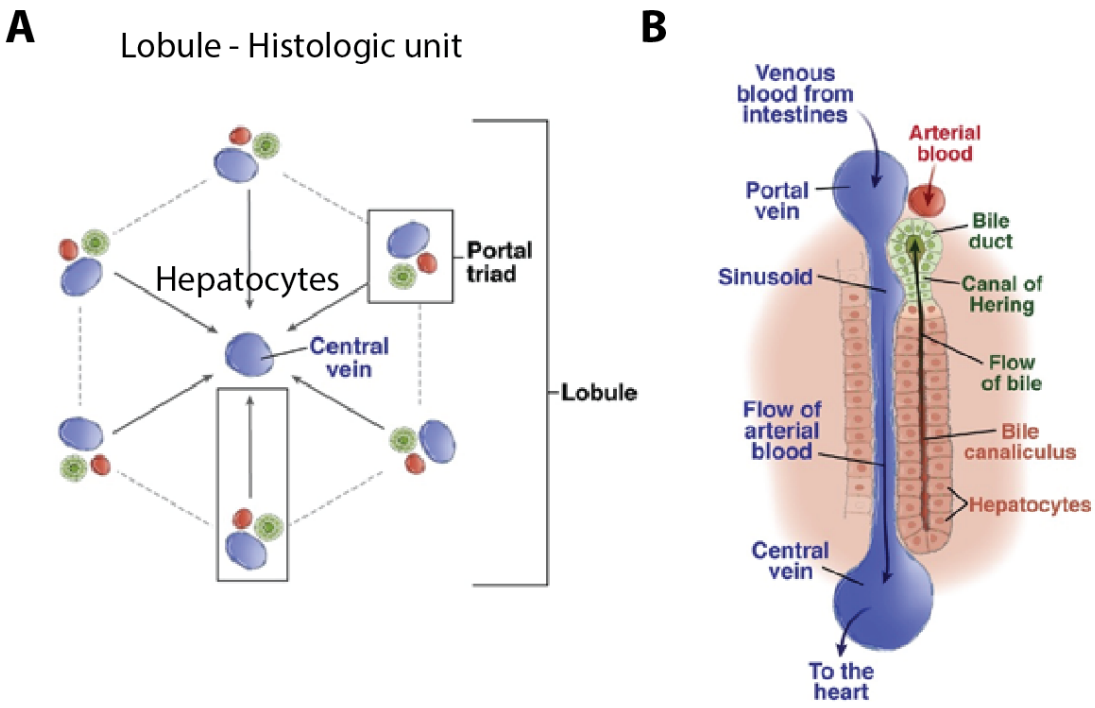

Figure 1-2: Microarchitecture of the liver
A) The liver appears as repeating hexagonal units of hepatocytes surrounded portal triads that drain into the central vein B) The portal triad consists of a portal vein, hepatic artery, and bile duct. *Adapted from Duncan et. al. 2009 with permission.*

Histologic sections of the liver reveal a basic architecture of repeating hexagonal arrays of hepatocytes lined by sinusoidal endothelium, with portal veins, bile ducts, and larger central veins arranged at the corners of the hexagons (**Fig 1-2A**). The basic functional unit of the liver is the liver acinus (**Fig 1-2B**). Portal venous blood from the intestines and arterial blood enter the acini at the portal triad. It flows across the acini through the fenestrated endothelium and facilitates the delivery of the blood to the basolateral surface of the hepatocyte. Bile is secreted from the apical side of the hepatoyctes into channels formed by the hepatocyte cell membrane itself called bile canaliculi. Bile flows in the central vein to portal vein direction. Near the portal tract, bile canaliculi connect to the bile ductules which are lined by epithelial cholangiocytes, or biliary duct cells in the canal of Hering, which

is the anatomical location where some have hypothesizes a quiescent bipotential stem cell resides. Bile exits the liver through the common bile duct into the duodenum or through the cystic duct for temporary storage in the gallbladder. Multiple other cells types reside in the liver parenchymal including macrophages or Kuppfer cells, hepatic stellate cells, portal fibroblasts, lymphocytes, vascular endothelial cells, and sinusoidal endothelial cells (see **Table 1-1**). Many of these cells are important mediators of liver pathophysiology.

Liver function and zonation

The liver plays a critical role in maintaining the body's homeostasis. Since hepatocytes perform hundreds of vital functions, diseases such as hepatitis and cirrhosis often result in significant morbidity and mortality. A partial list of hepatic functions includes the processing of dietary amino acids, secreting proteins such as clotting factors and albumin, conjugating bilirubin, removing microbes from the splanchnic blood, detoxifying xenobiotic compounds in the blood, excreting bile into the intestines to aide fat digestion, maintaining fat and carbohydrate levels (ie glycogen storage and gluoconeogenesis), and maintaining cholesterol homeostasis.

Interestingly, many of these functions are spatially separated across the liver lobule. Many forms of hepatic injury exhibit a zonal distribution, which underscores the differential expression patterns and vulnerabilities functions of hepatocytes across the lobule. Zone 1 hepatocytes nearest the portal triad receive the highest gradient of oxygenated blood. These hepatocytes express the highest levels of gluconeogenesis enzymes, for example. Zone 3 hepatocytes near the terminal

central veins are the furthest from the blood supply and express the highest levels of cytochrome P-450 enzymes that perform drug detoxification. Zone 2 hepatocytes lie in the middle of the zone and are less well defined. The highest levels of carbamoyl phosphate synthetase, the first enzyme in the urea cycle, are found in midzonal hepatocytes but also in some perivenous zone 1 hepatocytes. The zonal expression of specific enzymes can be partially reversed if the pattern of blood flow is disrupted or experimentally manipulated(8). Specific transcriptional programs also reinforce the zonation of the liver. Wnt-signaling molecular β-catenin, for example, is critical in maintaining the function of pericentral hepatocytes and expression of glutamine synthetase(9). A recent high resolution immunohistochemical study in normal human liver showed that immediate periportal hepatocytes express cholangiocyte-genes such as HNF1β expressed at low levels(10).

Table 1. Predominant Cell Types and Their Functions within the Adult Liver

Cell Type	Position in Liver	Developmental origin	Function
Hepatocyte 70% of liver cell population	Parenchyma	Endoderm (hepatoblast)	Bile secretion Cholesterol metabolism Protein secretion Drug Detoxification Urea metabolism Glucose/glycogen metabolism Acute phase response/innate immunity Blood clotting
Cholangiocyte/bile duct cell 3% of liver cell population	Duct epithelium	Endoderm (hepatoblast)	Form bile ducts to transport bile Control rate of bile flow Secrete water and bicarbonate Control pH of bile
Liver sinusoidal endothelial cell 2.5% of lobular parenchyma	Sinusoids	Mesoderm (septum transversum)	Form sinusoidal plexus to facilitate blood circulation Allow transfer of molecules between serum and hepatocytes Scavenger of macromolecular waste Cytokine secretion Antigen presentation Blood clotting
Kupffer cell 2% of liver	Sinusoids	Mesoderm (bone marrow)	Scavenge foreign material Secrete cytokines and proteases
Hepatic stellate cell 1.4% of liver cells	Perisinusoidal	Mesoderm (septum transversum)	Maintenance of extracellular matrix Vitamin A, and retinoid storage Controls microvascular tone Activated to become myofibroblast Secretion of cytokines
Endothelial cell	Vasculature		Form veins, arteries, venuoles, and arterioles Control blood flow Contribute toward parenchymal zonation
Lymphocytes	Periportal	Mesoderm (bone marrow)	Rare, but can expand during injury Cytotoxic activity (ie natural killer cells, or "Pit Cells"

Adapted from Si-Tayeb, Dev Cell 2010

Embryonic liver development and fetal liver stem cells

The mechanisms of organogenesis have attracted the attention of scientists and clinicians engaged in liver regeneration research because many of the basic developmental programs appear to be reactivated in injury. In fact, embryonic-specific genes such as alpha-feto protein (AFP) are expressed in adult progenitor cells in liver injury. Reactivation of the developmental signaling pathways involved in embryonic specification are sufficient to alter the function and fate of adult cells(11), and even initiate cancer(12,13).

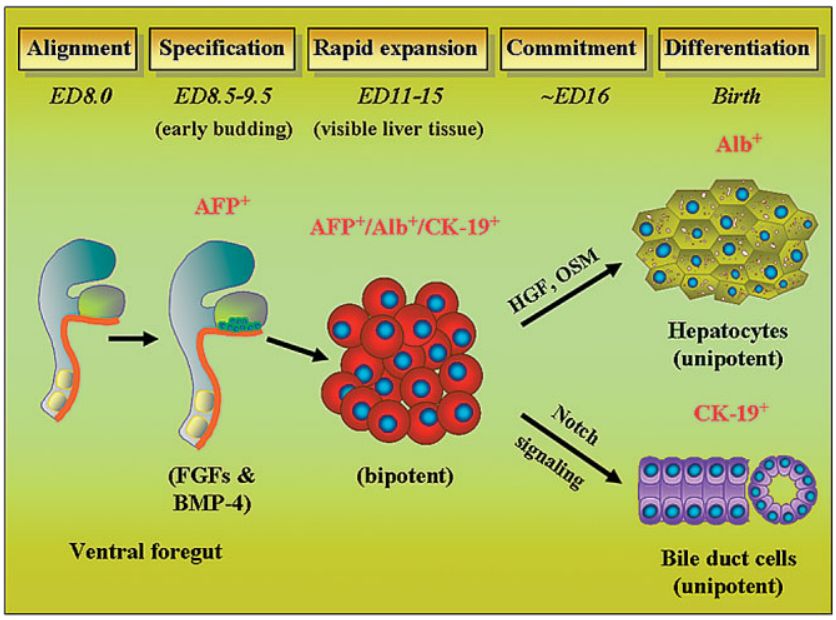

Figure 1-3: Schematic of mouse fetal liver development.
The liver bud emerges at embryonic day 8 (E8) and gives rise to biopotent hepatoblasts that eventually give rise to the two epithelial cell types of the liver: hepatocytes and cholangiocytes that line the bile ducts. *Adapted from Shafritz 2006 with permission.*

Liver specification in rodents first begins on embryonic day 8. At this time, the superior ventral wall foregut is positioned near the developing heart. The endodermal stem cells of the foregut begin to proliferate and differentiate. The cardiac mesoderm produces fibroblast growth factors (FGFs) and septum transversum mesenchyme (derived from lateral-plate mesoderm) secretes bone

morphogenic proteins that trigger hepatic specification and suppress pancreatic specification(14). FGFs signal directly through the MAPK signaling pathway to induce albumin expression and suppress the default pathway of pancreatic specification. Suppression of canonical Wnt-signaling is necessary to induce *Hhex* expression that drives liver specification; suppression of Wnt-signaling in the posterior endoderm is sufficient to induce ectopic liver development(15). By E9.5, the proliferating ventral foregut epithelium has budded out from the ventral wall into the adjacent septum transversum mesenchyme, which is the source of stellate cells and endothelial cells. Newly specified hepatic cells are termed "hepatoblasts" and are defined by expression of *Ttr, Hnf4a, Afp,* and *Alb*(16).

At E11, hematopoetic stem cells (mesoderm) temporarily invade the liver bud and the liver becomes the primary site for hematopoiesis. During this time hepatoblasts continue to proliferate rapidly in cords and express additional liver epithelial markers like alkaline phosphatase, GGT, CK18, and alpha1-antitrypsin. Hepatoblast morphology gradually transitions from cuboidal to pseudostratified epithelium.

At E16 hepatoblasts specify towards the two adult epithelial cell types of the liver: hepatocytes and cholangiocytes. The earliest sign of biliary differentiation is expression of SOX9 in hepatoblasts close to the portal vein. Fgf10 signaling through Fgfr2b is necessary to maintain Sox9 signaling and drives a feedforward loop in progenitor specification(17). These cells form the ductal plate, which is a continuous ring of cells arranged in a monolayer that surrounds the periportal

mesenchyme. As the ductal plate cells differentiate, they are reoriented into tubular biliary structures aligned parallel to the portal vasculature. TGF-β is necessary and sufficient to repress hepatic markers such as *Alb*, *Ttr* and induce biliary cell markers. Mutations in downstream TGF-β signaling causes defects in biliary tree maturation and differentiation(18). Notch signaling also promotes cholangiocyte differentiation; haploinsufficiency of notch ligand JAG1 or notch receptor NOTCH2 results in a paucity of bile ducts and hereditary Alagille Syndrome in both humans and mice. Additional signaling molecules involved in biliary specification include the Wnt/β-catenin family. Deletion of β-catenin in hepatoblasts results in a paucity of bile ducts while activation through deletion of *Apc* promotes biliary differentiation(19).

Hepatoblasts that remain SOX9-negative differentiate towards a hepatocyte lineage and gradually acquire hepatic functions. Hepatocyte growth factor (*Hgf*) and oncostatin M promote hepatocyte differentiation(15). Recent evidence has shown that Sox9-expressing ductal plate cells also give rise to a small subset of peribiliary hepatocytes(20) that may have unique properties in adult injury. Loss of function gene deletion studies detail a large number of other transcriptional regulators that control hepatic gene expression and hepatocyte maturation including *Hnf4a* and *Hnf1a* (reviewed by Si-Taeyeb)(16).

Liver development continues into the neonatal period. Hepatocytes maturation is marked by a downregulation of fetal hepatocyte genes such as alpha-fetoprotein

and glypican-3, induction of Cyp450 genes, and lobular patterning. At birth hepatocytes are exclusively diploid but rapidly increase in chromosomal number upon weaning as a product of failed cytokinesis(21). In the adult mammalian liver, approximately 80% of hepatocytes are tetraploid or octaploid.

Histopathologic findings in human liver disease

Many of the animal models used to understand liver disease are modeled on the histopathological findings present in the most common forms of liver disease. Thus, a brief review of clinical histopathological findings is important to understanding advantages and limitations of experimental liver injury models. The liver is vulnerable to a wide variety of metabolic, toxic, and microbial insults which primarily injure the hepatocyte. Ductular reactions are reported in all types etiologies of liver disease that impair hepatocyte function.

In both acute and chronic human liver disease the severity of the clinical impairment is correlated with the degree of histologically defined atypical ductal proliferation(22-25). The ductal reaction has been documented as a common feature of hematochromatosis, non-alcoholic steatohepatitis (NASH), alcoholic hepatitis, hepatitis C, and hepatitis B. Ductular reactions occur in the early stage of disease and typically preceded the development of extensive lobular fibrosis(26). The ductal reaction occurs at the interface of the hepatic lobule and the terminal branches of the ductual tree near the portal tract. Because the atypical ductal reactions do not form a lumen, they are often referred to as “pseudo-ducts”(27).

The ductal cells themselves are small epithelial cells (8-18 μm in diameter) with a relatively large oval nucleus and scant cytoplasm. The cells arrange in ductal cords and largely express biliary epithelial genes. Immunohistochemical stains are needed to definitively identify the cells in the ductular reaction. Typical immunohistochemical stains include neural cell adhesion marker (NCAM), CD133 (also known as Prom1), EpCAM, Keratin 7, and vimentin(24,26,28). Atypical ductal cells also express markers of the hepatocyte lineage such as albumin and c-met(27). **Figure 1-4** illustrates the range of intermediate hepatobiliary phenotypes that are directly observed. Additionally, the ductal reaction is typically accompanied by a strong lymphocytic infiltrate, hepatocyte necrosis, and hepatocellular injury.

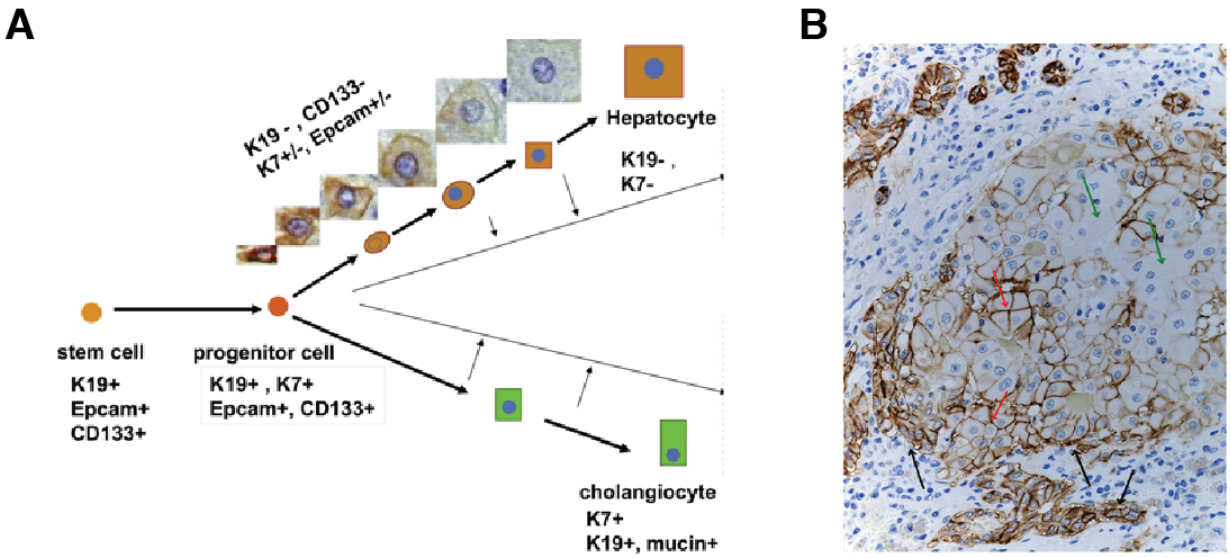

Figure 1-4: The liver stem cell hypothesis explains the origin of intermediate hepatobiliary. A) Diagram illustrates the liver stem cell hypothesis, which is proposed to activate a quiescent stem cell. The liver stem cell is not directly observed in tissue but is inferred through the observance of intermediate hepatobiliary cells that are Krt19-negative but express intermediate levels of EpCAM and Krt7. B) EpCAM staining in a "regenerative" nodule from a patient who lost more than 80% of hepatocytes from an acute liver injury. Ductal cells with scant cytoplasm stain most intensely (black arrows, top of image). Intermediate hepatobilliary cells are weakly positive for EpCAM (red arrows) and have a hepatocytic morphology. Hepatocytes at the center of the nodule are EpCAM-negative (green arrow) and thought to have differentiated earlier. *Adapted from Roskams 2010 and Hattoum 2013 with permission.*

In normal human liver, expression of EpCAM is limited to the biliary cells of the portal ducts and ductules. But in cases of severe hepatic damage (i.e. loss of more than 80% of hepatocytes), EpCAM is expressed in "regenerative nodules" containing hepatocytes interspersed with ductal cells (**Fig 1-4B**). The biliary-like cells with scant cytoplasm are most strongly positive for EpCAM, the ductal hepatocytes around the periphery of the nodule are weakly positive, and the small clusters of hepatocytes at the middle of the nodule are EpCAM-negative. Ductal hepatocytes expressing biliary markers such as EpCAM or KRT7 have a greater cell replication index than EpCAM-negative hepatocytes, suggesting these cells are participating in liver regeneration in chronic injury(27,29). In acute necrotic liver injury, an independent group also reported that ductal hepatocytes located immediately adjacent to the ductal reaction had the highest proliferative index of all hepatocytes(26).

Due to the bleeding risk of serial biopsy in patients with severe coagulopathies, few studies have systematically tracked the fate of atypical ductular reactions. A single case report in 2000 histologically followed the recovery of a patient who received an auxiliary partial orthotopic liver transplant (APOLT) for treatment of massive fulminant hepatitis B where 95% of the hepatocytes were lost is particularly revealing(30). In this procedure, 1/3 of the patient's liver was surgically removed and replaced with 1/3 of a healthy relative's liver. Both the new healthy liver and residual injured were biopsied 15 times over the course of 14 months. Strikingly, the ductular reaction peaked at 10 days post surgery and progressed into a

histology dominated by ductular hepatocytes weakly positive for CK19 by 30 days post surgery. The number of ductal hepatocytes continued to decrease over the next year. At 14 months post surgery, the donor and native liver showed no obvious differences in histology and immunosuppression was stopped. This study demonstrates that even a severely injured human liver has the capacity to regenerate with supportive therapy. The origin of the ductular reaction was impossible to determine, however, the sequential biopsies in the recovery period strongly suggest the existence of direct precursor-product relationship between the ductular reaction and regenerated hepatocytes.

Together, these observations are often interpreted as evidence that stem/progenitor cells are producing new hepatocytes; however, they are in fact static snapshots in time from single patients. As snapshots in time, these reports provide no information about the directionality of the process or origin of the ductular cells. Regenerative nodules (**Fig 1-4B**) may be the product of stem/progenitor cells that progressive lose biliary markers and differentiating into hepatocytes. But these static histopathologic observations on their own are also consistent with an alternative model where hepatocytes transiently acquire a biliary phenotype without the involvement of a stem cell. In the 1950s and 1960s, experimental liver biologists were evenly split between those who thought biliary cells gained hepatocytic characteristics and those who thought hepatocytes acquired biliary characterstics with injury(31). In recent years, the field has gravitated towards one prominent explanation: the liver stem cell hypothesis

(27,32-34). In the next section, I discuss the liver stem cell hypothesis and the experimental laboratory systems devised to test the liver stem cell hypothesis. Cell-tracking techniques in controlled model systems are needed to understand the directional relationship between the ductular reaction and hepatocytes.

CHAPTER 2: EXPERIMENTAL STRATEGIES TO IDENTIFY ADULT HEPATOCYTE PRECURSOR CELLS

The recent history of experimental adult liver stem/progenitor biology is one of confusion and controversy. In the past 15 years, no fewer than four different populations of cells have been proposed as reservoirs of hepatocyte precursors. Bone-marrow-derived hematopoetic stem cells(35-37), bile duct cells(38,39), stellate cells(40), unidentified non-parenchymal cells(41-43), and hepatocytes themselves(44,45) have all been proposed as the origin of new hepatocytes in chronic injury. These disparate reports are difficult to reconcile with one another and underscore the difficulty of identifying the cellular mechanisms of organ regeneration. This chapter begins by discussing the differences between regeneration from partial hepatectomy and chronic injury. Next, I examine the advantages and disadvantages of four major experimental approaches that have been used to build evidence for and against the adult liver stem cell hypothesis. Specifically, I discuss how *in vitro* progenitor assays, transplantation assays, label retaining assays, and genetic lineage tracing approaches are used to test progenitor activity in the liver.

Partial hepatectomy regeneration

A defining feature of the liver is its remarkable capacity to regenerate. In partial hepatectomy, 2/3 of the liver is surgically excised and the residual liver mass enlarges to make up for the mass of the removed lobes, though the resected lobes do not grow back. The regeneration process takes 5-7 days days in rodents and about 3 weeks in humans. The procedure does not cause any injury to remnant liver

tissue, and the subsequent regenerative process is considered to occur by the proliferation of each individual cell type in the liver without any role for an immature stem cell population(46,47). Normal homeostasis is also maintained without the apparent need for a stem cell. Briefly, the liver stem cell hypothesis (discussed next) has occasionally been extended to propose that stem cells are involved in normal liver homeostasis of the hepatocyte mass (38,42,48,49). These reports employed novel methodologies but generally could not be replicated in more rigorous studies that followed(39,45,50). Thus, the evidence against "streaming" in truly normal liver is overwhelming and has recently become an area of *near* consensus in the field(33,51).

The liver stem cell hypothesis

The liver stem cell hypothesis provides a model to explain the mechanism of liver regeneration in pathologic conditions that involve hepatocyte death, impairment of hepatocyte replication, fibrosis, and chronic inflammation. Under pathological conditions, the ability of hepatocytes to replicate is severely impaired or entirely blocked. A population of small cells with an ovoid nucleus and high nuclear:cytoplasmic ratio emerges from the portal tract. These cells are called many things including *oval cells, neocholangiole*, *hepatic progenitor cells,* or *atypical ductular* reactions. Because the cells are first observed at the interface of the hepatic plate and terminal ductuals, they may be derived from normally quiescent stem cells that reside in the terminal biliary tree within the canals of Hering. The quiescent *intrahepatic stem cell* has never been directly isolated or identified in tissue sections, but its presence is inferred based on the characterization of

intermediate hepatobiliary cells observed in injury and some lineage tracing experiments. Given that the canaliculi and biliary tract connect in multiple locations per portal triad, multiple stem cells would be expected in each portal tract. Multiple trophic factors and cell types participate in oval cell activation (reviewed by Erker)(52), but replication arrested hepatocytes somehow initiate the signaling cascade. Finally, oval cells appear heterogenous in size and morphology, likely due to their rapid differentiation towards a hepatocyte.

Is hepatocyte replication arrest sufficient to activate oval cells?

A tenant of the stem cell hypothesis is that oval cells are activated only when hepatocytes cannot replicate themselves. The prototypical oval cell activation model combines 2-AAF, an alkylating agent that blocks hepatocyte replication, with 2/3 partial hepatectomy in the rat. This injury does not work in mice because 2-AAF is only metabolized to its active form by a sulfatase expressed in rat hepatocytes(51).

Two commonly used model systems create exceptions to this rule. First, hepatocyte replications arrest with the alkaloid retrorsine followed by partial hepatectomy (PH) does not generate a significant oval cell response(53). Instead, small hepatocytes appear as clusters of 3-6 cells that are evenly distributed across the lobular zones 3 days after hepatectomy. These clusters rapidly grow into large hepatocyte nodules and occupy 50% of the liver parenchyma by day 14. The mode of repopulation is distinct from the 2-AAF/PH model even though it shares the common elements of replication arrest in the setting of a strong replication

stimulus. One interpretation of this this study is that a small population of hepatocytes inefficiently metabolize retrorsine and thus escape its effects.

Second, the *Fah*$^{-/-}$ mouse is widely used for hepatocyte transplantation assays because donor cells have a profound selective advantage when mice are cycled off NTBC and allowed to develop liver injury. Withdrawal of NTBC leads to accumulation of fumarylacetoacetate, a potent DNA mutagen that creates cell cycle arrest. When *Fah*$^{-/-}$ mice off NTBC were given partial hepatectomy, no hepatocytes incorporated BrdU by 40 hours(54) and only a few BrdU positive cells were observed at 96 hours(44). Strikingly, this regimen did not provoke an oval cell response.

Interestingly, a connection between the bile ducts and the periportal hepatocytes seems to be necessary to initiate the oval cell response. Toxic damage to the biliary cells with the chemical metheleyne dianiline prior to initiating the oval cell response with the 2-AAF/PH protocol eliminated the appearance of oval cells(55). Oval cells may not appear because the stem cell compartment was obliterated, the connection between the bile ducts and periportal hepatocytes is critical for oval cell activation, or because methelene dianiline blocks the activity of 2-AAF through a drug-drug interaction.

Interestingly the congenital disorder dsykeratosis congenital caused by a mutation in the telomerase complex, results in cirrhosis, among other symptoms. Some

patients with sporadic cryptogenic cirrhosis also carry mutations in telomerase complex genes, which implicates hepatocyte replication arrest in cirrhosis(56). On the contrary, EpCAM$^+$ hepatocytes that appear in liver injury are documented to have a higher replication index than EpCAM-negative hepatocytes in both chronic(29) and acute liver injury(26). Additionally, analysis of X-inactivation patterns(57) and hepatitis-B integration sites(58) suggests that over 1/3 of nodules in hepatitis B induced cirrhosis may be monoclonal outgrowths. This is evidence of continued hepatocyte cell division in fibrotic disease.

In summary, hepatocyte replication arrest may be necessary to activate the oval cell response. But it is not sufficient. Chemical caricinogens like 2-AAF that block hepatocyte replication may have additional signaling functions that are critical to oval cell activation.

In vitro clonogenic assays

The evaluation of individual cellular components of a complex organ involves the reductionist practice of separating tissues into single cell suspensions of its component cell types. With the use of cell surface markers and flow cytometry, different cell types can be isolated and their functions can be evaluated *in vitro*(3,4,59).

Two recent examples of prospective progenitor isolation were demonstrated from Foxl1$^+$ and MIC1-1C3$^+$ liver cells, respectively(60,61). A subset of isolated ductal epithelial cells isolated in these two studies shared similar gene expression patterns,

and clonogenic activity in defined culture media. The clonogenic progenitor cells could both self-renew and differentiate into cholangiocytes or hepatocyte-like cells depending on the culture conditions that were used. Importantly, MIC1-1C3^{+} progenitors could be isolated from both normal and DDC treated mice, suggesting this progenitor cell originated from the biliary tract. Progenitors derived from DDC treated liver were more numerous and had similar clongenic properties to those of the normal liver(61).

A different epithelial cell colony forming assay, Suzuki et al, showed that clonogenic cells formed from FACS isolated CD133^{+} cells from normal and DDC treated liver(62). But only clonogenic cells from DDC treated liver gave rise to large colonies in this study. When CD133^{+} cells were FACS isolated in bulk and cultured for 4 weeks, the transplanted cells were able to differentiate into hepatocytes and provide a functional rescue. Because the transplant was performed in bulk, it is not possible to prove whether the colony forming cells or another cell type present in the culture accounted for the *in vivo* rescue.

Huch and colleagues developed a 3-dimensional Wnt/Rspo1-based assay that allowed for the unprecedented expansion of normal liver epithelial cells(41). Self-renewing spherical colonies could be initiated from single cells. Upon culture, these cells expressed the intestinal stem cell marker Lgr5 and retained the general architecture of biliary epithelial cells. Of note, expanded spheroids were able to differentiate towards a hepatocyte-like phenotype in specific culture conditions.

Upon transplantation, the hepatocyte-like cells differentiated into hepatocytes at very low rate (~1 in 50,000 transplanted cells).

In contrast to ductal progenitor cells, mature hepatocytes cannot be expanded in culture. The inability to expand hepatocytes *in vitro* has hindered applications to cell transplantation and pharmacology. Standard culture techniques cause hepatocytes to rapidly lose expression of albumin and dedifferentiate. The collagen sandwich technique(63) was the first to maintain mature hepatocytes in their differentiated form for more than a few days. Interestingly, the collagen sandwich technique could even rescue albumin secretion rates in hepatocytes that had dedifferentiated in culture for 7 days, providing an early demonstration that hepatocyte dedifferentiation may be partially reversible. The ability of mature hepatocytes to give rise to $CK19^{+}$ ductular structures "akin to bile ducts" in the presence of hepatocyte growth factor was convincingly shown *in vitro* by Block et al(64). Several recent studies have also demonstrated that hepatocytes give rise to bile duct-like phenotypes. Transplantation or *in vitro* differentiation assays demonstrated that hepatocyte-derived bile ducts could efficiently convert back into hepatocytes. (65-67). These studies provide strong evidence that hepatocytes have the *potential* to acquire a phenotype similar to the ductular reaction observed in liver injury. Nevertheless, they have received little attention due to questions about the *in vivo* relevance of hepatocyte dedifferentiation.

Studying epithelial cells in defined growth factor conditions is an enormously powerful way to determine the potential of a cell type. But *in vitro* potentiality may not fully correspond to *in vivo* functionality(68). For example, *in vivo* lineage tracing of putative progenitor populations in lung(69) and breast(70) failed to show the same multi lineage differentiation achieved in culture. Moreover, *in vitro* hepatic gene expression and *in vitro* activity in genetically engineered hepatocyte-like cells does not fully correspond with *in vivo* hepatocyte functionality(71,72).

Transplantation

Transplantation assays are critical tools for assessing stem/progenitor potential to provide long-term physiologic function. The widespread availability of transplantation assays is a major advantage for the study of liver stem/progenitor cells. Cell transplantation has achieved considerable attention because of the potential translational applications for therapeutic cell transplantation to treat liver disease(73). Typically, cells of interest are isolated from a donor mouse that can be identified based on a distinct marker from the recipient, such as green fluorescent protein or sex-mismatch (i.e. Y-chromosome). When cells are transplanted into a diseased recipient model, donor cells can demonstrate *in vivo* physiologic function and rescue organ function. A disadvantage of transplantation assays is that many cells are simultaneously implanted, so the multi-lineage differentiation capacity of individual cells can be difficult to establish. When few cells engraft, it is difficult to exclude contamination of a mature cell type. To accurately assess progenitor activity, transplantation assays must meet several criteria, which I will discuss one at a time by using examples from the literature:

1) Progenitors must be purified from mature cell types in the donor organ.
2) The isolation procedures must maintain progenitor viability (and mature cells, if using a competitive repopulation design).
3) Donor cells must be delivered to and then trapped in the correct tissue niche
4) Donor stem cells must receive signals and be given sufficient time to differentiate into mature cell types in a multi-lineage fashion
5) Heterotypic cell fusion must be excluded as the mechanism of activity.

Cell Isolation and Purification

Progenitor cells, by definition, lack the activity of the mature cell, but can differentiate into mature cell type(s) upon differentiation. In order to prove that an immature cell matures upon transplantation, one must first rule out the presence of the mature cell type in the initial preparation. The development of monoclonal antibodies to cell-type specific antigens similarly revolutionized the study of hematopoetic stem cells(74) and liver progenitor cells(59,75,76). The current generation of FACS-based isolation allows for unprecedented ability to separate phenotypically homogenous cells from a heterogeneous tissue based on cell surface phenotype. Nevertheless, all purity is relative: purity exceeding 99% is difficult to achieve even for experienced experimentalists.

In the *Fah*$^{-/-}$ system, fewer than 500 transplanted hepatocytes can functionally rescue the mouse from acute liver failure caused by tyrosinemia(77). Therefore, a hypothetical transplant of 500,000 potential progenitor cells that is contaminated with just 500 mature hepatocytes could rescue the host from death and read out as

a positive graft in a transplantation assay—even if the 99.9% pure potential progenitor fraction had no activity.

A notable example of contamination in a highly selective model comes from the limb regeneration field. When the axolotyl limb is amputated, a proliferation of small, immature proliferative cells collects at the tip of the regenerating limb called the blastema. Muscle and Schwann cells were proposed to achieve a pluripotent state during limb regeneration based on transplantation assays into irradiated recipients(78). Later genetic lineage tracing experiments, however, showed that these preps were simply contaminated with exceedingly low levels with multiple other cell types. Each cell type regenerated itself according to its specified lineage without evidence of muscle contributing to a pluripotent population(79).

Delivery and immobilization in the niche

Liver directed cell therapy utilizes a vascular delivery route to evenly distribute donor cells throughout the liver. Embryonic liver stem/progenitor cells are significantly smaller than larger mature cells (ie hepatocytes) and engraft with only 20-30% efficiency if directly injected into the liver parenchyma. But when administered through a vascular route, more primitive cells are not efficiently trapped in the liver sinusoids as a function of cell diameter (80). Similar principles of cell delivery apply in other organs as well. For example, direct femoral injection of hematopoetic stem cells dramatically increases donor engraftment and repopulation time(81). Therefore, caution is required in interpreting a negative result in transplantation assays; the absence of activity—or reduced activity

compared with a mature cell type--may simply reflect a homing or delivery defect rather than a biological property of the putative progenitor. Since a vascular migration of a progenitor is not a feature of normal liver regeneration, negative result in a transplantation assay may not reflect the progenitor activity of a cell in situ.

Competitive repopulation and experimental considerations

The stringent criteria for determining the activity of a putative progenitor population is competitive transplantation against cells with known activity(82). In these experiments, progenitor population and mature cells from different genetic backgrounds are mixed together and co-transplanted into the same location (ie progenitors expressing tdTomato, mature cells expressing GFP). In a competitive repopulation assay to assess the regenerative capacity of murine liver oval cells, Wang et al tested the *in vivo* repopulating capacity of the "F2 nycodenz fraction" of DDC treated liver cells(83). In a competitive transplantation assay, the F2 cells were competed against pronase-isolated hepatocytes (high endotoxin, harsh method) for their ability to for hepatocyte regeneration nodules in a recipient mouse. Even though the F2 fraction contained 45% CD45 white blood cells and approximately 25% endothelial cells (which have no known liver repopulating capacity), the transplantation assay was interpreted to show the F2 fraction had equivalent regenerative potential to hepatocytes(83). One limitation of this paper was that that the F2 fraction competed against hepatocytes that were severely wounded by a harsh enzyme, which may have over-estimated the repopulation capacity of the bulk "F2" population. Thus the differential survival of cell types in the cell isolation

process may affect the interpretation of experiments.

A second important consideration with FACS isolation is the presence of two cell types sticking together. For example, $CD45^+$ cells can be found adhering to approximately 5% of hepatocytes isolated by collagenase digestion and gravity centrifugation. The use of surface markers to exclude a population is helpful (i.e. anti-CD45 antibody to exclude adherent blood cells). Rare cell populations that are double positive for two surface markers must be directly visualized under fluorescent microscopy to rule out cell doublets or adherent membrane fragments from a second cell type as the source of immunopositivity(84).

Differentiation and expansion signals

Liver size and cell number is tightly regulated across mammalian species. For example, in human orthotopic liver transplantation an undersize liver grows to the necessary size while an undersized donor liver shrinks to the requirement of the patient(85). Therefore, liver cell transplantation assays must utilize specialized rodent model systems that provide a donor cells a survival advantage. High levels of liver repopulation can be achieved when mature or immature hepatocytes are transplanted into a host with sustained liver injury where the host hepatocytes are incapable of proliferation. In such a model transplantation of mature hepatocytes or hepatocyte precursors can rescue the function of the host and demonstrate *in vivo* hepatic function that is not possible *in vitro*. Such animal models include:

1) The albumin-urokinase plasminogen activator (uPa) mouse that expresses a protease causing fulminant hepatic failure within 4-6

weeks in most animals unless they are transplanted with wild-type hepatocytes.(86)

2) In $Fah^{-/-}$ mice a mutation in the terminal enzyme of the tyrosine catabolism pathway causes the accumulation of toxic metabolites resulting in extensive liver failure. This mutation is a model for hereditary tyrosinemia type 1. Liver failure can be prevented by administration of the small molecule NTBC or by transplantation with hepatocytes.

3) Pretreatment of host animals with DNA crosslinking agents that act selectively in hepatocytes, such as retrorsine(87) or monocrotaline(88), can be combined with partial hepatectomy to give donor cells a selective advantage. These agents may be metabolized differently in mice than in rats (89).

4) Induction of DNA damage in focal regions of the liver by external beam irradiation can be combined with with hepatocellular injury(90). Similarly, lethal irradiation of the bone marrow followed by transplantation of hematopotetic progenitor fractions is utilized in transplantation assays for HSC function/rescue(74).

5) Immune-compromised versions of the uPA (uPA-SCID)(91) and *Fah*$^{-/-}$ (*Fah*$^{-/-}$ *Rag2*$^{-/-}$ *Il2rg*$^{-/-}$ triple knockout)(92) mice support repopulation with human hepatocytes or fetal hepatoblasts.

Most recently, the *Fah*$^{-/-}$ transplantation assay has been used to characterize the function of hepatocyte-like cells engineered by genetic reprogramming of fibroblasts. Hepatocyte-like cells demonstrates many basic hepatic function *in vitro*; however, reprogrammed hepatocyte-like cells consistently show only partial hepatocyte functionality *in vivo*(93-95). Thus, the transplantation assay demonstrated the hepatic reprogramming was incomplete despite convincing *in vitro* gene expression evidence.

While the models discussed here provide an assay for rescue of hepatic function, no transplantation assay currently exists to assay for multi-lineage differentiation. For example, no transplantation assay currently exists to read out *in vivo* biliary cell function. Notably, transplantation of putative of hepatic progenitors in the *Fah*$^{-/-}$ recipients has resulted in unipotential hepatic differentiation(41,83). In contrast, bipotential oval cells isolated from 2-AAF/PH rats and transplanted into retrorsine/partial hepatecomized rats showed evidence of donor derived immature hepatocytes and bile-duct-like cells(96). A limitation of this approach was that the assay could not conclusively determine whether single oval cells gave rise to both hepatocytes and bile-duct-like cells. In contrast, Sandhu and Shafritz showed that trangenically marked E14 hepatoblasts transplanted into retrorsine/PHx rats behaved as stem cells: they could differentiate into both hepatocyte and mature bile ducts, proliferate extensively, and maintain long term repopulation.(97) The observation that the bulk of repopulation clusters contained both hepatocytes and cholangiocytes was good evidence for bilineage differentiation.

Cell fusion

Cell fusion is a physiological phenomenon that occurs normally in immune cells, placental trophoblasts, osteoclasts and following viral infection with Sendai or Cytomegalovirus. Cell fusion is a rare but important consideration in the interpretation of rare events in transplantation assays. In 2000, Lagasse and colleagues reported that bone marrow transplantation was sufficient to rescue hepatocyte function in *Fah*$^{-/-}$ mice, suggesting that hematopoetic stem cells had the ability to differentiate into tissues of a different germ layer(36). This interpretation was plausible because several published reports suggested that bone-marrow-derived cells were oval cell precursors(35). Unexpectedly, follow up studies indicated that bone-marrow derived hepatocytes were a product of cell heterotypic cell fusion between bone-marrow derived cells and hepatocytes(3,98). Recently, Dorrell reported that pancreatic epithelial progenitor cells propagated in culture were able to differentiate into hepatocytes at a low rate following *in vitro* differentiation(99). Dorrell appropriately ruled out cell fusion as a potential mechanism by transplanting donor cells from a Cre-reporter mouse (ie R26R-lacZ or ROSA-mTmG switcher mouse) into a *Fah*$^{-/-}$ mouse that constitutively expressed Cre under the control of the albumin promoter.

Label retaining cells and autoradiography

When a resident tissue stem cell is activated, it must both self-renew and give rise to a progenitor cell through an asymmetric cell division. Progenitor cells, or transiently amplifying cells, then rapidly proliferate and differentiate into mature functional cells. A label-retaining assay exploits the tendency for stem cells to

replicate through asymmetric cell division and to remain relatively quiescent compared with transiently amplifying progenitor cells. If replicating DNA is marked with a pulse of BrdU or H3-thymidine nucleotide pulse given during an asymmetric stem cell division, both daughter cells will be marked. The DNA mark will be diluted and lost after 3-5 rounds of cell division in any cell that was marked during the brief pulse period (**Fig. 2-1**. Because stem cells are thought to be relatively quiescent, they will retain the marked DNA for a longer period of time than a transiently amplifying cell.

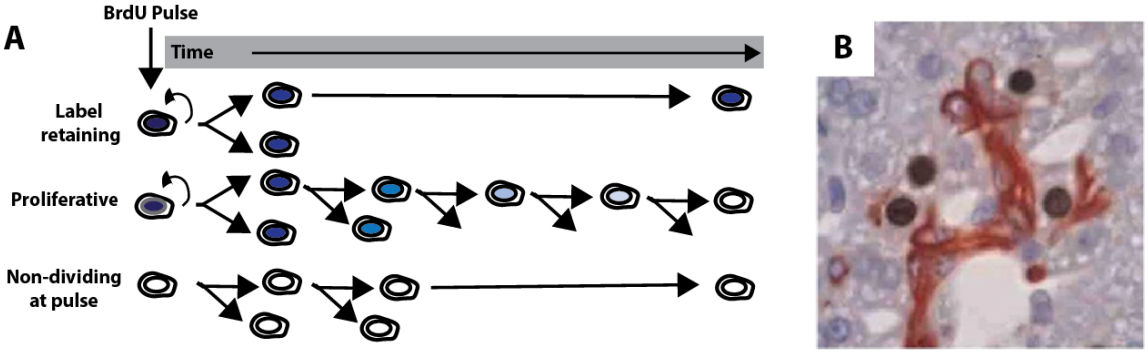

Figure 2-1: Label retaining assays mark stem cell niches. A) A label retaining assays mark cells that are proliferating at the time of a BrdU pulse (marked cells shown in dark blue). Label retaining cells will retain the dark blue label, but proliferating cells will dilute the BrdU label through cell replication and appear unmarked at the end of injury. In the liver, an injury is typically given to induce replication. B) periportal hepatocytes (dark brown nuclei) adjacent to Krt7^{+} ductal cells (reddish brown) preferentially retained BrdU after acetaminophen injury. *Adapted from Kuwahara 2008 with permission.*

Label-retaining assays have the advantage of locating niches of cell and can be applied to all species with few prior assumptions. The disadvantage is that multiple cell types may divide in parallel regeneration structures with complex, and separate regeneration kinetics. Since label-retaining cells are defined in relative terms, a label-retaining cell may have no relationship to regenerating tissue of interest.

In short, label-retaining cells are not necessarily tissue stem cell but provide an

important measure of tissue homoestasis. Recent evidence from multiple organ systems suggests more complex interactions maybe at play between active and quiescent tissue stem cell populations(100) which complicate the interpretation of label retaining assays. In the small intestine, for example, non-self-renewing secretory precursor cells are the label-retaining cells that can differentiate into mature paneth cells or enteroendocrine cells(101). In the hematopoetic system, label retention was relatively enriched in long-term stem cells, but found to be relatively non-specific in absolute terms: only 6% of stem cells were BrdU+ and 0.5% of all BrdU+ cells were stem cells(102). In contrast, studies in the skin hair follicle confirmed that bulge stem cells were indeed label retaining; however, the authors noted considerable variability in the cycling behavior of the bulge stem cells(100).

The normal liver is relatively quiescent in homeostasis. BrdU pulse chase experiments indicate that approximately 1 in 40,000 hepatocytes is replicating at any time; over the course of a year, a hepatocyte will replicate between 1 and 3 times. Therefore, label retaining assays in the liver are typically combined with injury regimens to promote both initial labeling and regeneration.

Kuwahara and Theise performed a label retaining assay in mouse liver combined with acetaminophen injury(43). They identified four compartments that retained labels including proximal biliary cells, intralobular bile duts, periductular “null cells”, and peribiliary hepatocytes. At the final time point of 56 days post injury, the most statistically significant label-retaining compartment was the peribiliary

hepatocytes. These BrdU positive hepatocytes were always "directly contiguous with PanK-positive cells" and occasionally showed faint PanK-staining. The authors proposed that their data supported a model where transiently amplifying oval cells simply differentiated into peribiliary hepatocytes, possibly involving an additional round of cell division. A more straightforward interpretation of this data, however, is that the periportal hepatocyte in the canal of Hering is the origin of some transiently amplifying progenitor cells.

Finally, a variation on the BrdU-label-retaining assay was performed in the setting of oval cell activation in the rat 2-AAF/partial hepatectomy model(103). The investigators administered BrdU to rats at the peak of the oval cell/progenitor response to mark ductal cells. 24 hours after the pulse was given, the majority of labeled cells had ductal morphology and expressed biliary genes. But over the course of the next week, the BrdU label was transferred to nodules of newborn hepatocytes that expressed albumin and other ductal markers. These studies demonstrated a precursor-product relationship existed between the oval cells and hepatocytes. This study is often cited as the strongest evidence for the liver stem cell hypothesis (M. Grompe*, personal communication*). A limitation of the study is that it did not address whether the oval cells were derived from normal mature hepatocytes or a biliary duct cells.

Single cell genomics

Novel single cell transcriptional profiling techniques will provide a powerful, perhaps even essential, approach for establishing the identity of putative

progenitors. For example, MARS-seq (Massively parallel single-cell RNA-seq) provides a cost-effective approach to acquire low-depth transcriptional profiling of up to 1500 single cells using next-generation sequencing(104). This technique correctly categorized mature white blood cells to known cell types and ruled out contamination of other cell types, such as circulating epithelial cells. A similar technique was used to identify the signature of bipotential adult lung progenitor cells. As of this writing, single cell genomics have not yet been applied to understanding cell hierarchies in normal or injured liver. A huge advantage of this approach is that human tissue samples can be used. For example, single cell genomics could be used to unravel the lineage hierarchies in cirrhotic liver disease.

Genetic *in vivo* lineage tracing

Genetic *in vivo* lineage tracing is often referred to as the gold-standard method for determining the actual potential of a stem or progenitor cell(68). The technique has the advantage of examining the biology of a particular cell type in the native microenvironment. In the past 5 years, a large number of different transgenic mice have been generated to specifically ask if a non-parenchymal liver cell significantly contributes to the restoration of the hepatocyte mass following liver injury. **Table 2-1** provides a summary of these studies and underscores the widespread disagreement about whether non-parenchymal biliary cells differentiate into hepatocytes, even when the same injury protocols are used. Rather than discuss each of these studies separately, I will focus on the technical aspects of liver lineage tracing and focus on methodological issues that may explain the apparent discrepancies between these studies.

Table 2-1: Summary of lineage tracing studies tracking liver non-parenchymal cells

Author	Mouse	Injury (approximate percent of hepatocyte mass replaced per unit time) Normal	Partial hep	DDC injury	CCL4 injury	CDE injury	Other	Conclusion/model Liver stem cell?
Sackett, 2009	FoxL1-Cre			~1% (3w)			~1% BDL	Yes
Furuyama, 2010	Sox9-IRES-CreERT2	60% (6m)	~5% (3w)	0% (3w)	~5%	~20% (3w)	>20% BDL	Yes
Carpentier, 2011	Sox9-CreERT2 (BAC)	0% (8w)						Yes
Malato, 2011	rAAV8-Ttr-Cre	0% (6m)	1.40%	0% (8w)	1.3% (6w)			Yes
Dorrell, 2011	Sox9-CreERT2 (BAC)			1.3% (2w)				Yes
Espanol-Suner, 2012	Opn-iCreERT2	0.006% (6m)	0%	0%	0.038% (6w	2.45%		Yes
Huch, 2013	Lgr5-IRES-CreERT2			~1%	~5%	~1%		Yes
Michalotti, 2013	a-SMA-CreERT2						~25% BDL; GFAP-Cre	Yes
Rodrigo-Tores, 2014	Hnf1b-CreERT2	0% (2m)	0%	0%	<0.1%	1.86%		Yes
Tarlow, 2014	Sox9-CreERT2 (BAC)	0% (6m)		0%	<0.1%	<0.1%	Chimera validation	No
Stanger, unpub.	Krt19-CreERT2	0%	0%	0%	0%	0%	AAV-TBG-Cre valid.	No
Willenbring, unpub.	Krt19-CreERT2	0%	0%	0%	0%	0%	AAV-Ttr-Cre valid.	No
Feisel, unpub.	Hnf1b-CreERT2	0%	0%	0%	0%	0%		No
Miyajima, unpub.	Cd133-CreERT2			<5%				Yes

* Color coding reflects a subjective interpretation significance of each result, as reflected by the author's title and discussion. Green = high signficance, red = low

Lineage tracing relies upon the function of a promoter that is assumed to be transcribed in specific cell types, thus allowing a subset of defined cells to be marked in heterogeneous tissue. Many native promoters are well characterized but none are fully understood in all circumstances, including injury. Transgenic approaches involve the insertion of a foreign genetic element into genomic DNA of an animal through site-directed homologous recombination or random insertion of a bacterial artificial chromosome (BAC).

BAC transgenic animals can show cell type specificity differences from the native promoter or even between different founders, reflecting influence of the DNA insertion site on the Cre-promoter. Homologous recombination can also be used to insert a Cre gene directly into the endogenous locus, thus minimizing ectopic expression from adjacent regulatory elements. For example, Furuyama and colleagues inserted an internal ribosomal entry site (IRES) into the 3' untranslated region of the endogenous Sox9 locus(38). But subsequent reports suggest the

dosage of Sox9 expression might be altered even though the CreER cassette contained an IRES sequence(44,51,105).

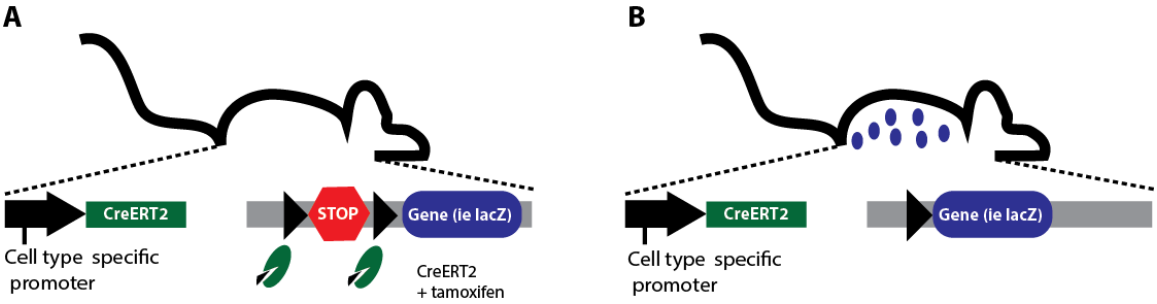

Figure 2-2: Spatial temporal control of lineage marking with tamoxifen inducible cre-recombinase. A) Cre-recombinase fused to a tamoxifen-sensitive estrogen receptor (ERT) is expressed under the control of a cell-type specific promoter. When tamoxifen is present, CreERT2 dimers translocate to the nucleus and bind to specific loxP sites (black triangles) and mediate site-specific recombination. B) Recombination is typically used to switch on a reporter protein such as lacZ that permanently marks cells of interest and their progeny.

Liver lineage tracing often utilizes spatial and temporal control with a cell type specific promoter driving a tamoxifen-inducible Cre-recombinase fused to a mutant estrogen receptor that binds tightly to tamoxifen but not estrogen (CreERT2). Recombination occurs only in the cell types where the promoter is expressed and only when tamoxifen or its active metabolites are present (**Fig. 2-2A)**. Recombination then causes the irreversible removal of a stop cassette that leads to expression of a reporter marker in that cell and all daughter cells (**Fig. 2-2B)**. Tamoxifen, the drug used to induce recombination, is a hydrophopic selective estrogen receptor modulator that is widely used in clinical practice and its pharmacologic properties are well appreciated. Tamoxifen has a large volume of distribution (50L/kg) and a long elimination half-life in mice ($t_{1/2}$= 5-7 days) and humans ($t_{1/2}$=7 days)(106,107). Nevertheless, some authors still insist tamoxifen half-life is only a few hours(108). If tamoxifen metabolites remain active at the time of injury, they may inadvertently mark a different cell type if the promoter becomes

activated in an injury or other experimental perturbation. The long half-life is thought to have confounded lineage tracing experiments in both the pancreas(106) and liver(44).

Tamoxifen also induces considerable cardiac(109) and hepatic toxicity(110) which may alter the biology of the organism. For example, high dose tamoxifen induces the expression of the biliary transcription factor Sox9 in periportal hepatocytes where it is not normally expressed(20). Thus, investigators can end up tracing the fate of two different cell populations simultaneously, which makes it difficult to draw conclusions about lineage relationships(38). The generation of new reporters and imaging techniques recently permitted clonal tracking of putative progenitor populations in the small intestine(111), kidney, lung(69), and liver(44). Bilineage differentiation from well-characterized clonally marked cells is strong evidence of a tissue stem cell and can guard against confounding technical factors.

A growing number of genetic lineage tracing studies have now demonstrated that mature hepatocytes have the potential to convert into biliary ductal cells in cholestatic injuries such as bile duct ligation and DDC injury(112,113). These studies labeled the hepatocyte compartment using cell transplantation or a Cre-expressing AAV virus that only marked hepatocytes. When bile duct ligation or DDC injury was induced, the hepatocyte lineage mark appeared in ductal biliary cells in the ductal reaction. Subsequent work by two independent groups demonstrated that hepatocytes could also be the source of cholangiocarcinoma(13,114), a biliary-

like tumor long though to arise from a bipotential liver stem cell or cholangiocyte(27). These lineage-tracing studies have challenged the interpretation of the liver stem cell hypothesis. But these studies did not fully answer whether the hepatocyte-to-ductal conversion was reversible.

While genetic lineage tracing may remain the gold standard approach, these experiments require careful controls and validation with independent approaches. Curiously, cell lineage tracing in the liver have led to many discrepancies discussed that are not easily resolved (discussed in several recent reviews ((34,51). In short, the Heisenberg uncertainty principle applies just as well to particle physics as *in vivo* lineage tracing: the act of observing alters the reality being observed.

CHAPTER 3: *IN VITRO* ASSAYS TO PROSPECTIVELY ISOLATE PUTATIVE LIVER PROGENITOR CELLS

Chapter summary*

- *The antibody MIC1-1C3 identifies a surface antigen corresponding to the integrin-α3β1 heterodimer*
- *MIC1-1C3+ identifies the clonogenic spheroid forming cells in the liver*
- *A subset of DHIC5-4D9+ ductal cells from the human liver have clonogenic in vitro spheroid forming potential*

In vitro colony forming assays play a critical role in identifying adult stem cells with self-renewal and differentiation capacity. For example, the use of novel antibodies that identify surface proteins coupled with *in vitro* colony forming assays led to the isolation of hematopoietic stem cells(74). To better understand the liver oval cell response, our group previously generated a large panel of monoclonal antibodies that identified cell surface antigens on different constituent cell populations in the mouse liver under injury and homeostasis (59). Subsequently, we adapted this strategy to identify sphere-forming cells from enzyme dispersed human liver cells. More than half my tenure in the Grompe laboratory was dedicated to these projects. In this chapter, I will discuss unpublished work to characterized potential liver stem cell populations using *in vitro* assays.

* Author contributions: Experiments were planned and conducted primarily by B. Tarlow with assistance from C. Dorrell. This work is mostly unpublished . A modified version of Figure 3-1 appeared in the supplemental figures of Dorrell et al 2014(99). Dr. Bin Li in the laboratory has built on this work with subsequent experiments which may be published at a later date.

Surface antigen identification

One particular monoclonal antibody, MIC1-1C3, identified a biliary/ductal population in the murine liver capable of colony formation and modest hepatocytic differentiation potential *in vitro*(61). This antibody also identified pancreatic ductal epithelial cells with colony forming potential (Dorrell, in press). Further functional characterization of this population was slowed because the gene producing the MIC1-1C3 antigen was unknown. Antigen identification is critical to functional characterization of colony forming cells. When the gene is known, one can validate the purity of cell isolation using transcriptional analysis, use genetics approaches to understand the functional significance of the marker gene, or generate transgenic mice to track the fate of the cells *in vivo*.

To explore the identity of the MIC1-1C3 antigen, we took a biochemical approach. Flow-cytometry analysis identified the cell line H2.35, a murine biphenotypic hepatobiliary cell line that strongly expressed the MIC1-1C3 surface antigen. A second cell line HUH7 did not react with MIC1-1C3. Cell lysates were generated from both cell lines and the MIC1-1C3 antibody was used to immunoprecipitate the antigen. An irrelevant antibody MIC0-6B10 was used as a control.

A single unique band of approximately 120 kDa was visualized by coomasie in a acrylamide gel (**Fig. 3-1A**). The band was excised, trypsinized, and analyzed by mass spectrometry. Only two genes were identified that met the criteria of correct size, mouse origin, and known surface expression. 31 total spectra mapped to

mouse integrin-alpha3 (15 unique peptides) and 44 total spectra to mouse integrin-beta1 (28 unique peptides) (**Fig. 3-2B**). The integrin α3β1 heterodimer, also known as VLA3 or CD49c, is reported to migrate as a single band with an apparent mass of 130 kDa in reducing conditions. Itga α3β1 is highly expressed in the H2.35 cell line(115), the liver ductal epithelium, and in ductal progenitors in the developing pancreas.

Expression analysis of MIC1-1C3 sorted liver cells strongly supported Integrin-α3β1 as the correct antigen. *Itga3* was 17.6-fold upregulated in 1C3+ positive FACS sorted primary liver cells compared with 1C3- negative cells (unpaired parametric t-test, n=5, p=0.0046). Similarly, FACS isolated 1C3+ cells from injured liver showed a similar increase in *Itga3* mRNA (12.6-fold, unpaired t-test, n =4, p = 0.0035). Itgb1 is ubiquitously expressed in the liver, including in ductal cells, supporting the plausibility that the MIC1-1C3 monoclonal antibody recognized *Itgb1-Itga3* heterodimers. *Itgb1* was not differentially expressed in 1C3+ compared with 1C3- cells.

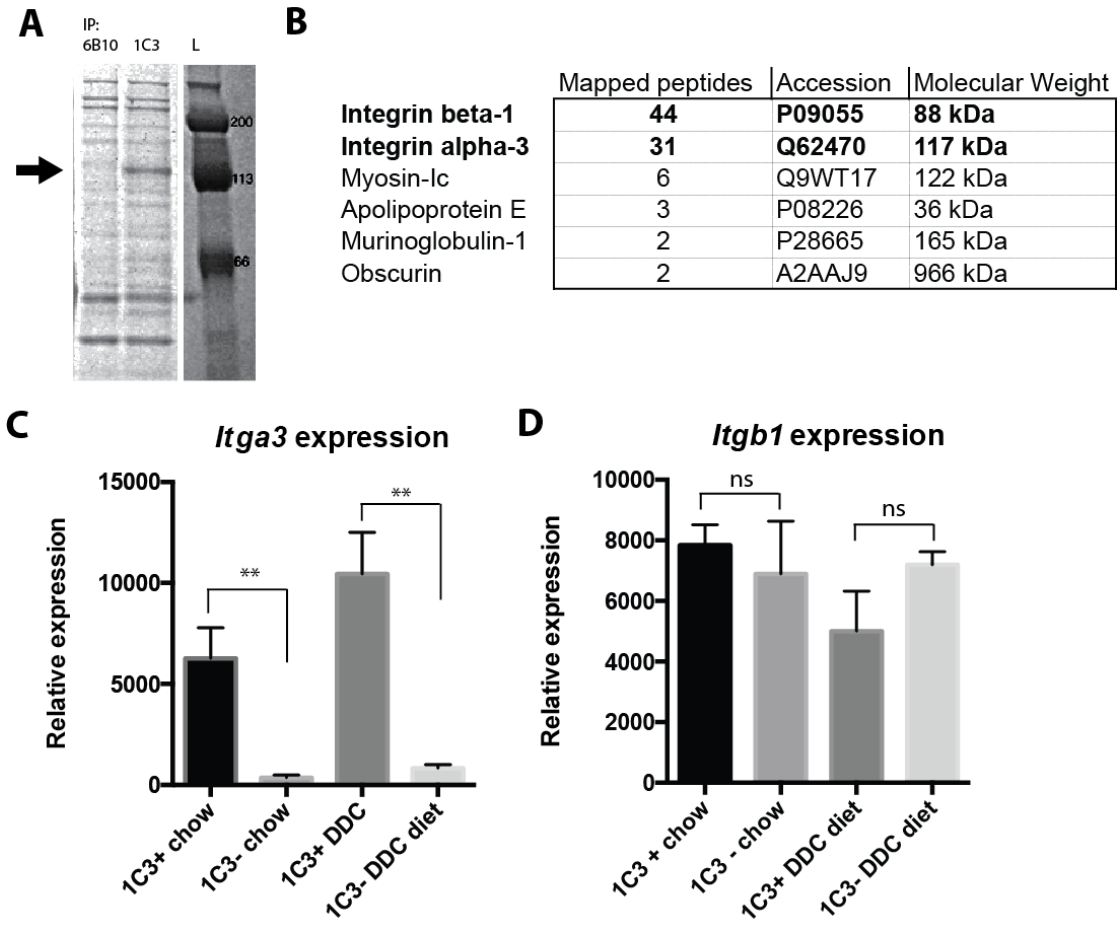

Figure 3-1: Integrin-alpha3 beta1 is the antigen for monoclonal antibody MIC1-1C3
A) Immunoprecipitation with MIC1-1C3 identifies 130kd band under reducing conditions B) band analysis by tandem mass spectrometry identifies two non-contaminant proteins integrin beta-1 and integrin alpha-3 C) FACS isolation of MIC1-1C3^{+} cells from heterogenous liver tissue significantly enriches *Intga3* mRNA but D) not *Itgb1* mRNA.

The identification of the MIC1-1C3 antigen was critical in validating our assays for surface isolation of defined populations in peer-reviewed publications that are described in Chapter 4 and 5. Moreover, a literature review on the function of integrin α3β1 suggested is was a critical mediator of epithelial-to-mesenchymal (EMT) signaling in chronic injury models of another endoderm-derived epithelial tissue(116). EMT-signaling in liver injury developed into major theme of this thesis work (Chapter 5).

Organoid initiation from defined populations

Next, we used FACS-based cell phenotyping to ask whether MIC1-1C3 cells, which formed colonies in a 2-dimensional colony forming assay(61), also accounted for organoid-like colony formation in a novel 3-dimensional matrigel-based *in vitro* system including Fgf10, Egf, Hgf, Wnt3a and Rspo1 growth factors. This novel system allowed for propagation of putative liver, intestinal, and pancreatic epithelial stem/progenitor cells indefinitely (41,117).

To test the hypothesis that liver organoids initiate from MIC1-1C3^{+} CD133^{+} progenitors(61), we dissociated normal liver and enriched for the non-parenchymal cell fraction. Different fractions of FACS isolated cells were then seeded into *in vitro* conditions and allowed to grow for 10 days (**Fig. 3-2A**, n=2). Nearly all spheroids formed from the MIC1-1C3^{+} fraction. The greatest spheroid initiating activity was found in the CD133^{+} CD26^{-} population (8.5-9.5%, n=2; **Fig. 3-2B**). These spheres were self-renewing and could be passaged more than three times. Neither the polyploid hepatocyte fraction nor the antibody negative (MIC1-1C3^{-}, Cd45^{-}, Cd31^{-} population, comprised of portal fibroblasts and stellate cells), showed sphere forming potential above expected contamination rates. FACS isolated MIC1-1C3^{+} cells did not express detectable levels of *Lgr5* at the time of isolation, however, *Lgr5* became highly expressed after 1-week culture (not shown). *Lgr5* is a known Wnt3a target gene, and is transcriptionally activated in high Wnt-conditions(118).

Two potential interpretations exist to explain why only ~9% of MIC1-1C3$^+$ cells are consistently found to form spheroids (n~10). One possibility is that spheroid formation, the clonogenic outgrowth of single cells into >20 cell spheres, is a stochastic event occurring in a homogenous population. A second possibility is that the MIC1-1C3$^+$ CD133$^+$ population is a functionally heterogeneous mixture of clonogenic and non-clonogenic cells. Recent evidence that the sphere forming population can be enriched with additional surface markers may support the latter model (Li and Grompe, *manuscript in preparation).*

In the small intestine, organoids form from single Lgr5+ crypt base columnar cells in high Wnt conditions. Interestingly, the rate of organoid formation was greatly enhanced when Lgr5+ cells were seeded into culture still attached to adjacent paneth cells as a "doublet" event(117). To explore whether liver organoid/spheroid formation was enhanced by a niche-cell, MIC1-1C3$^+$ cells were FACS isolated as either singlet or doublet events and then seeded into matrigel(**Fig 3-2C,D**). Spheroid formation from MIC1-1C3$^+$ doublets was not enhanced when compared with single cells in either high Wnt3a or conditions without added Wnt3a. Thus, no niche cell was found to support organoid formation in the liver. This highlights a key difference between the small intestine and liver.

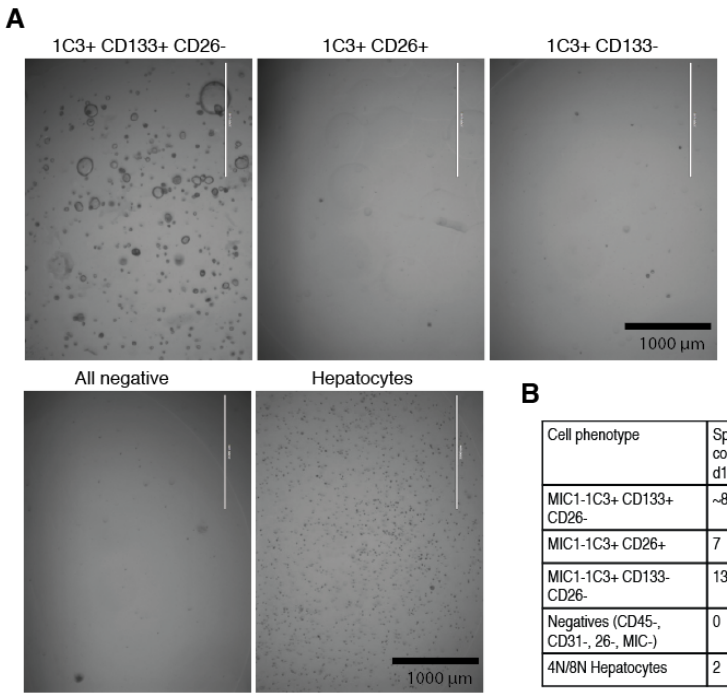

Cell phenotype	Spheroids counted on d10	Sorted cells per droplet	% organoid initiation
MIC1-1C3+ CD133+ CD26-	~860	10,000	**8.5 % - 9.5%**
MIC1-1C3+ CD26+	7	851	**0.8 %**
MIC1-1C3+ CD133- CD26-	13	1100	**1.2 %**
Negatives (CD45-, CD31-, 26-, MIC-)	0	10,000	**0 %**
4N/8N Hepatocytes	2	10,000	**0.02%**

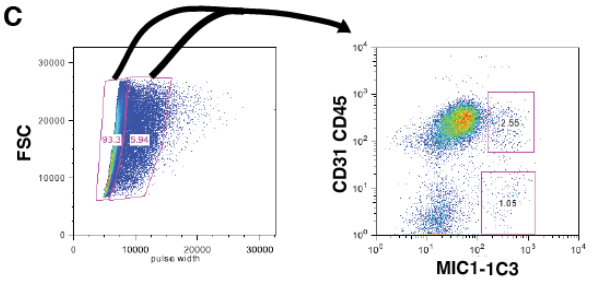

Phenotype	Media	Colony formation efficiency on d10
CD45+ MIC+ doublet	Standard	9.1%
CD45-- MIC+ doublet	Standard	9.7%
MIC1-1C3+ CD133+ singlet	Standard	8.5 - 9.5%

Figure 3-2: MIC1-1C3⁺ cells form self-renewing colonies *in vitro*
A) Five fractions of FACS isolated cells from a normal 8-week old male mouse were seeded into matrigel culture conditions. Spheres greater than 10 cells were counted after 10 days of culture. B) Spheroid/organoid forming capacity was quantified. C) Dissociated liver cells could be divided into single and doublet cells based on the trigger width parameter in FACS analysis, allowing for the isolation of MIC1-1C3⁺ singlet and doublet cells. D) Spheroid/organoid forming rates were similar between different types of doublet events and single cell events.

Defined human ductal epithelial cells form self-renewing spheres *in vitro*

The feasibility of hepatocyte transplantation to correct enzyme deficiency and provide a bridge to liver transplantation has been demonstrated in human trials(119), but this approach is limited by a severe shortage of liver donors and human hepatocytes. Therefore, a long-term aim in the field is to identify alternative sources of hepatocytes that could potentially be useful for cell therapy(73). Initial

reports that adult mouse liver spheroids could differentiate into hepatocytes upon transplantation(41), raised the prospect that a human liver organoids may represent a clinically important source of cells for cell therapy. We hypothesized that human liver progenitor cells could be selectively expanded *in vitro* in a 3-dimensional matrigel culture. The goal of this study was to test the ability to establish long-term cultures of human liver progenitor cells in this defined culture condition. Second, we wished to define surface markers to prospectively isolate human liver organoid forming cells.

To enable fractionation of dispersed human liver tissue by flow cytometry, our lab generated monoclonal antibodies by immunizing mice with dispersed human pancreas or liver cells. Monoclonal antibody clones that reacted with ductal epithelial subsets by immunohistochemistry were further investigated in colony formation assays. Two monoclonal antibodies, DHIC5-4D9 and DHIC2-4A10, recognized a cell population that expressed KRT19^{+} ductal epithelium in cirrhotic human liver sections (Fig 3-3A,B). Interestingly, DHIC5-4D9 but not DHIC2-4A10 identified KRT19^{low} intermediate hepatobiliary cells. KRT19^{low} cells appearing in liver injury are suggested to be an intermediate cell type between hepatocyte and cholangiocyte (see Chapter 5 for further discussion).

Human liver tissues were obtained from patients undergoing surgical resection, liver transplantation, or from cadaveric livers unsuitable for orthotopic transplantation. Cells were dissociated with a 2-step collagenase digestion, depleted

of hepatocytes by gravity centrifugation and stored in UW solution for up to 18 hours prior to analysis. To obtain normal tissue, tissue was taken ~ 2cm or more from tumor. Culture media conditions were similar to previously discussed and included R-spondin1-Fc, hWNT3A, hNoggin, hEGF, hHGF, Nicotinamide, and hFGF10. Media was changed twice per week and cultures were passaged every 10-14 days.

Analysis of FACS sorted human liver cells indicated that 6-12% of DHIC5-4D9+ cells formed spheroids, which is similar to rates observed in mouse liver epithelial cells (**Fig. 3-3C**). Spheroids were initiated from 15/18 patient samples (83%, **Fig. 3-3D,E**) but could only be propagated for more than 5 passages in 7/18 samples (38%). Spheroid initiation was defined as the formation of >10-cell spheres in matrigel when counted on day 10 to 12. Cells were seeded at low density in a semi-solid matrigel matrix and sphere formation was observed. Single cell experiments suggested that spheres were clonal outgrowths rather than cell accumulation (not shown). A single sample was expanded for more than 10 passages over 80 days (**Fig. 3-3F**), demonstrating a potential for exponential expansion for cell therapy applications.

To determine the hepatocyte differentiation potential of human liver organoids, cells were expanded and differentiated towards a hepatocyte fate. Organoids were then transplanted into *Fah*$^{-/-}$ *Rag2*$^{-/-}$ *Il2rg*$^{-/-}$ triple knockout mice to determine if they could differentiate into hepatocytes *in vivo*. 0/29 mice formed detectable Fah+

human hepatocyte nodules after 2-4 months of *in vivo* selection by cycling NTBC, however, trace levels of human genomic DNA were detected (not shown). Further characterization of engrafting cells by other researchers in our laboratory showed that human organoids maintained a ductal phenotype (EpCAM+, human nuclear antigen+) and expressed low levels of albumin by immunofluorescence (Li, Tarlow & Grompe, *manuscript in preparation*).

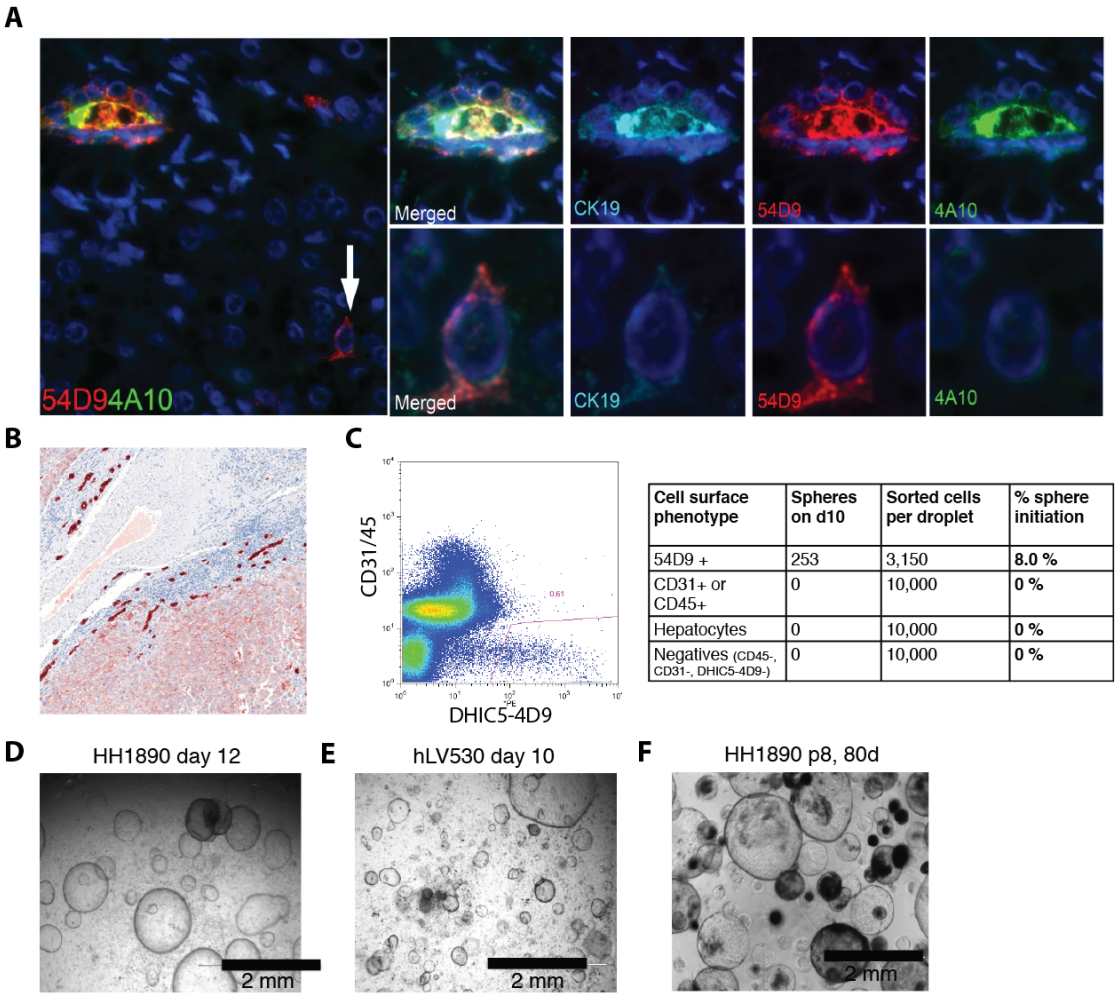

Cell surface phenotype	Spheres on d10	Sorted cells per droplet	% sphere initiation
54D9 +	253	3,150	**8.0 %**
CD31+ or CD45+	0	10,000	**0 %**
Hepatocytes	0	10,000	**0 %**
Negatives (CD45-, CD31-, DHIC5-4D9-)	0	10,000	**0 %**

Figure 3-3: Ductal marker DHIC54D9 identifies spheroid initiating cells
A) Monoclonal antibodies DHIC5-4D9 and DHIC2-4A10 colocalize with ductal marker CK19 in cirrhotic human liver tissue. But only DHIC5-4D9 identifies CK19-low intermediate hepatobiliary cells. B) DHIC5-4D9+ ductal cells surround a cirrhotic nodule in a hepatitis B patient. C) DHIC5-4D9+ isolated by FACS formed colonies in a 3-dimensional *in vitro* colony forming assay. D,E) Large multicellular spheres (~10 – 200 cells) formed by day 12 of culture. F) Multiple cell lines showed extensive proliferative capacity and could be propagated for more than 2 months.

The failure to see organoid-to-hepatocyte differentiation in these studies is not evidence for the absence of a liver progenitor. These results must be interpreted with caution. Many technical factors may have limited our ability to detect hepatocyte-to-duct differentiation. For example, trapping cells in the liver, the first step in engraftment, may be reduced when with smaller diameter cells. Smaller cells can pass through the vasculature and pass directly to the lungs(120). These studies did not administer adenoviral urokinase-plasminogen activator, which may increase hepatic congestion and improve engraftment. Second, mouse organoid-to-hepatocyte differentiation is incomplete *in vitro*, therefore, it may rely on factors provided in the mouse liver to complete the differentiation process. Mouse trophic factors in the recipient may not be sufficient to stimulate donor human ductal progenitor-like to differentiate. Finally, we cannot rule out the possibility that the rare duct-to-hepatocyte differentiation effect observed in mouse organoids (41) occurs through a rare and non-physiologic mechanism that is difficult to identify and is not recapitulated in human cells.

Hepatocytes are maintained in organoid cultures

To further explore the selectivity of the organoid culture system, we performed *in vitro* lineage tracing by separately marking hepatocytes and cholangiocytes with fluorescent proteins. Previously, we established that only cholangiocytes contribute to organoid, however, the fate of hepatocytes in long-term cultures was unknown. One feature of the *Fah*$^{-/-}$ transplantation model is that it allows for the selective repopulation of the mutant animal with fluorescently marked hepatocytes. This

allows for highly specific marking of the hepatocyte compartment but not the ductal progenitors (44,121). In this case hepatocytes were marked with the mTomato+ red fluorescent marker and organoid initiating cholangiocytes were unmarked. In experiments discussed in further detail in Chapter 5, self-renewing spheroids only initiated from the biliary compartment. On no occasion did spheroids form from marked hepatocytes (See Fig. 5-5). Interestingly, organoid cultures initiated from crude preps showed fluorescent marked hepatocytes were observed intercalating in approximately 5% of all spheroids at passage 3 (**Fig. 3-4**). Additional hepatocytes were present in the culture and maintained as small ~20μm diameter cystic structures (**Fig. 3-4B**). Upon dissociation into single cells and subsequent passage, the mTomato+ cells were unable to initiate organoids (not shown). mTomato+ cells were present in culture up to 2 months, or 6 passages, when the experiment was terminated.

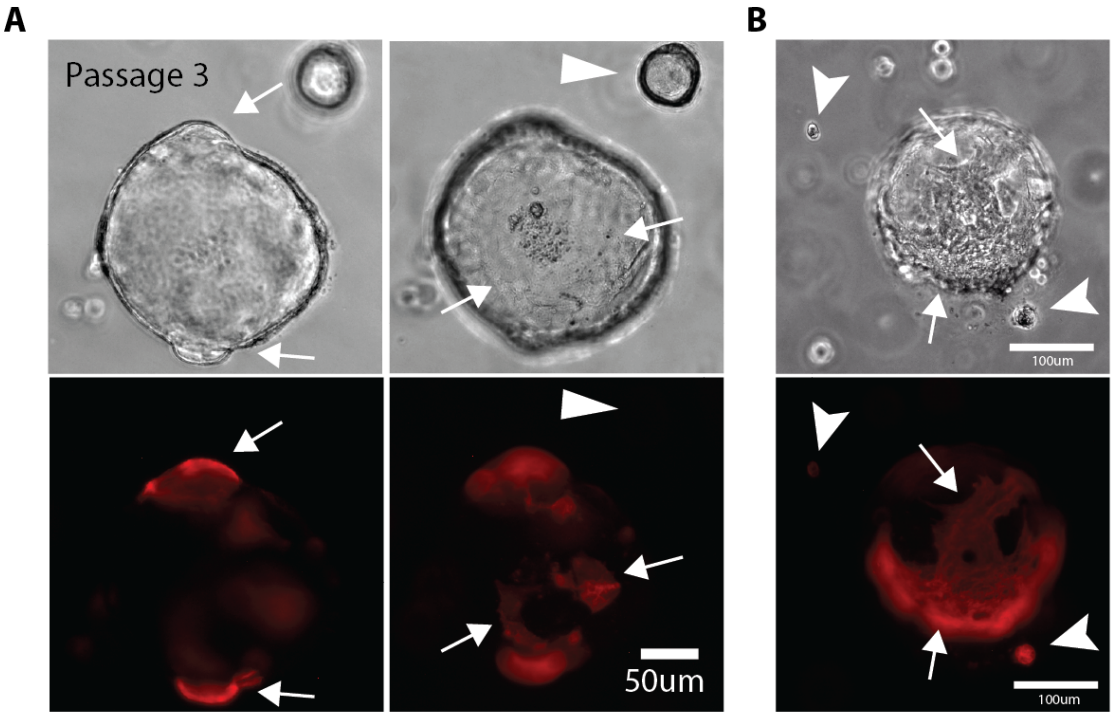

Figure 3-4: Viable hepatocytes are maintained in long-term spheroid/organoid cultures. A) Approximately 1 in 20 organoids initiated from an admixture of unlabeled cholangiocytes and mTomato+ hepatocytes had a mTomato+ cell located in the sphere (arrow). Most spheroids were entirely composed of unlabeled cholangiocytes (arrowhead). B) Areas of hepatocytes incorporation (arrow) had higher granularity. Hepatocytes were also present in culture long-term as cystic structures (arrowhead).

These data indicate that although hepatocytes do not form self-renewing spheroids, they still may be present and viable in a dedifferentiated form after at least 6 passages. These results raise the possibility that low-level heterogeneity in the culture system may read out as a rare hepatocyte differentiation event in transplantation assays.

Discussion

In vitro culture systems are helpful in defining the potential for cell types to both self-renew and differentiate *in vitro*. The development of antibodies to cell-type specific surface antigens are invaluable in the development and characterization of prospective progenitor populations. Fractionating live cells into subsets permits the isolation of functionally defined cells in heterogeneous tissues. These studies demonstrated that ductal cells from the liver of two species had similar colony forming abilities. But rapid expansion *in vitro* in defined cultures or the partial differentiation of one cell phenotype to another may not reflect physiologic properties. Physiologically important cell types, such as mature hepatocytes, have a nearly unlimited self-renewal capacity *in vivo* yet they cannot be expanded *in vitro*(121). Thus, this *in vitro* assay on its own could be erroneously interpreted to say that hepatocytes are neither hepatocyte precursors nor capable of extensive self-renewal.

CHAPTER 4: CLONALLY TRACED SOX9+ CELLS ARE NOT BIPOTENTIAL IN MURINE OVAL CELL INJURY

Chapter summary[†]

- *Sox9-lineage tracing primarily marks ductal cells with low density labeling*
- *Clonal marking rarely identified biliary cell-to-hepatocyte conversion*
- *Hepatocytes themselves generate new hepatocytes in oval cell injury*

Proliferating ducts, termed "oval cells", have long thought to be bipotential, i.e. produce both biliary ducts and hepatocytes during chronic liver injury. The precursor to oval cells is considered to be a facultative liver stem cell (LSC). Recent lineage tracing experiments indicated that the LSC is Sox9+ and can replace the bulk of hepatocyte mass in several settings. However, no clonal relationship between Sox9+ cells and the two epithelial liver lineages was established. We labeled Sox9+ mouse liver cells at low density with a multicolor fluorescent confetti reporter. Organoid formation validated the progenitor activity of the labeled population. Sox9+ cells were traced in multiple oval cell injury models using both histology and FACS. Surprisingly, only rare clones containing both hepatocytes and oval cells were found in any experiment. Quantitative analysis showed that Sox9+ cells contributed only minimally (<1%) to the hepatocyte pool, even in classic oval cell injury models. In contrast, clonally marked mature hepatocytes demonstrated the ability to self-renew in all classic mouse oval cell activation injuries. A hepatocyte chimera model to trace hepatocytes and non-parenchymal cells also demonstrated the prevalence

---

[†] This work published was in, July 2014(44). First author: Branden Tarlow. Additional authors: Milton J. Finegold and Markus Grompe. I acknowledge Leslie Wakefield, Feorillo Galivo, Annelise Haft, Angela Major, Stefanie Kaech Petrie, and Mandy Boyd for their excellent technical assistance. I thank the Oregon Health & Science University for use of the Advanced Light Microscopy Core, Flow Cytometry Core, and Molecular Virology Support Core and the Texas Medical Center Digestive Disease Center Molecular Morphology Core for their services.

of hepatocyte-driven regeneration in mouse oval cell injury models. Conclusion: Sox9+ ductal progenitor cells give rise to clonal oval cell proliferation and bipotential organoids but rarely produce hepatocytes *in vivo*. Hepatocytes themselves are the predominant source of new parenchyma cells in prototypical mouse models of oval cell activation.

Introduction

The proliferation of ductal liver progenitor cells, or "oval cells", is a hallmark of chronic human and experimental liver injuries(23,122,123). In humans oval cells are prominently observed in common forms of chronic liver disease leading to cirrhosis(23). They are thought to provide an alternative path to parenchymal regeneration when hepatocyte replication is blocked(34,122,123). Oval cells are proposed to originate from a quiescent, facultative stem cell anatomically located at the interface between bile ducts and hepatocytes in the "Canal of Hering". However, a debate regarding their precise origin dates back over 50 years(31,83,122-124). In rodent chronic liver injury models, oval cells can differentiate into hepatocytes upon recovery(23,125), transplantation (34,62,83) and *in vitro* differentiation (75,126). Interestingly, phenotypically defined duct-like cells isolated from normal liver do not demonstrate the same efficiency of hepatocyte differentiation, especially in transplantation assays(41,61). Defining the cell of origin responsible for the regeneration of hepatic parenchyma is key to devising pharmacologic strategies to modulate the oval cell response in chronic liver disease and for advancing cell-based liver therapy.

Recent lineage tracing experiments have yielded disparate results in well-studied mouse oval cell activation models (38,39,41,45). Furuyama et al. used a Sox9-IRES-CreERT2 lineage tracing approach and found the Sox9+ biliary compartment contributed the majority of new hepatocytes even during normal liver homeostasis(38). This was further accelerated by injury. Subsequent work by Malato et al. labeled all hepatocytes with Cre-recombinase delivered by adeno-associated virus(45). In contrast to Furuyama, they found that only a small percentage of hepatocytes were derived from non-parenchymal (NPC) precursors and only following certain injuries. A limitation of these and other prior studies (39,41,42) is that the biliary or non-parenchymal compartments were traced en masse, which precludes the identification of clonal relationships between hepatocytes and ductal progenitors. Evidence that tamoxifen can induce "ectopic" expression of ductal markers in hepatocytes (20) and that biliary transcription factors are expressed in normal hepatocytes (10) suggested that a clonal labeling strategy was needed to directly identify the origin of hepatocyte precursor cells in liver repair.

The aim of our study was to use *in vivo* clonal analysis to directly identify bipotential adult liver stem cells and understand their function in injury. We used low density clonal labeling in classic models of oval cell activation to separately track the progeny of adult biliary cells and hepatocytes. As a second approach we used hepatocyte-chimeras generated by transplantation to determine the contribution of NPC in models of oval cell activation. Our results indicate that bipotential hepatic

progenitors of Sox9+ ductal origin do not contribute significantly to hepatocyte replacement even in traditional mouse oval cell injury models. Instead, hepatocytes themselves are the predominant source of new parenchymal cells.

Experimental Procedures

Mice husbandry and Cre-recombination

Sox9-CreERT2 mice(127) were backcrossed 3 generations with C57BL/6 mice and then bred with R26R-Confetti mice(111). Tamoxifen (Sigma) was dissolved in sesame oil (20 mg/ml) and administered intraperitoneally to 4-6 week old mice. Dosing ranged from 8-250mg/kg. As a negative control for recombination, mice were given sesame oil. A two-week washout period was allowed for tamoxifen levels to dissipate prior to starting injuries. For AAV8-Ttr-Cre lineage tracing, heterozygous R26R-Confetti mice were given 2 x 10^{10} viral genomes by retro-orbital injection. Two weeks later, 50-66% partial hepatectomy was performed. Two weeks were allowed for recovery/regeneration prior to injury initiation. The Oregon Health and Science University IACUC approved all animal experiments described.

Hepatocyte transplantation and chimeric *Fah*$^{-/-}$ mice

C57BL/6 *Fah*$^{-/-}$ mice were maintained on 8mg/L NTBC (2-(2- nitro-4-trifluoromethylbenzoyl)-1,3-cyclohexanedione) (Yecuris Corp.) drinking water until 1 day prior to transplant. Primary hepatocytes were freshly isolated by a 2-step collagenase perfusion from Fah-wildtype mice carrying either ROSA26-lacZ or ROSA26-mTomato/mGFP genes. Hepatocytes were enriched by a series of low

speed (1' x 50g) centrifugation steps(77). Then 500,000 live hepatocytes resuspended in 150uL in DMEM/10% FBS/0.5% green food coloring were injected percutaneously into the spleen of *Fah*$^{-/-}$ mice 3-6 weeks of age. *Fah*$^{-/-}$ mice that showed evidence of weight stabilization by 4 weeks were allowed to repopulate for 6 additional weeks before injuries were initiated.

Diets and injury regimens

Mice were maintained on Purina 5015 diet with or without supplementation with 0.1% wt/wt DDC (3,5-diethoxycarbonyl-1,4-dihydrocollidine)(61) (Harlan Laboratories). To induce steatosis, mice were fed a diet deficient in choline (MP Biomedicals)(39,41) supplemented with 0.1% (wt/vol) ethionine water (Sigma) for 3 weeks and allowed to recover for 2 weeks on Purina 5015 before harvest. CCL_4 injury was induced with i.p. injection of 1uL/kg CCL_4 (acute injury; Sigma) or 0.5uL/kg body weight 2 times/week for 5-10 weeks (chronic) and examined 1 week after the last injection CCL_4 (41,45). Control mice were given an equal volume of corn oil vehicle. BrdU was injected 2 hours prior to sacrifice (150mg/kg) or given continuously in drinking water (0.5mg/mL) supplemented with 1% dextrose where indicated.

Immunohistochemistry and imaging

Livers were perfused with cold 4% paraformaldehyde/PBS and post-fixed for 2-6 hours. Tissues were then either cut on a vibrating microtome in 50-100 μm sections or cryopreserved in 25% sucrose/PBS for cryosectioning in 8-10μm sections. Immunohistochemistry was performed on fixed/frozen cryosections with all steps

conducted at 4°C. mCerulean, eYFP, tdimer(RFP), and mTomato were directly detected on a Zeiss LSM780 with similar laser and filter settings as previously described(111). High-level Cre-expression is required to produce nGFP recombination, and was not observed with the doses of tamoxifen used. Primary antibodies (Supplementary Table 1) were detected with AF647-conjugated secondary antibodies (Jackson ImmunoResearch), counterstained with Hoechst 33258, and mounted with Prolong Gold (Invitrogen).

Cell culture

Biliary ducts were isolated by collagenase-based perfusion(61). Isolated ducts were either FACS sorted into single cell suspensions or directly mixed with matrigel, as previously described(41). Organoid cultures were analyzed or passaged after 10-14 days.

FACS sorting and analysis

Hepatocytes and NPCs were isolated with a multiple-step collagenase dissociation and gravity centrifugation protocol as described previously(61). Cells were immunostained for FACS with antibodies listed in the supplementary table. PI was used as a cell viability indicator. Cells were analyzed and sorted with a Cytopeia inFluxV-GS equipped with 405, 488, 561, and 640nm excitation lasers.

Cell Counting and Image analysis

Fluorescent and brightfield mages were captured with Zeiss AxioImager.M2 with Xen Blue 2011 software and a computer controlled motorized stage (Zeiss Inc.). Images were analyzed and scored with ImageJ/FIJI (www.fiji.sc). For analysis of

injured chimeric liver tissue, sections were immunostained for Fah and nuclear counterstained with hemotoxylin or Hoechst 33258. mTomato direct fluorescence was also captured. Multiple high-resolution images were collected and the total numbers of positive and negative hepatocytes were scored from multiple liver lobes and sections from each animal. For clonal AAV8-Ttr-Cre analysis in the R26R-Confetti mouse, direct fluorescence from fluorescent proteins was collected on a LSM780 laser scanning confocal microscope. Stitched z-stack images were collected and colony size was scored from a single 6um optical plane in all treatment groups for consistency. The thin section is may underestimate of hepatocyte cluster size. For hepatocyte clonal analysis, single clones were defined as cells of an identical color combination that were in direct contact with each other. To evaluate the position of AAV8-Ttr-Cre-marked hepatocytes on the portal-central axis liver, 20uM thick fixed-frozen sections were first immunostained for osteopontin (AF647) and counterstained with Hoeschst 33258 to identify portal tracts. Multiple immunofluorescent images were collected from RFP, Opn-647, and Hoeschst channels using a Zeiss Apotome upright microscope outfitted with a (Xen Blue 2011, Carl Zeiss Inc). Images from adjacent fields were stitched together (ImageJ) to approximately 3300 x 2500 micron dimensions. Pixels were converted to micron measurements based on established calibration (1.550px/micron). The distance from the center of the marked cell to the nearest portal vein was measured for each Cre-marked clone (ImageJ).

For Sox9-CreER lineage tracing, 3-color direct fluorescence was collected from 50-100μm thick sections or 10μm sections co-labeled with a ductal marker (Opn or

A6/AF647). After injury clones were scored as single color ductal cells that were at least 5 cells away from another marked cell of the same color.

Assumptions for clonal marking

Based on FACS based analysis of Sox9-CreER R26R-confetti$^{+/-}$ mice treated with 32mg/kg tamoxifen we assumed that 3% cholangiocytes were marked with mCerulean, eYFP, or tdimer-RFP. We did not observe double positive Sox9+ cells when tamoxifen was allowed to washout. We assumed that 20 cholangiocytes were present at each portal triad in a single section in a normal liver at the time of marking. Given our assumptions, we calculated there was greater than an 88% chance that single color cell in a portal triad represented a distinct clone. For hepatocyte clonal analysis, single clones were defined as cells of an identical color that were in direct contact with each other.

Extended tamoxifen recombination

Adult male *Fah*$^{-/-}$ mice were given IP tamoxifen 100mg/kg (dissolved in sesame oil) 7 days or 24 hours prior to intrasplenic hepatocyte transplantation. Sesame oil vehicle was given 24 hours prior. *Fah*$^{-/-}$ mice were maintained on 8mg/L NTBC water until 24 hours prior to transplant when NTBC was permanently discontinued. Then, hepatocytes were isolated from a *ROSA*-$^{CreERT2/mTmG}$ mouse (128,129) by standard collagenase perfusion and gravity centrifugation. The donor mouse also harbored a Scx-GFP (cytoplasmic) transgene that is not expressed in the liver(130). Donor cells were directly injected into the spleen of pre-treated recipient *Fah*$^{-/-}$ mice. Transplanted mice were sacrificed after 7 days and livers, fixed in 4%

paraformaldehyde for 3 hours, cryopreserved in 30% sucrose, and frozen in OCT. 8 µm frozen sections were counterstained with Hoechst 33342 and analyzed on a fluorescent microscope.

For *in vitro* experiments, cells were plated in DMEM/F12 supplemented with 10% FBS, pen/strep, and 10mM Hepes. After cell attachment, tamoxifen citrate (dissolve in ethanol) was added to media overnight at a final concentration of 400nM. Media was then replaced every 2 days thereafter. Cells were imaged 2 or 6 days after tamoxifen administration on a flourescent microscope (Evos, Life Technologies) and images were identically processed with ImageJ.

Statistical analysis

Image quantification graphs and statistical tests results were generated with Prism 6.0b (Graphpad Software, Inc, La Jolla, CA, including histograms, bar graphs, standard error and confidence intervals, and unpaired parametric t-test.

Results

Clonal labeling of ductal progenitors

We hypothesized that clonally marking Sox9+ cells followed by oval cell injury would reveal bipotential clones containing both ducts (self-renewal) and hepatocytes (stem cell differentiation). Towards this end Sox9-CreERT2 R26R-Confetti multi-color stochastic reporter mouse was generated and used to establish the tamoxifen dose suitable for clonal labeling. Recombination of the confetti allele irreversibly turned on one of three mutually exclusive fluorescent proteins. Given that high doses of tamoxifen induces Sox9 expression in hepatocytes (20), we first

sought to determine quantities that would avoid significant levels of hepatocyte marking (**Fig. 4-7**).

With limiting doses of tamoxifen, the Sox9-CreERT2 recombination rate was roughly a linear function of tamoxifen dose, as assessed by immunofluorescence and FACS-based analysis in phenotypically defined MIC1-1C3^{+} ductal progenitor cells (**Fig. 4-1a**)(61). Confetti-marked periportal hepatocytes were readily observed in uninjured animals treated with 250mg/kg tamoxifen and rarely after 125mg/kg tamoxifen. In contrast, hepatocyte marking was undetectable in animals treated with ≤62mg/kg tamoxifen.

In order to verify that low doses of tamoxifen indeed labeled ductal progenitors we applied the organoid formation assay(41). This progenitor assay identifies clonogenic cells with extensive self-renewal capacity that are bipotential *in vitro* and give rise to hepatocytes upon transplantation. Single FACS isolated Sox9-CreERT2 marked cells were seeded into organoid cultures. Organoid initiation was observed at all tamoxifen doses after 10 (**Fig. 4-1b**) or 14 days (**Fig. 4-1c**), demonstrating the stochastic marking of a functionally homogenous population. Organoids were of a single color, confirming they clonally initiated from single cells (**Fig. 4-1c**). The self-renewal potential of Sox9-CreERT2 marked organoids was shown by serial passage (**Fig. 4-1d**). This result establishes that low doses of tamoxifen marked the Sox9+ clonogenic progenitors *in vivo*.

Sox9+ tracing without injury

To determine whether Sox9+ cells are a continuous source of new hepatocytes in homeostasis, labeling was carried out in adult mice without hepatic injury. Adult Sox9-CreERT2 R26R-Confetti mice were injected with either 32 or 125 mg/kg tamoxifen (n=2). On a normal diet clonally labeled (32mg/kg) Sox9+ labeled cells continued to express only the biliary duct markers Sox9, A6, and Osteopontin but never the hepatocyte marker Hnf4a after 3 months (n=500 clones, **Fig 4-1e**) and 6 months (**Fig. 4-8**). When periportal hepatocytes were labeled with high levels of tamoxifen (>125mg/kg), they remained in the periportal location and did not stream or replace the hepatic parenchyma after 3 or 6 months (**Fig. 4-8**).

Sox9+ tracing in CDE induced oval cell injury

Steatotic injury induced by the CDE diet is one of the prototypical and most widely used oval cell induction regimens (38,39,41,42,131). To trace the fate of Sox9+ cells after CDE injury, cells were first marked by recombination followed by a two-week rest period for tamoxifen to dissipate (**Fig. 4-2a**). Mice were then treated according to previously described injury regimens associated with Sox9+/Opn+ progenitor-to-hepatocyte differentiation(39). After 3 weeks of CDE diet followed by a 2-week recovery period, sections were examined for evidence of duct-to-hepatocyte differentiation(39). Prominent ductal proliferation and branching was observed in animals when 2.5-4% of Sox9+ ducts were marked one of three colors each (mCerulean, YFP, or RFP; the total of MIC1-1C3^{+} cells was 8-11%, **Fig. 4-2b**). Unexpectedly, no clones containing both oval cells and hepatocytes were found. In fact, hepatocyte marking was extremely rare. Co-immunohistochemistry with

Hnf4a, A6, Osteopontin, and Sox9 confirmed the progeny of Sox9-Cre marked cells were only biliary cells. 500 Confetti+Opn+ or A6+ clones were scored in multiple sections treated with CDE (**Fig. 4-2c**, n=4 mice). Only a single YFP+ hepatocyte clone was identified adjacent to a portal vein (**Fig. 4-2d**) but adjacent ductal cells were mCerulean+ or RFP+, indicating that the marked hepatocyte was not clonally related to the marked ductal cells.

FACS analysis of single cell dissociated livers was used as a second method to quantify and phenotype Sox9-marked cells. MIC-1C3 is a reliable surface marker for biliary duct cells, including progenitors(61). Conversely, 2F8 is a hepatocyte-specific surface marker(41). Fluorescently marked cells were mostly MIC-1C3 positive, indicating a ductal phenotype. In concordance with the histological results, labeled 2F8+ hepatocytes were rare, comprising less than 0.1% of the total (**Fig. 4-9**). Importantly, FACS sorted Sox9-CreER-Confetti+ cells from CDE injured animals retained their ability to form organoids *in vitro* at all labeling densities (**Fig. 4-10**).

Sox9+ tracing in CCl_4 injury

We next assessed the fate of clonally labeled Sox9+ cells in chronic and acute CCL_4 injury. After five-weeks of chronic CCL_4 injury and a one-week recovery period, livers were examined for evidence of hepatocytic differentiation. In clonal tracing experiments, we found confetti-marked cells continued to co-localize with Opn+/Sox9+ ductal structures but never with Hnf4a+ hepatocytes (n=500 clones, n=3 animals; **Fig. 4-3a**). FACS-based hepatocyte quantification confirmed histologic findings that Sox9-CreERT2 marked hepatocytes were extremely rare after injury

(**Fig. 4-8**). Acute CCl_4 injury tracing produced the similar results (**Fig. 4-11**). Finally, Sox9-CreERT2-Confetti+ cells from CCl_4 injured animals formed organoids *in vitro* at all labeling densities (**Fig. 4-10**).

Sox9+ tracing in DDC induced oval cell proliferation

After Sox9-CreERT2 clonal labeling and a 2-week washout period, mice were given DDC (3,5-diethoxycarbonyl-1,4-dihydrocollidine) for 4 weeks(61,126). Similar to the CDE and CCl4 injury regimens we found that Confetti-marked cells exclusively localized with A6 or Opn+ ductal cells (500 clones, n=3 mice, **Fig. 4-3b**). This indicated that proliferating ducts do not differentiate into hepatocytes in this model.

Generating mice with chimeric livers

We next wished to validate our unexpected findings with a second approach independent of Cre-recombination. Chimeras generated by transplantation have previously been used to track the respective contributions of adult cell types in organ regeneration(79). Our overall approach was similar to the one used by Malato et al by generating animals with genetically marked hepatocytes, followed by oval cell injury(45). As in their study, the goal was to determine whether nonparenchymal precursors (not only ductal cells) would significantly contribute to hepatocyte regeneration following injury.

To obtain a high labeling efficiency of mature hepatocytes, we used the *Fah*-mutant mouse model which allows for the specific and reproducible replacement of >95% of hepatocytes with donor-marked hepatocytes through therapeutic liver

repopulation(77). *Fah*-mutant hepatocytes accumulate toxic metabolites and are unable to proliferate(54). Importantly, the deleterious effects of *Fah*-deficiency and hepatocyte replication arrest are completely reversed by treatment with the small molecule nitisinone (NTBC) (**Fig. 4-16**)(77).

We generated chimeric mice by transplanting syngeneic hepatocytes from ROSA-lacZ or ROSA-mTomato marker strains into recipient *Fah*-mutant mice (**Fig. 4-4a**). Liver repopulation was assessed 10-weeks after transplantation. 95-99.4% of hepatocytes were donor derived as measured by Fah-immunostaining or FACS (**Fig. 4-5b,c**). For histologic analysis, we focused on tissue away from the capsule where donor hepatocyte content consistently was >99% before injury (n=6).

No transplanted donor cells were found to express biliary progenitor markers (CK19/Osteopontin/MIC1-1C3) (>4,500 ducts surveyed, n=3 mice, **Fig. 4-4**) or other non-parenchymal cell markers (**Fig. 4-12**) by immunohistochemistry or FACS. *In vitro* organoid formation showed that all progenitors were host-derived (198/198, n=2 animals) (**Fig. 4-4e**). Because hepatocytes but not non-parenchymal cells were specifically replaced with marked transplanted cells, we proceeded to use chimeric mice to study the non-parenchymal cell compartment in oval cell injuries.

Lineage tracing in hepatocyte chimeras

Current models regarding oval cell response hold that the putative LSC is activated because the hepatocytes themselves cannot regenerate(34). This model predicts that the percentage of hepatocytes derived from non-hepatocyte precursors will

significantly increase at the expense of the disabled donor hepatocytes during oval cell injury. In hepatocyte chimeric animals these cells can be readily identified, because they are of host origin and hence negative for the marker (either lacZ or mTomato). Newly born progenitor derived hepatocytes would be protected from the deleterious effects of *Fah*-deficiency if treated with NTBC (**Fig. 4-13a**). Conversely, new *Fah*$^{-/-}$ hepatocytes would be expected to be functionally impaired if the animal is off NTBC (**Fig. 4-15**). Thus, we hypothesized that only NTBC-treated chimeras would survive the oval cell injury, if progenitor derived new hepatocytes were necessary for survival.

After complete repopulation, chimeric mice were given the CDE diet for 3 weeks with or without NTBC. A control cohort received NTBC alone. After injury, mice recovered for two weeks to permit progenitor differentiation(39). Injury on NTBC therapy (newly born hepatocytes are functional) was associated with only a minimal increase in mean marker-negative host-derived hepatocytes (0.77% ± 0.12%) compared with injury alone (0.67% ± 0.25%, p=0.8) or NTBC alone (0.49% ± 0.11%, p=0.4) (n=3 per group, **Fig 4-5b,c**). Animal survival, body weight, or liver weights were also similar between groups, indicating the small differences between groups were not functionally significant (**Fig. 4-13**). A two-hour BrdU pulse given at the peak of CDE injury showed proliferation of NPC in the portal tract and microvesicular steatosis in hepatocytes(**Fig. 4-5e**). Upon recovery, we detected robust hepatocyte regeneration and proliferation with 2-week continuous BrdU

treatment (**Fig. 4-5f**). Serial section analysis indicated BrdU+ hepatocytes were derived from lineage-marked, mature hepatocytes.

Next, repeated toxic injury with twice-weekly CCL_4 (0.5ul/kg) was given for 10 weeks with or without NTBC. Overall, only 0.24-0.92% of all hepatocytes were of host origin in animals after injury (n=3 per group, **Fig. 4-5b**). NTBC protection during injury produced no significant increase of host-derived hepatocytes (p = 0.18) or global measures of animal health compared with injury alone. BrdU uptake was observed in non-parenchymal cells 72 hours after injury and in donor-marked hepatocytes upon recovery from chronic injury (**Fig. 4-13**).

Finally, we tested whether chimeric *Fah*$^{-/-}$ mice required NTBC to adapt to 5 weeks of DDC injury. As in CCL_4 and CDE injury, putative progenitor-derived mTomato-negative hepatocytes were only rarely found next to proliferating ducts (**Fig. 4-5d**). mTomato negative hepatocytes trended higher in the DDC-plus-NTBC group (1.03% versus 0.62%, p=0.4, **Fig. 4-5b**), but these differences did not effect survival or global measures of liver function (SFig. 7). FACS-based quantification confirmed that NTBC did not increase progenitor-derived hepatocytes compared with injury alone (p=0.88, n=3, **Fig. 4-13**).

Mature hepatocytes self-renew in oval cell injuries

To further test this self-renewal potential of hepatocytes, we examined the clonal dynamics of mature hepatocytes in oval cell injury. R26R-Confetti$^{+/-}$ mice were injected with AAV8-Ttr-Cre to establish sparse, specific hepatocyte labeling (**Fig. 4-**

14). Each allele in a R26R-Confetti$^{+/-}$ mouse randomly recombined to mark cells in one mutually exclusive fluorescent color. This produced 6 observable color patterns due to the sometimes polyploid nature of adult hepatocytes. At baseline, over 95% of marked cells were identifiable as single cells (**Fig. 4-6b**). Two weeks later, partial hepatectomy was performed to eliminate residual rAAV by cell replication. Upon regeneration from partial hepatecomy, we observed either single marked cells or clonally related clusters of two cells, in agreement with others (132). Colonies of hepatocytes were stable as mostly one and two cell clones for up to 6 months (**Fig. 4-6c**).

Next, we induced prototypical chronic liver injuries previously associated with oval cell activation two weeks after recovery from hepatectomy. Mean hepatocyte clone size increased considerably following injury (1.5-4.5 fold, **Fig. 4-6g**), indicating that mature hepatocytes marked prior to injury were an important source of new hepatocytes. In CDE and DDC injuries 20% of surviving hepatocytes were part of a cluster of 5 cells or more (**Fig. 4-14**). After chronic CCl_4 injury, a majority of marked surviving hepatocytes were part of a clone of 10 or more cells.

Discussion

First, our results indicate that Sox9+ precursors do not continuously generate new hepatocytes in normal physiologic conditions, consistent with multiple other reports(20,39,45,50). Even when periportal hepatocytes were marked with Sox9-CreERT2 (high tamoxifen), marked hepatocytes did not continuously replace the parenchyma (38,42)(**Fig. 4-8**). rAAV clonal tracing (**Fig. 4-6**) similarly underscored

the low turnover rate of hepatocytes in normal homeostasis and positional stability along the portal-central axis (**Fig 4-14f**).

Second, our data show that Sox9+ ductal proliferation makes only a minor contribution to parenchymal regeneration in diverse liver injuries. Low-density clonal lineage tracing in oval cell activation injury, showed that Sox9+ cells gave rise to highly proliferative oval cells (20) but we found little evidence that oval cell activation was associated with efficient hepatocyte differentiation. Our results in DDC induced injury are similar to several previous studies (38,39,45,131) but in contrast to other reports (41,61,133). Our findings in CCl4-mediated regeneration are in closer agreement with older studies suggesting CCl4-mediated regeneration is primarily driven by hepatocyte self-renewal (34) and less consistent with a stem-cell based mechanism (38,41,45). We also find little evidence for hepatocytic differentiation of progenitors in the CDE oval cell activation regimen, in contrast to a recent study using Opn-lineage tracing(39).

Given the long half-life of active tamoxifen metabolites in mice ($t_{1/2}$= 5-7 days)(107) and the sensitivity of CreERT2 at low tamoxifen at low levels (**Fig. 4-1a**), it is likely that cre-recombination continues for several half-lives after tamoxifen administration. In fact, we have directly shown that tamoxifen persists in the liver one week after injection (**Fig. 4-17**), the time at which CDE injury was initiated in the Opn lineage tracing study(39). Consistent with our own result, others have found that tamoxifen can persist up to 4 weeks after injection(106). Thus the low

hepatocyte labeling frequency observed by Español-Suñer et al. could be the result of CDE-induced Opn-expression in hepatocytes(134).

Formally, the results raise the possibility that our low-tamoxifen dosing strategy simply failed to mark a hypothetical biphenotypic Sox9^{low} Krt19^{low} resident stem cell. Two experiments argue against this. First, Sox9-CreERT2 marked cells behave functionally similar in an *in vitro* functional assay for progenitor activity regardless of tamoxifen dose, suggesting that high and low doses of tamoxifen label the same population of cells.

Second, in our chimera lineage-tracing experiments, transplantation only replaced mature hepatocytes. Thus, this model system generally tests whether any NPC, such as a Sox9^{low} biliary cell or even a Sox9-negative stellate cell (40), has the capacity to differentiate into hepatocytes. Therefore, it is unlikely that our strategy systematically overlooked a subset of biliary cells. Evidence that Sox9 and other biliary cell genes are expressed in mature hepatocytes (10,20) raises the possibility that the hypothetical Sox9^{low} Krt19^{low} Opn^{low} progenitors are simply injured periportal hepatocytes.

Our chimera experiments further confirmed the scarce contribution of NPC precursors to the hepatocyte pool after oval cell activation. NTBC treatment had no effect on animal survival or global measures of liver function in response to any of the oval cell injury regimens used (**Fig. 4-13**), providing functional evidence that

rescue of a progenitor population was not required for adaptation to these injury models. This result strongly suggested *Fah*$^{+/+}$ donor hepatocytes contribute significantly to liver function and that a newborn progenitor had only a minor contribution in oval cell injury.

Our study assessed liver function by survival, liver size, and animal weight (**Fig. 4-5**, **Fig. 4-13**) as previously described (133,135) but we could have missed other differences detectable by more sensitive synthetic liver function tests (135). Our results do not determine conclusively whether rare marked hepatocytes are a result of stem cell differentiation, transdifferentiation of a biliary progenitor, or direct Sox9-CreERT2-marking of hepatocytes themselves. Our experiments would have readily detected a hepatocytic contribution of 5% or more, the level we deem to have a functional impact in the short term. However, it is important to note that the cumulative effect of progenitor-to-hepatocyte differentiation at a constant low rate could hypothetically reach a functionally significant level over time in long-term chronic injury. Our experiments therefore do not rule out a functionally significant contribution of progenitors in long-term liver injury, such as chronic hepatitis in humans.

The ease of detecting self-renewing hepatocytes—in all injuries—starkly contrasted with the paucity of potential progenitor-derived hepatocytes in Sox9-CreERT2 clonal tracing experiments with the same R26R-Confetti reporter. The distribution AAV8-Ttr-Cre marked hepatocytes clone size indicates that a subset of hepatocytes

divided many times while other hepatocytes did not expand in DDC and CDE injuries.

Continued hepatocyte replication raises the possibility that existing mouse injury regimens are not sufficient to evoke true progenitor activation (34). Due to the lack of lineage tracing tools in other organisms, it is currently unknown whether our results are generalizable to human liver injuries or rats, the organisms in which oval cell progenitors were first described(23,122).

While our study found no difference in the survival of chimeric animals with ducts that lacked hepatocyte potential, cholangiocyte and oval cell proliferation may still be important to overall regeneration. Two recent studies showed that blocking ductal proliferation in DDC injury decreased survival (133,135). Therefore, while ductal proliferation does not provide a significant source of new hepatocytes, expansion of the ductal compartment could instead act as a scaffold for periportal hepatocyte regeneration or by altering hepatocyte gene expression through juxtacrine or paracrine signaling.

Recent reports that mature hepatocytes retain the potential to morph into duct-like cells, raise the possibility that hepatocytes can become Sox9+ after injury and appear similar in morphology and gene expression to cholangiocytes (112,113,136). Our data provide an opening for the hypothesis that hepatocyte-regeneration in chronic injury models is entirely a result of hepatocyte-self renewal and

differentiation of hepatocyte-derived oval cells—rather than activation of a resident facultative stem cell. Future work will be required to characterize the function of hepatocyte subsets in regeneration and develop better models of hepatocyte senescence to study putative progenitors.

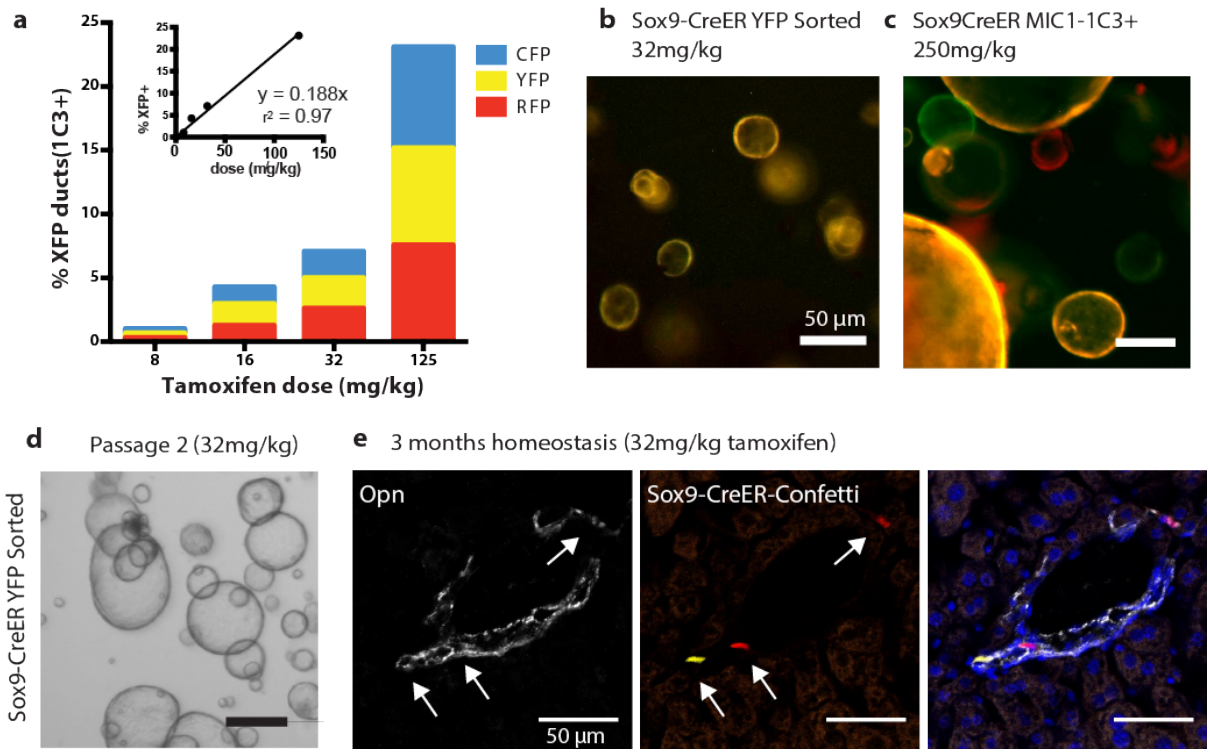

Figure 4-1: Sox9 clonal lineage tracing identifies ductal progenitors but not hepatocytes in homeostasis

(a) Sox9-CreERT2 R26R-Confetti$^{+/-}$ mice dosed with tamoxifen at limiting dilutions produced recombination in ductal progenitor cells (CD45- CD31- MIC1-1C3+) (b) FACS sorted MIC1-1C3+, Sox9-CreERT2 Confetti+ marked single cells initiated self-renewing organoids (YFP sorted) after 10 days culture or (c) 14 days (YFP+, mCerulean+, or RFP+ sorter) (d) Clonally labeled organoids self-renewed after passage. (e) Sox9-CreERT2 clonally marked cells (arrows) continued to express ductal marker Opn after 3 months of homeostasis (scale bars = 50µm).

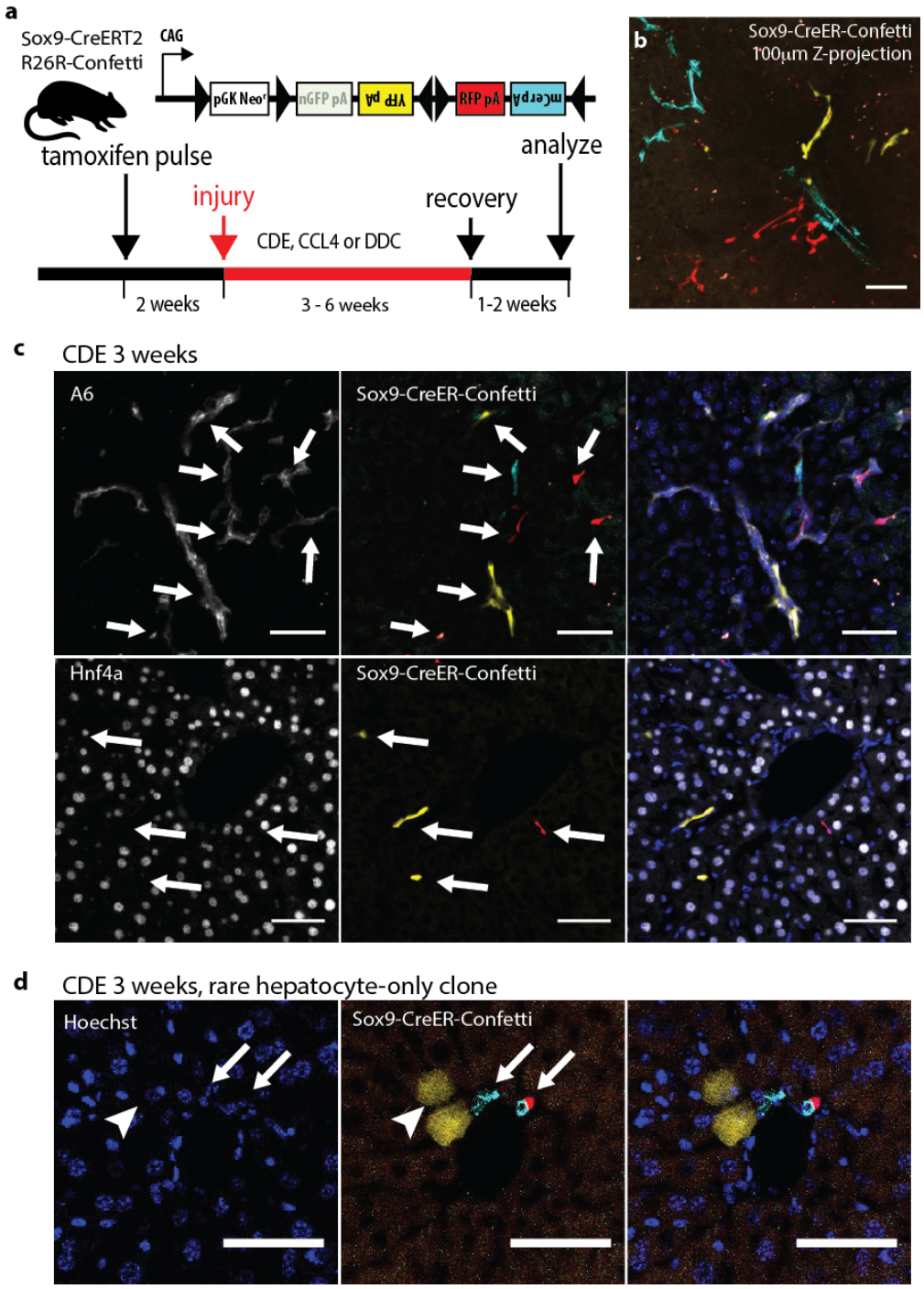

Figure 4-2: Sox9+ ducts rarely give rise to hepatocytes in CDE injury.
(a) Experimental scheme: 4-6 weeks old Sox9-CreERT$_2$ R26R-Confetti$^{+/-}$ mice were given a single dose of tamoxifen followed by oval cell injury two weeks later (b) CDE diet produced ductal proliferation after low density Sox9-labeling. A Z-projection generated from confocal analysis of 100 μ m thick liver section (32mg/kg tamoxifen). Ductal proliferation was not associated with hepatocyte-differentiation (c) Immunostaining for ductal markers A6 (top), Hnf4a (bottom) confirmed Sox9-CreERT2 marked cells (arrows) did not differentiate into hepatocytes after recovery from CDE injury. (d) 2 YFP+ cells with distinct hepatocyte morphology (arrowhead) were adjacent to clonally unrelated mCerulean+ and RFP+ cholangiocytes (arrows). Scale bars = 50μm.

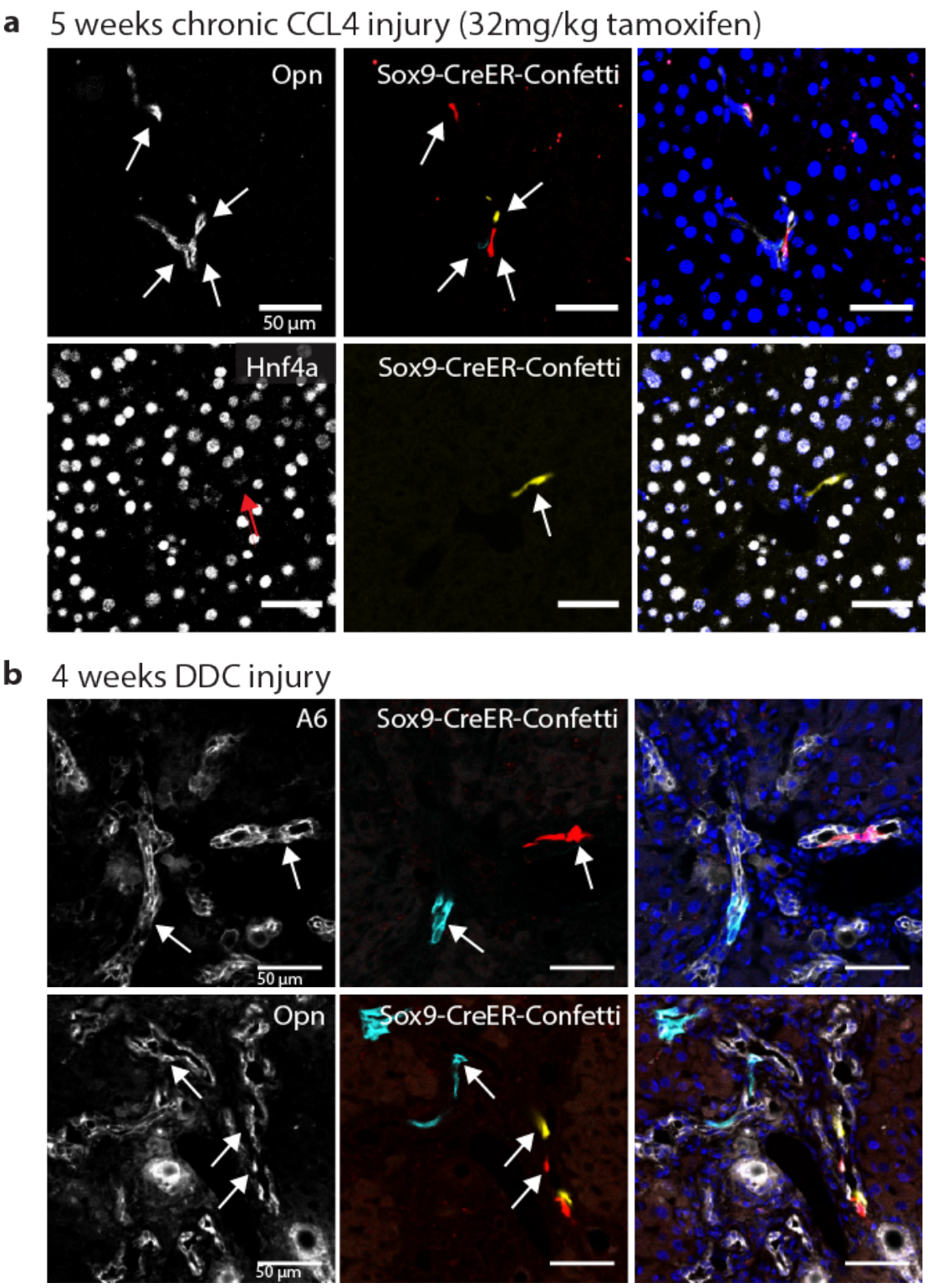

Figure 4-3: Sox9+ ducts do not differentiate into hepatocytes in DDC or CCl_4 injury. (a) Immunofluorescence for ductal marker Opn (top) and hepatocyte marker Hnf4a (bottom) showed Sox9-CreERT2 marked cells (arrows) retained ductal fate after regeneration from 5 weeks CCl_4 injury (arrows indicate a unique clone). (b) Immunofluorescence for ductal markers A6 (top) and Opn (bottom) continued to co-localize with Sox9-CreERT2 marked clones (arrows) after 4 weeks of DDC injury. Scale bars = 50µm.

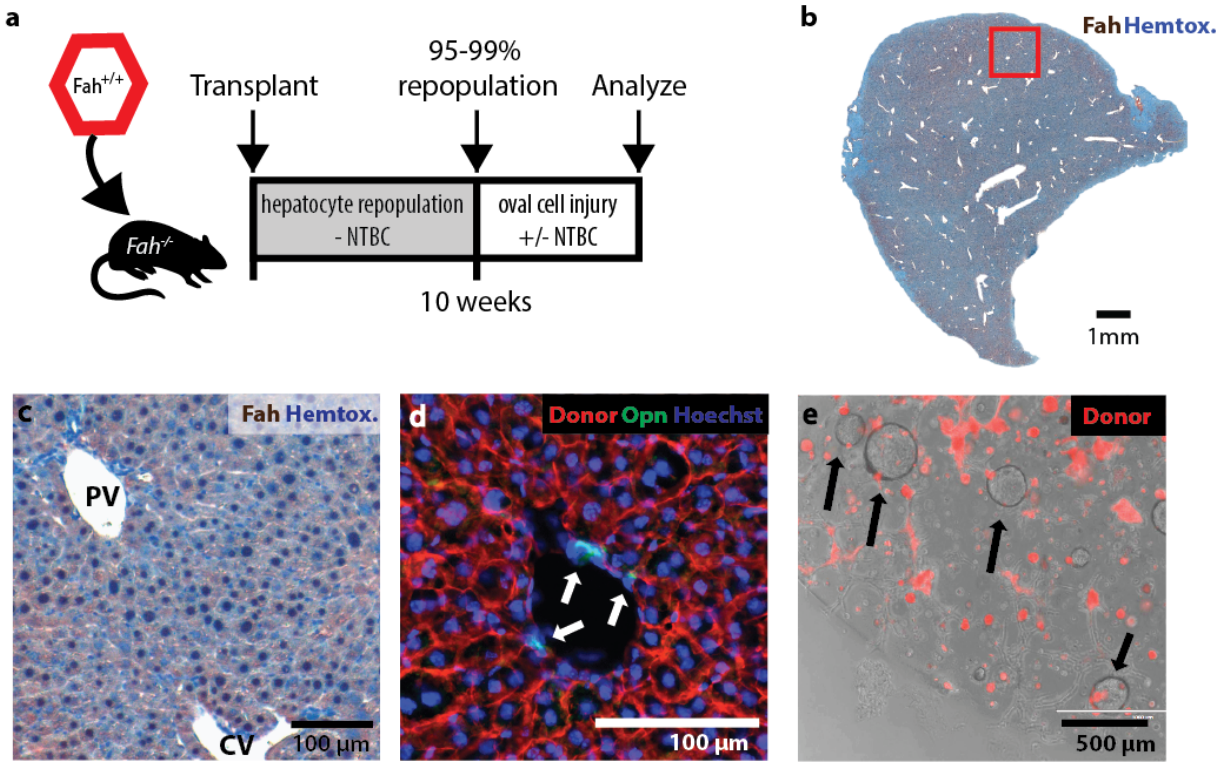

Figure 4-4: Robust and specific replacement of adult hepatocytes but not other cells in Fah-chimeric mice.
(a) Experimental scheme: gravity enriched wildtype or mTomato Fah$^{+/+}$ hepatocytes were transplanted into the spleen of Fah$^{-/-}$ mice and allowed to repopulate (95-99%).
(b) Fah-immunostaining (brown) shows >99% of hepatocytes were donor derived after 10 weeks repopulation (bar = 1mm) (c) Complete central vein (CV) to portal vein (PV) repopulation with donor Fah+ hepatocytes (brown). (d) Donor cell marker (mTomato red) did not colocalize with Osteopontin+ (green) host duct cells. (e) Organoids (arrows) formed from dissociated chimeric liver were host derived (mTomato negative). mTomato+ hepatocytes did not form organoid spheres after 12 days culture.

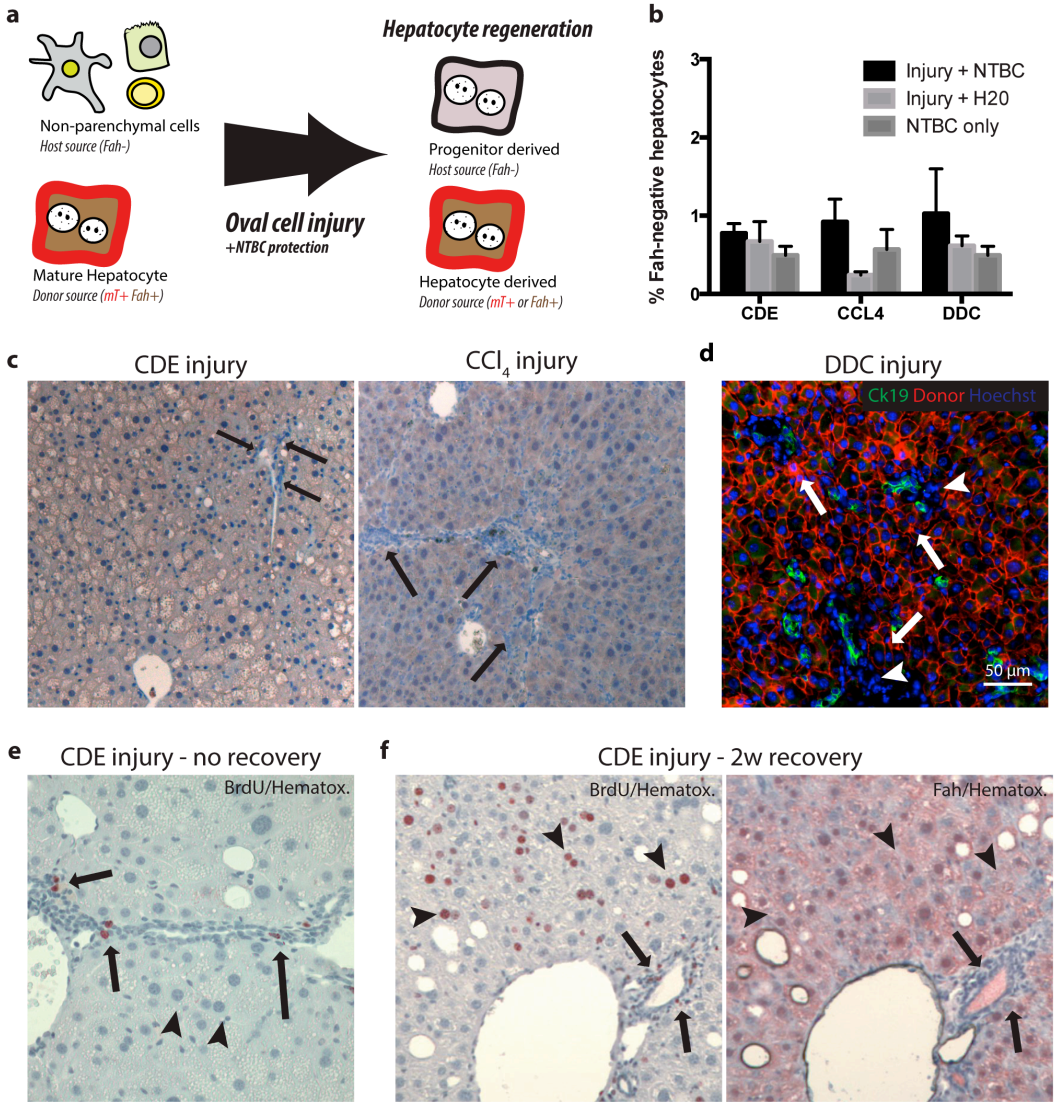

Figure 4-5: Progenitor derived hepatocytes are not required for adaptation to oval cell injury in chimeric mice.

(a) Schematic: Hepatocyte transplantation into *Fah*-/- mice generated chimeric mice, host nonparenchymal cells were *Fah*- and unmarked. Donor hepatocytes were Fah+ and mTomato-marked. If nonparenchymal cells gave rise to hepatocytes after oval cell injury, we hypothesized that progenitor-derived Fah- hepatocytes would displace marked Fah+ hepatocytes. (b) Image quantification of Fah-negative hepatocytes demonstrates approximately 1% of hepatocytes remain host derived after injury. (c) No Fah-negative progenitor derived hepatocytes were observed at the majority portal regions (arrow = ductal proliferation) after 3 weeks CDE injury plus NTBC rescue or 10 weeks CCl_4 injury plus NTBC (arrow = portal inflammation, ductal proliferation but no Fah-hepatocytes). (d) After 4 weeks DDC injury plus NTBC treatment CK19+ (green) ductal proliferations were adjacent to donor mTomato (red) hepatocytes (arrows) and inflammatory nonparenchmal cell (arrowhead, mTomato-negative) (bar=50µm). (e) BrdU uptake (2-hour pulse) was observed in proliferating ductal and nonparenchymal cells (arrow) but not hepatocytes at the peak of CDE injury. Hepatocytes show microvesicular steatosis. (f) BrdU uptake (2 weeks BrdU water) during recovery from CDE injury was observed in hepatocytes (arrowheads), inflammatory cells, and cholangiocytes (arrows). Serial sectioning demonstrates that regenerating hepatocytes are lineage-marked mature hepatocytes (Fah+) and not derived from a nonparenchymal progenitor (Fah-).

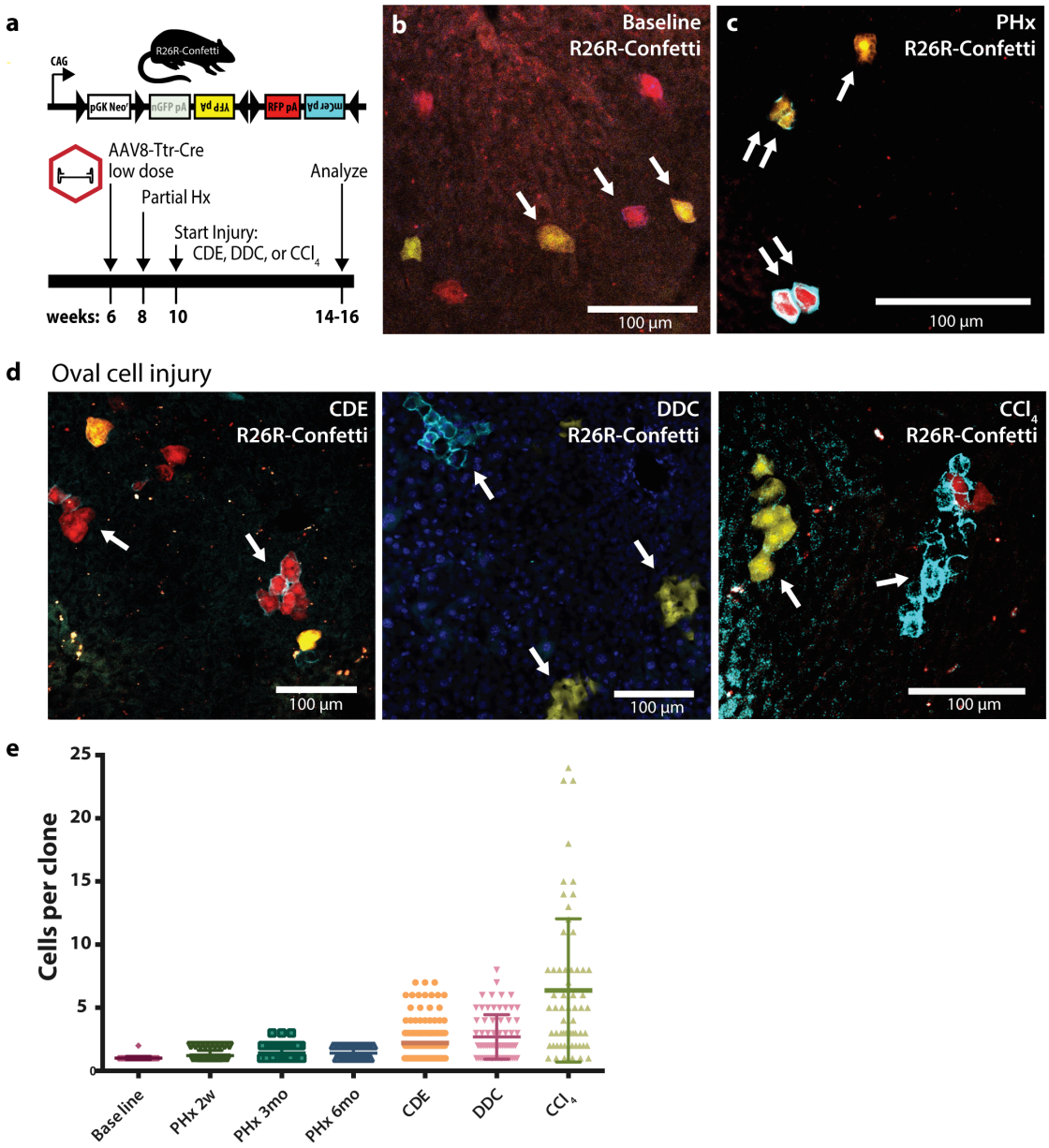

Figure 4-6: Mature hepatocytes self-renew in oval cell injuries
(a) Experimental scheme: Hepatocytes were marked at low density in heterozygous R26R-Confetti$^{+/-}$ mice using low dose rAAV8-Ttr-Cre. Partial hepatectomy was performed and injuries were initiated after complete regeneration. (b) Prior to hepatectomy single hepatocytes were marked. (c) Partial hepatectomy induced hepatocyte replication producing clones of 1 (single arrow) or two identically marked cells (double arrow). (d) Oval cell injury with CDE diet, DDC diet, or chronic carbon tetrachloride induced mature hepatocyte replication and self-renewal or clonal expansion. (e) Dot plot histogram of mature hepatocyte colony size at baseline, partial hepatectomy followed by 2 weeks to 6 months homeostasis, and after oval cell injury (line = mean ± SD). Scale bars = 100µm.

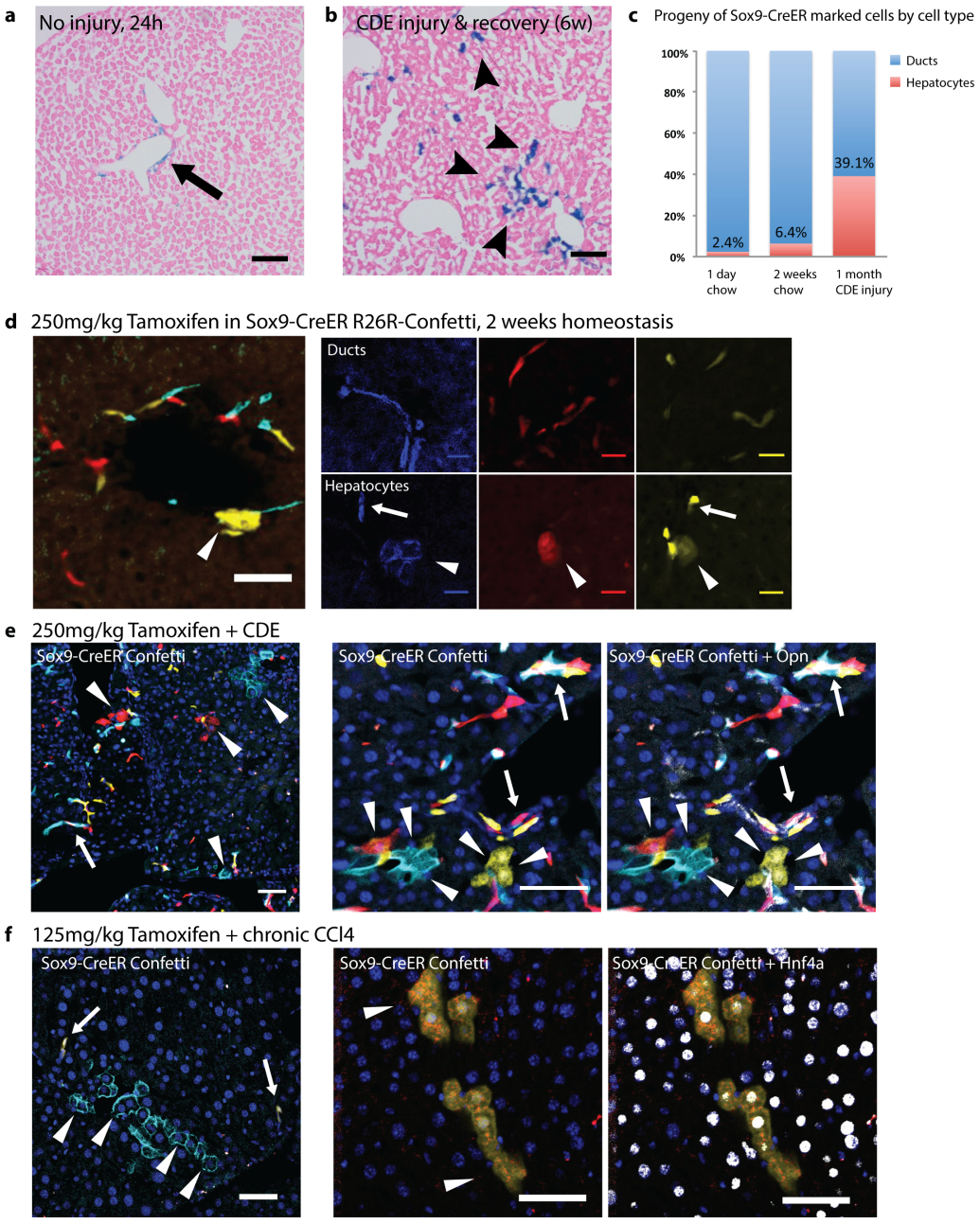

Figure 4-7: Sox9-CreERT2 marks hepatocytes with high tamoxifen doses.
Recombination was induced in Sox9-CreERT2 R26R-lacZ mice with 250mg/kg tamoxifen. Mice were examined (a) after 24 hours normal chow or (b) after prototypical steatosis injury that included a 1-week rest period, 3 weeks choline-deficient, ethionine supplemented diet, and a 2 week recovery period. (c) Quantification of Sox9-CreERT2 marked cells by epithelial cell type after normal chow or CDE injury recreates the increase in marked hepatocytes after injury previously reported in the literature. (d) 250mg/kg tamoxifen induced recombination Sox9-CreERT2 R26R-confetti recombination in both hepatocytes and ducts. Hepatocytes and ducts were identified in each of three Confetti colors (mCerulean, RFP, and YFP). (e) High dose tamoxifen tracing in Sox9-CreERT2 R26R-Confetti mice injured with CDE for 3 weeks and a 1-week recovery results in marked hepatocytes (arrow head) and Opn+ ductal cells (arrow). (f) High dose tamoxifen tracing in Sox9-CreERT2 R26R-Confetti in mice injured with repeated CCl4 administration results in marked HNF4a+ hepatocytes (arrowhead) and ductal cells (arrow).

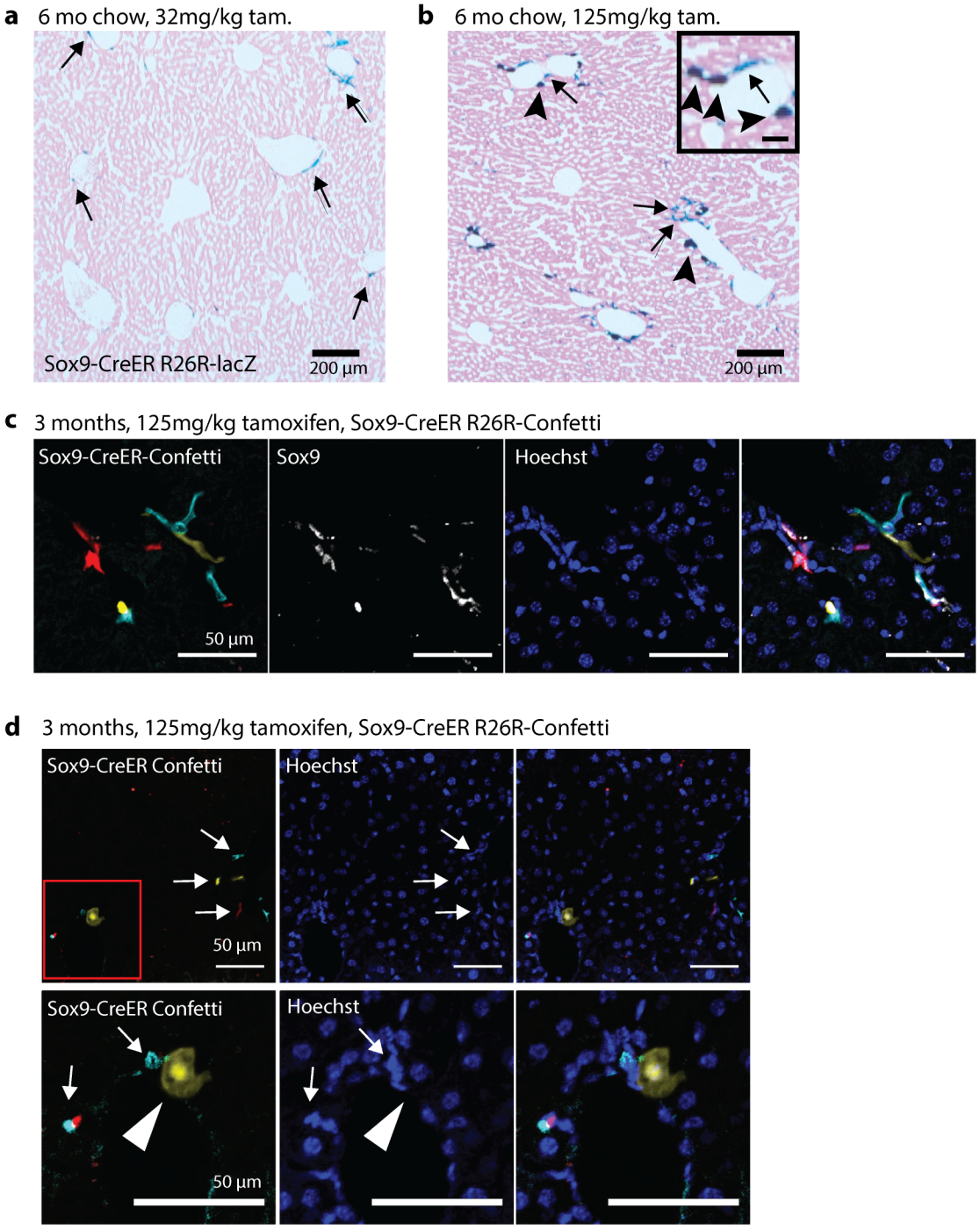

Figure 4-8: Sox9-CreERT2 marked ducts and periportal hepatocytes do not continuously "stream" in homeostasis

Sox9-CreERT2 R26R-lacZ mice were treated with (a) 32mg/kg tamoxifen or (b) 125mg/kg tamoxifen and maintained on normal chow for 6 months. Marked ducts (arrows) or periportal hepatocytes (arrowheads) did not progressively replace the bulk of the hepatocyte mass (bar = 200 µm, inset bar = 50µm). (c) Recombination in Sox9-CreERT2 R26R-Confetti mice treated with 125mg/kg tamoxifen showed recombination primarily in Sox9+ cells that did not give rise to hepatocytes after 3 months homeostasis. (d) Rare perioportal hepatocyte (arrowhead) maintained a periportal position and did not proliferate or replace the bulk of hepatocytes after 3 months homeostasis.

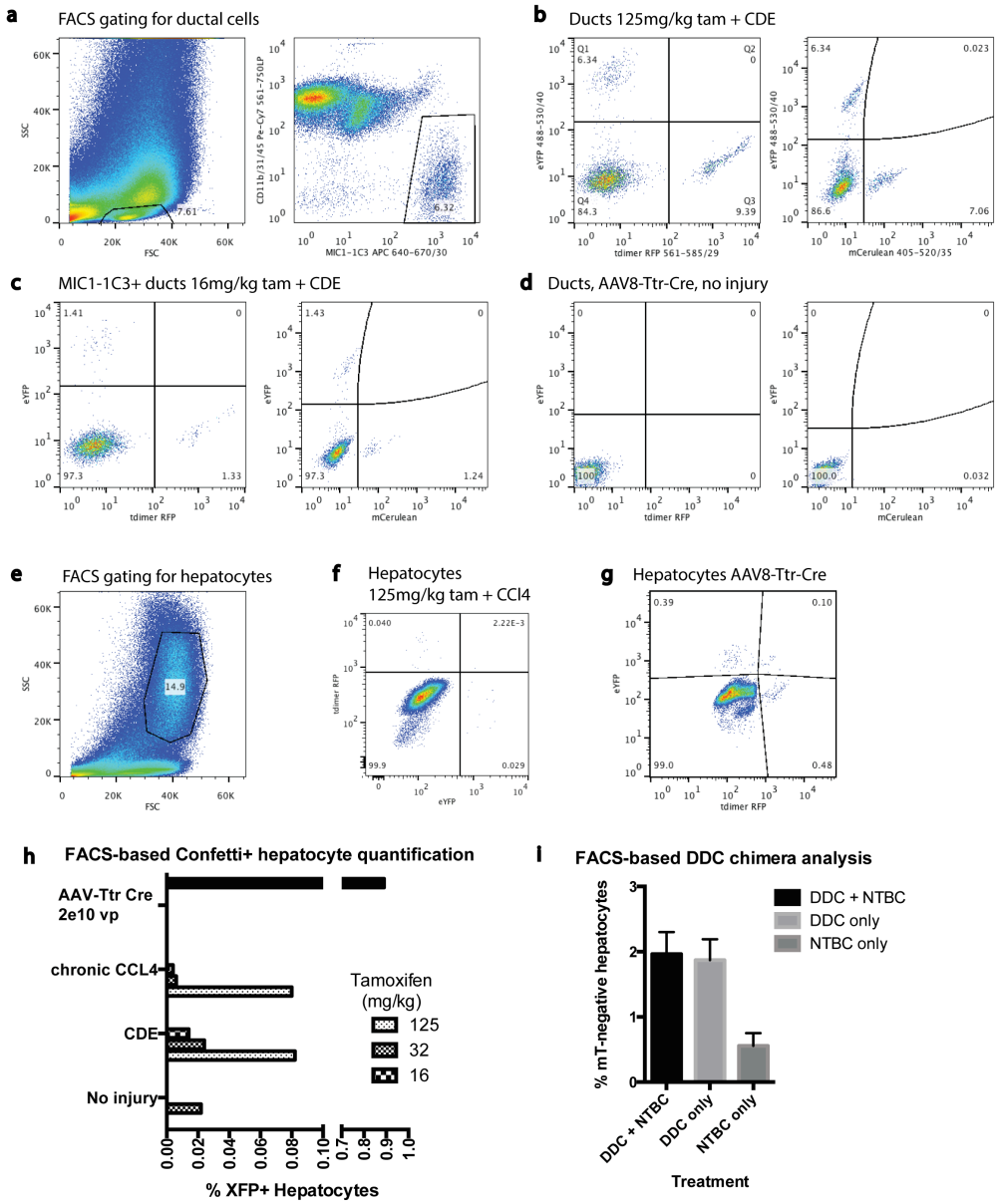

Figure 4-9: FACS-based analysis of Cre-marked Confetti cells

(a) Single-cell suspensions of liver nonparenchymal cells were FACS sorted with the following gating strategy to identify biliary progenitors. Gates were FSC/SSC, low trigger pulse width (not shown), propridium iodide negative (live cells, not shown), followed by MIC1-1C3+ Cd31- Cd45- Cd11b-. (b) MIC1-1C3 cells were then scored based on eYFP, mCerulean, and tdimer RFP status in a mouse treated with CDE and 125mg/kg tamoxifen (c) or CDE and 16mg/kg tamoxifen. (d) MIC1-1C3 ductal cells were unmarked in AAV-Ttr-Cre treated Confetti mice (and sesame oil treated Sox9-CreERT2 R26R-Confetti mice). (e) Gravity enriched hepatocytes were identified based on FSC/SSC and were PI-, OC2-2F8+, Cd31-, Cd45-. (f) Hepatocytes were interrogated for eYFP and tdimer RFP in injured Sox9-CreERT2 R26R-Confetti animals and (g) virally marked AAV8-Ttr-Cre marked hepatocytes (1-3% marked). (h) FACS-based quantification of Sox9-CreERT2 R26R-Confetti marked hepatocytes confirmed they were rare. (i) FACS-based analysis was used to confirm image based scoring of chimeric *Fah*$^{-/-}$ mice mTomato hepatocyte chimeras. The percentage of host mT-negative hepatocytes were plotted for each of three groups (mean± SEM, n=3 per group).

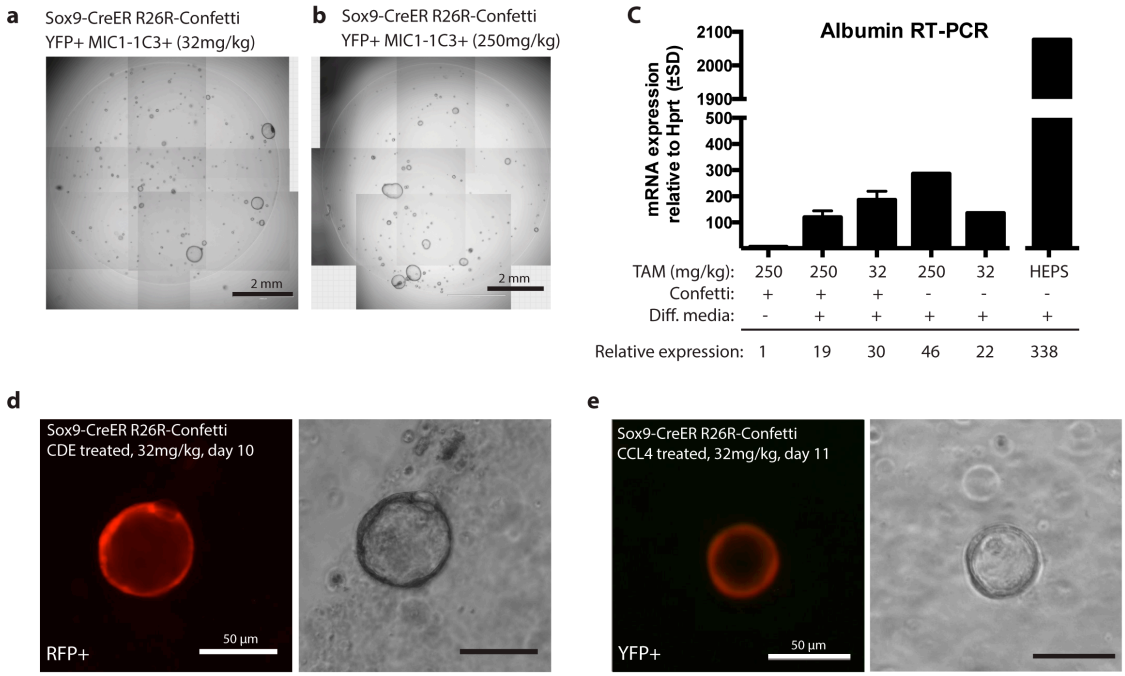

Figure 4-10: Sox9-CreERT2 marks phenotypically defined MIC1-1C3+ cells that form liver organoids.

Non-parenchymal liver cells from Sox9-CreERT2 R26R-Confetti FACS were FACS sorted (YFP+ MIC1-1C3+ CD31- CD45- CD11b-) and seeded into organoid culture conditions. Organoids formed from YFP+ cells at equivalent rates in mice treated with (a) 32mg/kg or (b) 250mg/kg tamoxifen after 12 days culture. (c) Albumin mRNA expression in confetti+ MIC1-1C3+ CD31- CD45- CD11b- marked with high (250mg/kg) or low tamoxifen (32mg/kg) and differentiated towards a hepatic fate. (d) Clonally labeled ducts formed organoids retained the ability to form organoids *in vitro* after injury with CDE diet or (e) chronic CCl_4 injury.

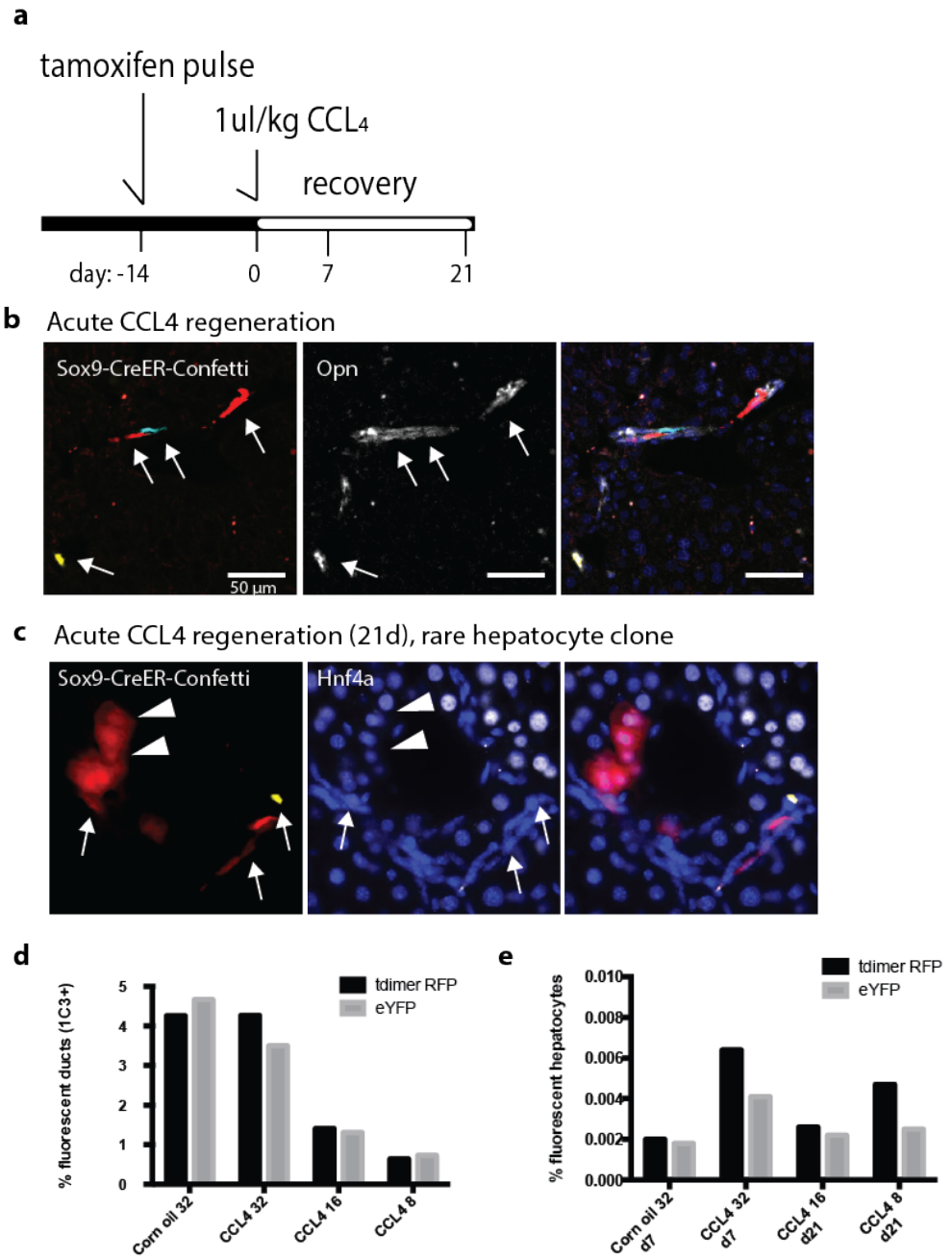

Figure 4-11: Sox9+ ducts rarely give rise to hepatocytes in acute CCl_4 injury
(a) Scheme for acute CCl_4 tracing: Sox9-CreERT2 R26R-Confetti$^{+/-}$ mice were given a single acute toxic injury (1ul/kg CCl_4) (b) 21 days recovery after injury, most Sox9-CreERT2 marked cells (arrows) co-localized with ductal marker Opn (arrow = unique clone). (c) A single RFP+ Hnf4a+ cluster of Sox9-CreERT2 marked hepatocytes (arrow head) adjacent to a cell with a ductal Hnf4a- ductal cell is suggestive of a clonal relationship. (d) FACS quantification of Sox9-CreERT2 marked cells after acute CCl_4 regeneration in phenotypically defined biliary cells (MIC1-1C3+) where approximately 4% of ducts are marked RFP or YFP+ with 32mg/kg tamoxifen. (e) OC2-2F8+ hepatocyte fractions show regeneration following CCl_4 injury is associated with a 2.5-fold increase marked hepatocytes compared with in corn oil only. Less than 0.01% of hepatocytes were Confetti marked.

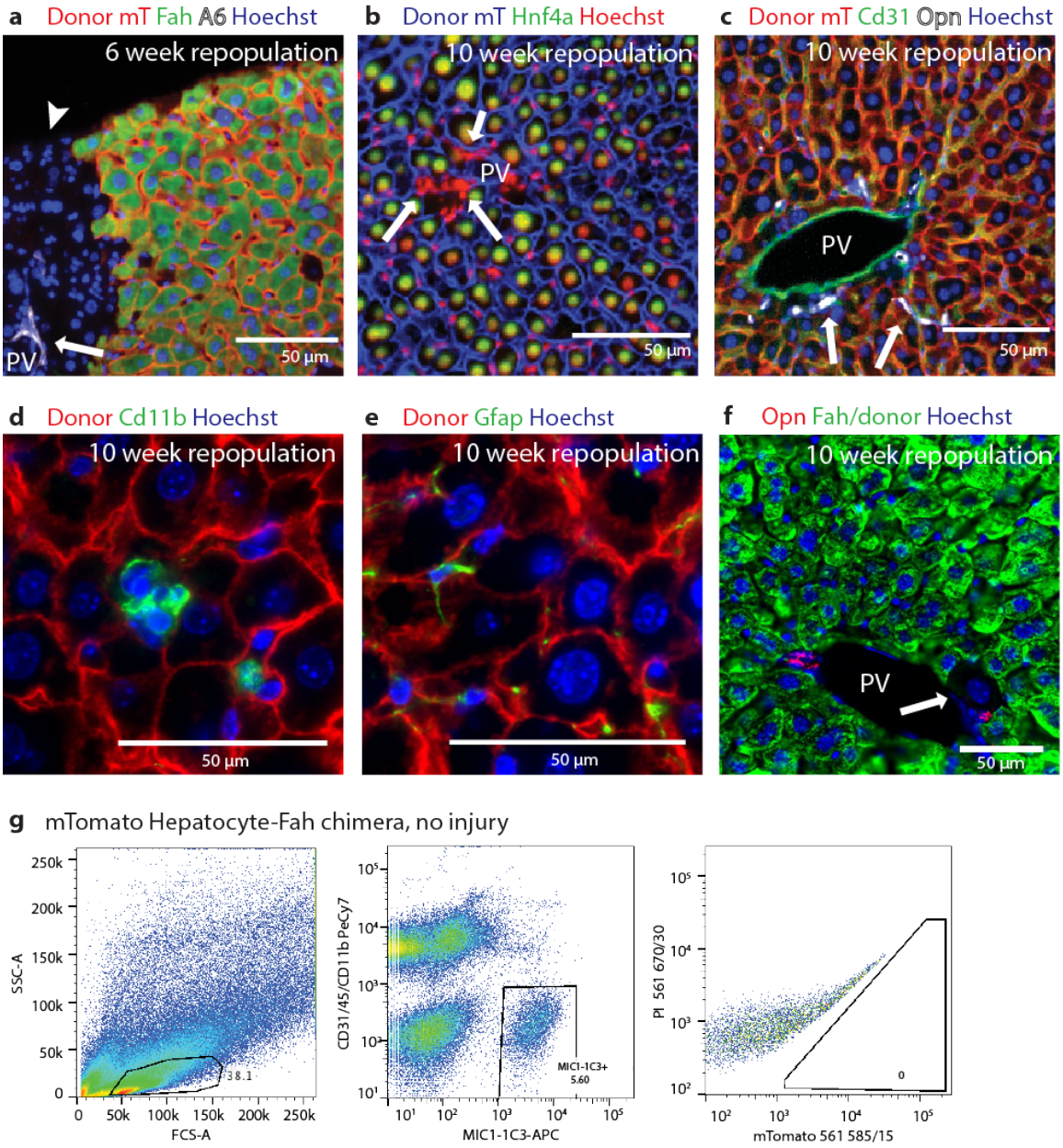

Figure 4-12: Hepatocyte transplantation into Fah-/- mice specifically replaced hepatocytes but not other cell types.

(a) 6 weeks after transplant with mTomato (red) marked mature donor hepatocytes, donor cells express hepatocyte marker Fah (green), but not duct marker A6 (white), demonstrating the detection of Fah-negative mTomato-negative host hepatocytes near the capsule (arrowhead), (bar = 50 µm). (b) mTomato donor marker (blue) surrounds Hnf4a+ hepatocytes (green) but not nonparenchymal cells nuclei (Hoescht only = red) c) CD31+ endothelium large vessels and sinusoids (d) CD11b+ mononuclear cells, and (e) GFAP+ stellate cells, and do not localize with mTomato, indicating these nonparenchymal cells are of host origin. (f) Fah immunostaining (green) shows donor hepatocyte repopulation was near complete but some *Fah*$^{-/-}$ hepatocytes (arrow) were retained in the periportal region adjacent to Opn+ cells (g) FACS-based analysis mTomato repopulated chimeric animals indicated no ductal cells were donor derived (0/4308 MIC1-1C3+).

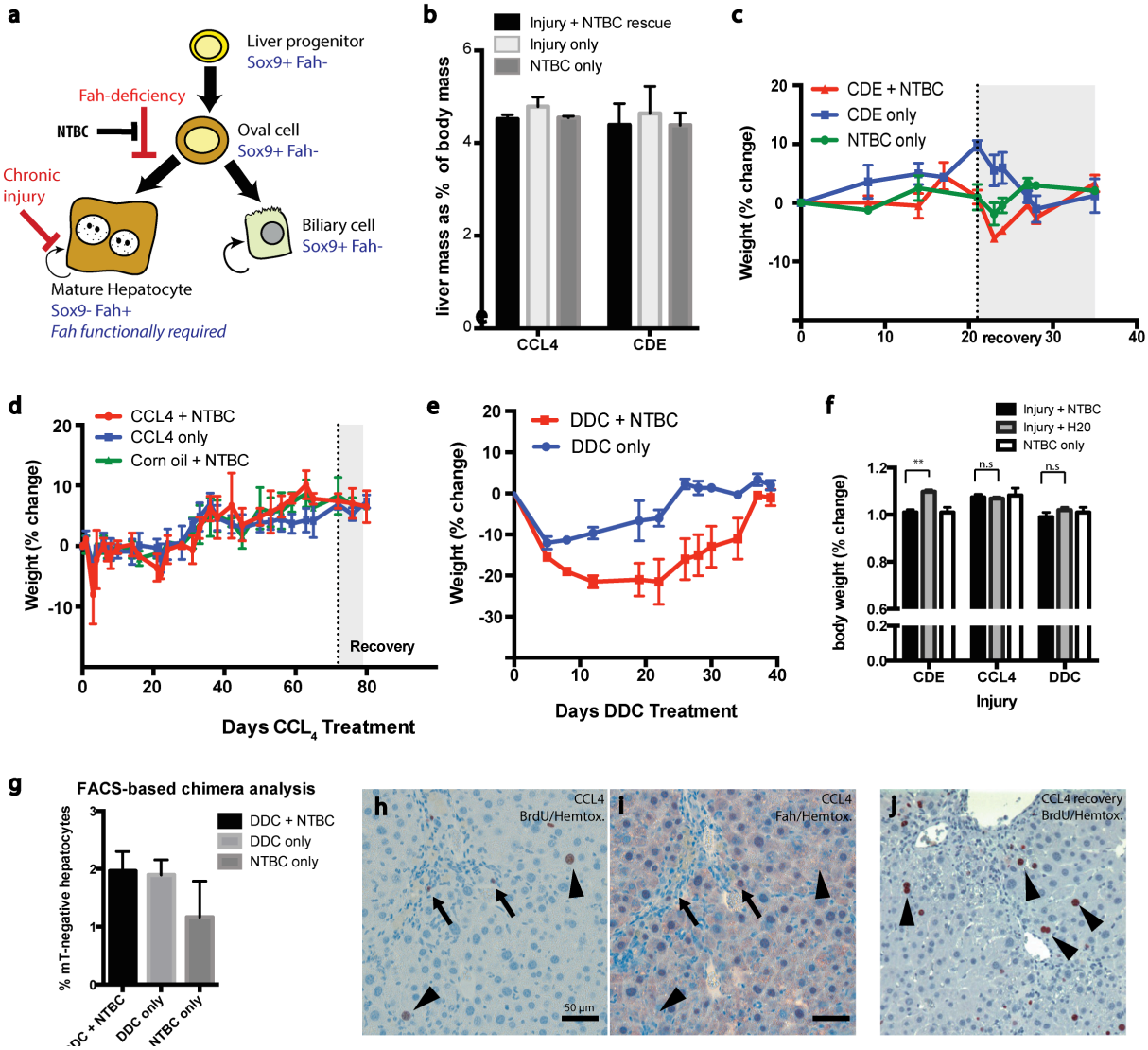

Figure 4-13: Chimeric Fah mice treated with DDC and CDE do not require NTBC (a) Schematic for testing the function of new progenitor derived hepatocytes in chimeric mice. Biliary and nonparenchymal cells are Fah-deficient. Fah-mutant hepatocyte require treatment with compound NTBC for normal survival. The liver stem cell model predicted NTBC rescue of progenitor-derived hepatocytes would be necessary for regeneration in when hepatocyte replication was disabled in oval cell/chronic injury. (b) Liver weights as a percentage of body weight were measured in chimeric animals treated with 10 weeks CCl_4 injury with 1 week recovery or 3 weeks CDE. NTBC rescue of putative progenitor-derived hepatocytes was not required for chimeric animal survival or to maintain global measures of liver function such as body weight. (c) Body weight changes in chimeras treated with CDE injury (±NTBC) or NTBC only (d) chronic CCl_4 injury and (e) DDC injury. (f) Quantification of body weight changes in cohorts of chimeric animals at the peak of oval cell injury. (g) FACS-based quantification of mTomato-negative hepatocytes in chimeras after DDC injury (n=3 per group). (h) Chimeric mice recovering from chronic CCl_4 injury (2 hour BrdU pulse) showed BrdU incorporation in both host portal non-parenchymal cells (arrow) and hepatocytes (arrowhead). (i) Fah-immunohistochemistry in serial sections showed replicating hepatocytes (arrowhead) to be donor derived mature hepatocytes. (j) BrdU+ hepatocytes (arrowhead) marked after 1 week BrdU administration in the recovery period following 10 weeks CCl_4 . (k) Hepatocyte BrdU incorporation (2 hour pulse) in uninjured chimeras was observed in ~1 in 25 high-powered fields.

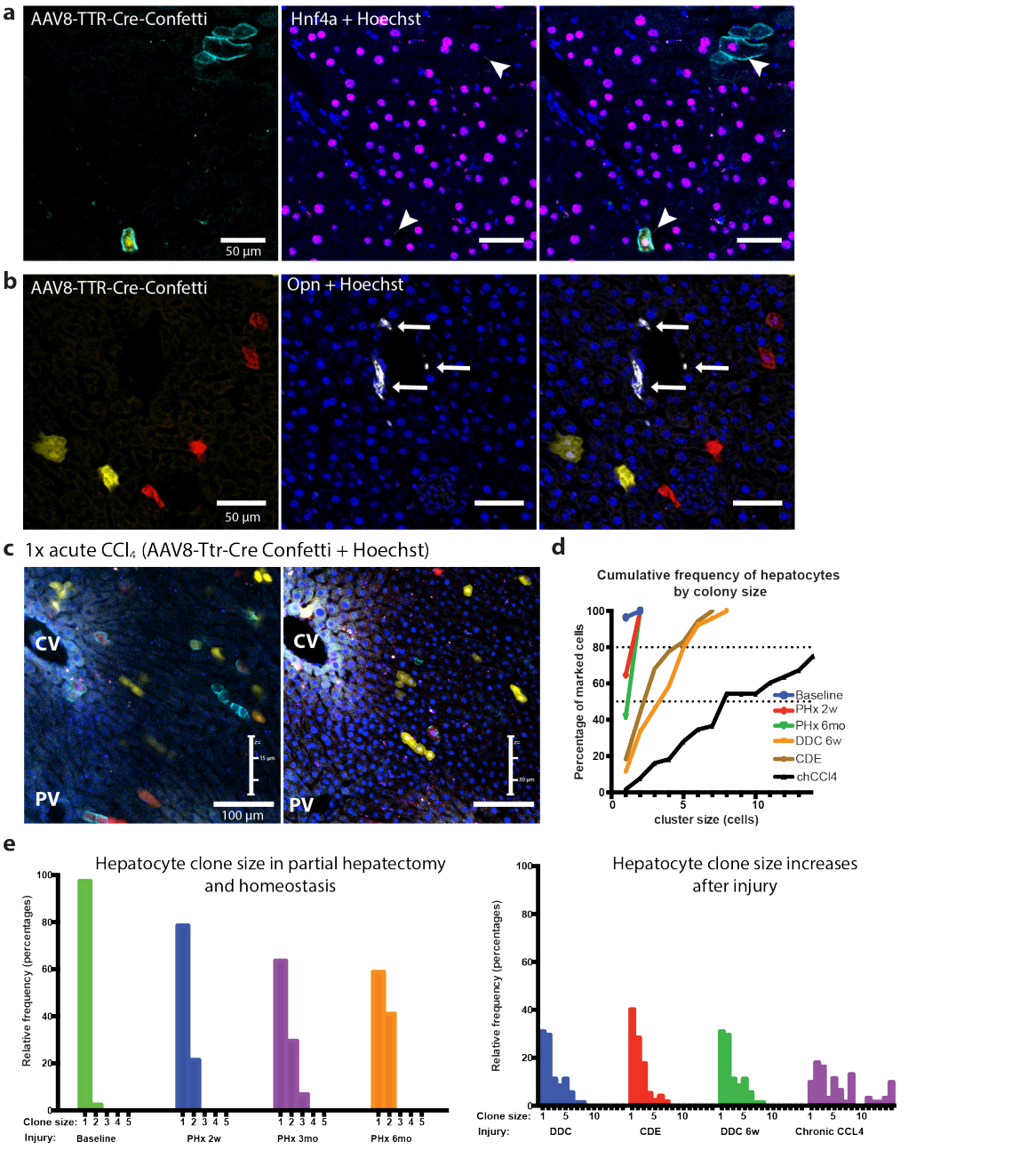

Figure 4-14: AAV8-Ttr-Cre specificity and hepatocyte clonal dynamics. AAV8-Ttr-Cre induced recombination in R26R-Confetti+/- mice specifically in (a) Hnf4a+ hepatocytes but not (b) Osteopontin+ ducts. (c) Confetti marked clones after acute CCl4 (1ul/kg) mediated pericentral hepatocyte injury and 21 days regeneration (d) The cumulative percentage of clonally marked hepatocytes that are part of a large cluster increases following injury, demonstrating that mature hepatocytes are a common source of new hepatocytes. (e) Histogram representation of hepatocyte colony size following regeneration. (f) Distance of each Confetti marked clone to the nearest portal vein was measured at baseline (n=4) and after 3 or more months of homeostasis (n=2).

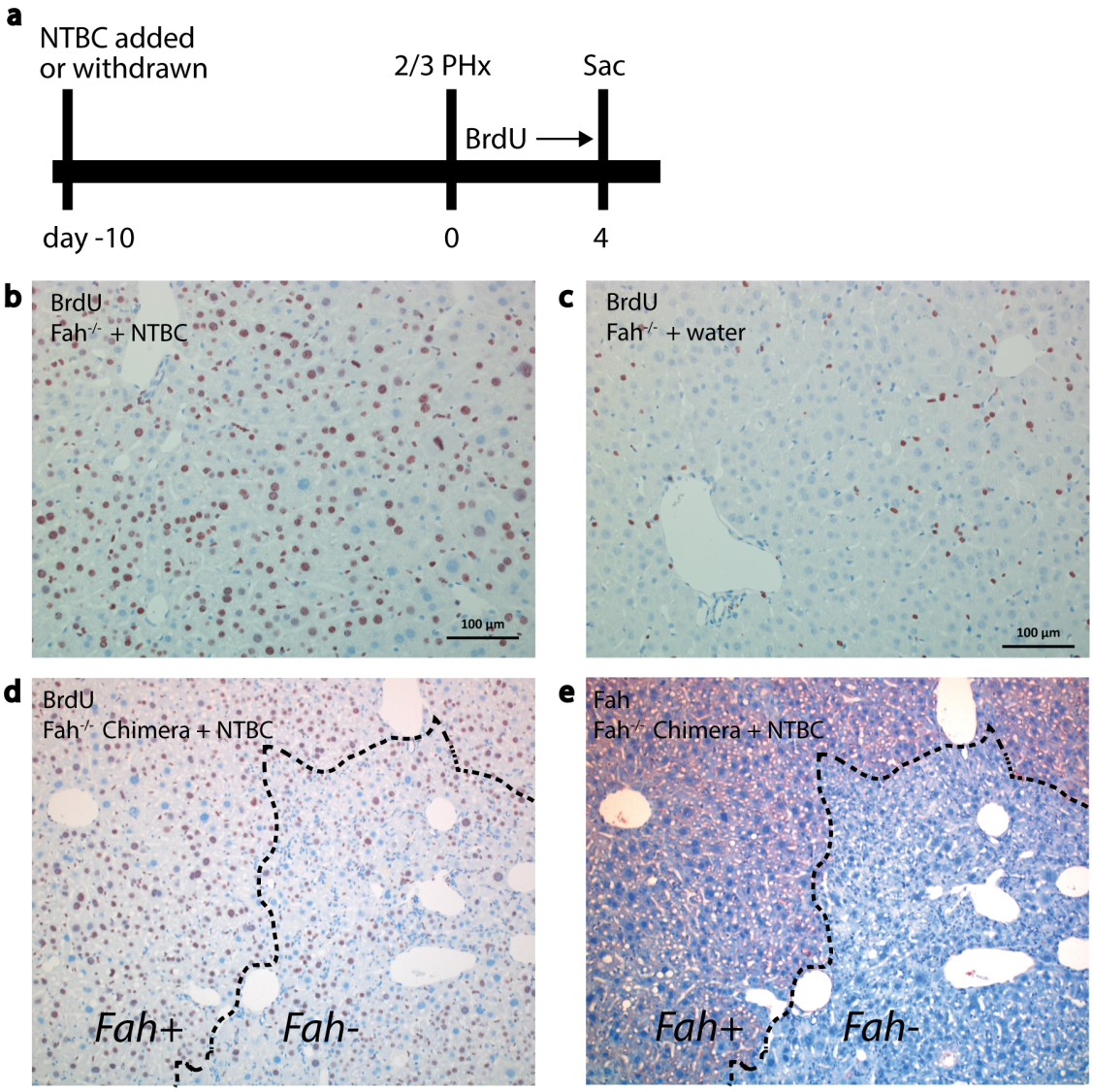

Figure 4-15: NTBC rescues Fah-/- hepatocyte replication in regeneration from partial hepatectomy.(a) Ten days prior to 2/3 partial hepatectomy *Fah*$^{-/-}$ animals were assigned to continue receiving NTBC (8mg/L water) or taken off the drug. Partially repopulated *Fah*$^{-/-}$ hepatocyte chimeric mice were put back on NTBC at this time. Upon 2/3 partial heptectomy, BrdU was continously administered in the drinking water. Replication was assessed after 4 days partial hepatectomy. (b) Fah-/- animals on NTBC showed robust BrdU incorporation in parenchymal and non-parenchymal cells following regeneration from partial hepatectomy. (c) Fah-/- off NTBC showed BrdU incorporation primarily in non-prenchymal cells following partial hepatectomy due to hepatocyte replication blockade. (d) Chimeric *Fah*$^{-/-}$ animal put back on NTBC showed BrdU incorporation in parenchymal cells that (e) were both *Fah*$^{-/-}$ and *Fah*$^{+/+}$ based on Fah-immunostaining in a serial section.

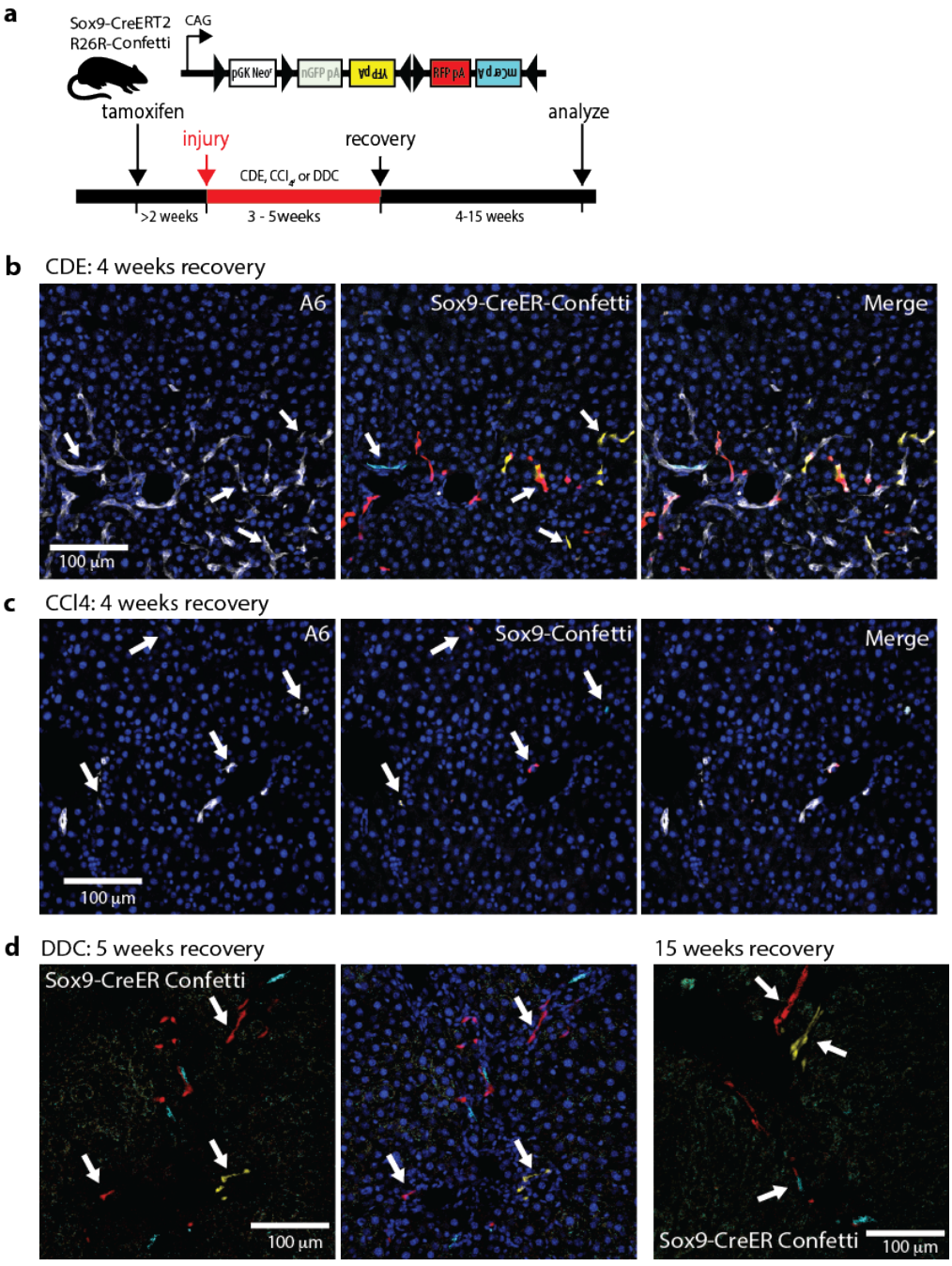

Figure 4-16: Extended recovery does not induce hepatic differentiation in Sox9-derived oval cells. (a) 32mg/kg tamoxifen was administered i.p. to Sox9CreERT2 R26R-Confetti mice at least two weeks prior to initiate of oval cell activation injury, as previously described (Fig. 2).
CDE injury was given for 3 weeks, chronic CCl4 and DDC injury were given for 5 weeks. For recovery, animals were given normal chow (5LOD diet) for 4-15 weeks, as indicated.
(b) Following CDE injury and 4 weeks recovery A6+ ductal proliferations persist. Confetti+ cells (arrows) continue to colocalize with A6+ cells (200/200 clones, n=1 animal). (c) Following CCl4 injury and 4 weeks recovery limited ductal proliferation is observed. Confetti+ cells continue to colocalize with A6+ cells (75/75 clones, n=1 animal). (d) Following DDC injury and 4 or 15 weeks recovery, mild ductal proliferation still persists. Confetti+ cells (arrows) were arranged in distinctly ductal morphology (200/200 clones, n=1 animal).

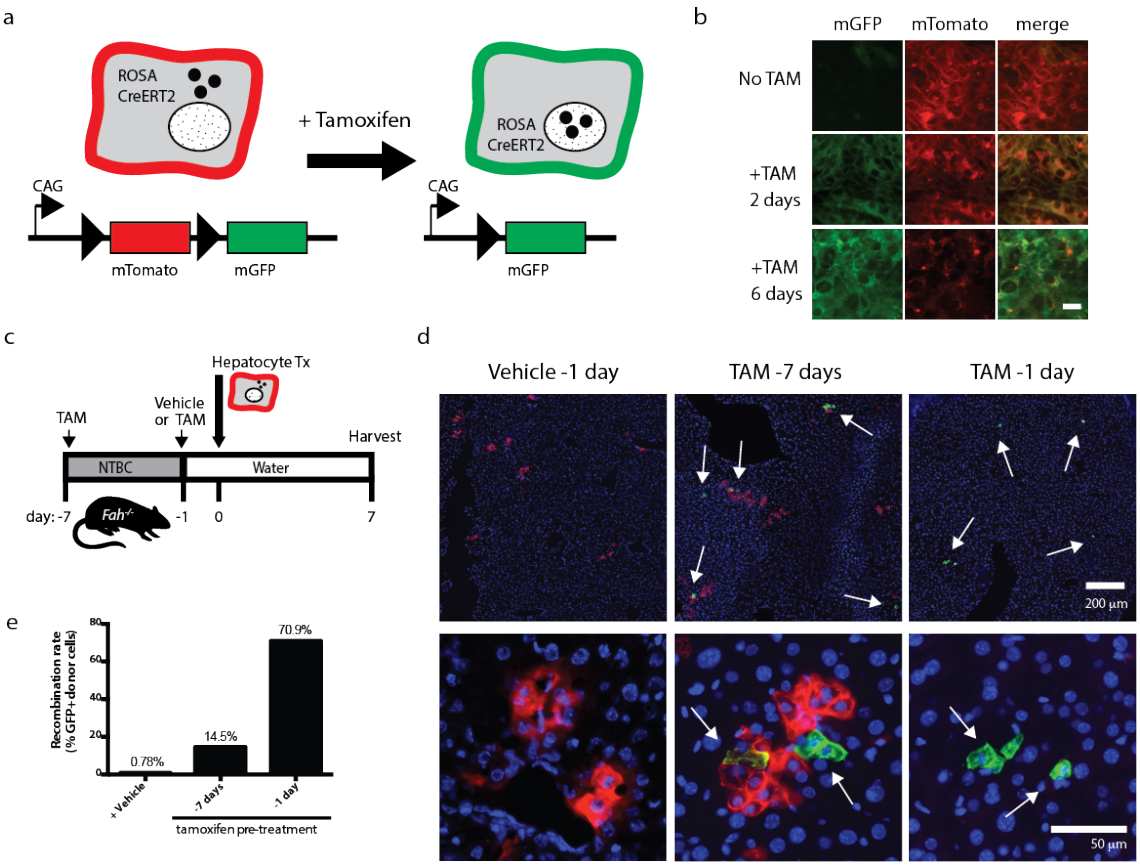

Figure 4-17: CreERT2 recombination continues a week after tamoxifen administration. (a) ROSA^{CreERT2} were crossed with ROSA$^{mT/mG}$ mice to generate a mouse line that irreversibly switches from red to green fluorescence upon tamoxifen-mediated recombination. (b) *In vitro* tamoxifen administration to ROSA$^{CreERT2/mTmG}$ primary hepatocytes switched cells from red to green fluorescence (bar =20 um). Fluorescence was monitored 2 and 6 days after tamoxifen treatment. (c) Transplantation experiment schematic: *Fah*$^{-/-}$ mice were given 100mg/kg i.p. tamoxifen (or vehicle) 1 or 7 days before intrasplenic transplant with ROSA$^{CreERT2/mTmG}$ hepatocytes. NTBC water was withdrawn 1 day before transplant and 7 days were allowed for graft selection and fluorescent protein turnover. (d)The recombination rate in donor ROSA$^{CreERT2/mTmG}$ hepatocytes was assessed by immunofluorescence in the livers of transplanted mice and (e) was quantified as the percentage of donor cells that were mGFP+.

CHAPTER 5: BIPOTENTIAL ADULT LIVER PROGENITORS ARE DERIVED FROM CHRONICALLY INJURED MATURE HEPATOCYTES

Chapter Summary[‡]

- *Mouse hepatocytes give rise to biliary-like progenitors after extended chronic injury*
- *Hepatocyte-to-ductal conversion is associated with a mesenchymal/EMT phenotype*
- *Hepatocyte-derived progenitor cells can differentiate back into hepatocytes in vivo*
- *Human hepatocytes morph into biliary ducts in oval cell injury in vivo*

Adult liver progenitor cells are biliary-like epithelial cells that emerge only under injury conditions in the periportal region of the liver. They exhibit phenotypes of both hepatocytes and cholangiocytes. However, their origin and their significance to injury repair remain unclear. Here, we used a chimeric lineage tracing system to demonstrate that hepatocytes contribute to the progenitor pool. RNA-sequencing, ultrastructural analysis, and *in vitro* progenitor assays revealed that hepatocyte-derived progenitors were distinct from their cholangiocyte-derived counterparts. *In vivo* lineage tracing and serial transplantation assays showed that hLPCs retained a memory of their origin and differentiated back into hepatocytes upon cessation of injury. Similarly, human hepatocytes in chimeric mice also gave rise to biliary progenitors *in vivo*. Our results show that human and mouse hepatocytes can

[‡] This chapter was submitted to *Cell Stem Cell* June 23, 2014 and is under revision with the opportunity to resubmit at the time of this writing. First author: Branden Tarlow. Additional authors: Carl Pelz, Willscott Naugler, Leslie Wakefield, Lisa Wilson, Milton J. Finegold, Markus Grompe. Author contributions: B.T. and M.G. designed experiments and wrote the chapter. M.F. provided electron microscopy analysis. E.W. and W.N. generated humanized mice and generated data. L.W. generated data and performed with experiments. C.P. designed and generated the RNAseq analysis data. M.G. edited the manuscript.

undergo reversible ductal metaplasia in response to injury, expand as ducts and subsequently contribute to restoration of the hepatocyte mass.

Introduction

Liver stem/progenitor cells, or hepatic oval cells, appear and undergo a massive expansion in chronic liver disease. In human disease, the extent of biliary-like progenitor proliferation emanating from the portal triads consistently correlates with the degree of clinical impairment (22,24,25). Experimental injury models in rodents designed to model this biliary progenitor proliferation have demonstrated that duct-like "oval cells" can differentiate into both hepatocytes and cholangiocytes (83,96,103). This finding suggested that the progenitor compartment represents a clinically important cell population that could be pharmacologically manipulated to improve liver function in advanced liver disease where mortality is high and few treatment options currently exist.

A long-standing debate in the field has centered on whether progenitors are derived from biliary-like stem cells that acquire hepatocyte functions or from hepatocytes that lose hepatocyte functions(51,122,124). Recently, we showed that clonally traced cholangiocyte-derived Sox9+ progenitors rarely contribute to regeneration of the hepatocyte pool in several classic mouse oval cell injury models(44). Several other groups have also demonstrated a very limited ability of non-hepatocytes progenitors to contribute to mouse liver regeneration in homeostasis and certain injuries with increasingly sophisticated lineage tracing tools(39,45).

On the contrary, good evidence now exists that hepatocytes can "transdifferentiate" into cholangiocytes in certain injury models(67,108,112,113) and/or by forced genetic modulation of the developmentally important Notch (11,136) and Hippo pathways(137). In the context of cancer, multiple groups have shown that hepatocytes can be transformed into a biliary-cell-like tumor, cholangiocarcinoma, previously thought to originate exclusively from cholangiocytes(13,114).

Nevertheless, it remains unclear whether hepatocyte-to-duct conversion is reversible or how this process may contribute to liver regeneration. The observation that "dedifferentiated" or "mesenchymal" hepatocytes are primed to reacquire hepatic functions *in vitro*(63,66,67,138) raised the question whether hepatocyte-derived progenitors could differentiate back to hepatocytes *in vivo*. Here we characterized hepatocyte-derived progenitors cells in a mouse model of oval cell activation. We utilized hepatocyte-chimeric mice to test the hypothesis that hepatocyte-to-ductal metaplasia is a reversible process. Our results indicate that both human and mouse hepatocytes undergo metaplasia to a distinctive progenitor state that can be reversed following recovery, and therefore, may represent a physiologically important pool of hepatocyte precursors in chronic liver injury.

Experimental procedures

Mouse strains, chimera generation, and diet

Sox9-CreERT2 (gift from Dr. Maike Sander), *Fah*$^{-/-}$, and ROSA-mTomato/mGFP ("ROSA-mTmG") reporter mice maintained on a C57bl/6 background. To generate chimeras, donor *Fah*$^{+/+}$ hepatocytes were gravity purified (3 x 1' x 50 x g) and 4 x 10^5 liver hepatocytes were injected into the spleen of *Fah*$^{-/-}$ mice as previously described. (44). *Fah*$^{-/-}$ animals were weaned from NTBC on the day of cell transplantation and maintained on water thereafter. Liver injury was induced by feeding 0.1% DDC (3,5-diethoxycarbonyl-1,4-dihydrocollidine, TCI America, Portland, OR) in Purina 5015 chow (TD.120495, Harlan Tekland). To isolate ductal cells from DDC-treated livers, post-perfusion digestion was performed with Collagenase II and TrypLE(61). Cells that did not pellet after 2 x 1' x 50g were considered the non-parenchymal fraction and used for FACS and serial transplantation experiments. Tamoxifen was resuspended in sesame oil (30mg/mL) and given by intraperitoneal injection to Sox9-CreERT2 ROSA-mTmG chimeric mice.

Short name	Scientific name	Jax Stock #	Reference
ROSA-mTmG	B6.129(Cg)-*Gt(ROSA)26Sortm4(ACTB-tdTomato,-EGFP)Luo*/J	007676	(128)
R26R-Confetti	B6.Cg-Gt(ROSA)26Sortm1(CAG-Brainbow2.1)Cle/J	017492	(111)
Sox9-CreERT2	Tg(Sox9-cre/ERT2)1Msan/J	018829	(127)
Fah$^{-/-}$	Fah tm1Mgo	N/A	(139)

Modifications for serial transplantation experiments enrichment of nonparenchymal cells by gravity centrifugation (2 x 1' x 50g, non-pelleting cells). Recipient mice were given adenoviral urokinase-plasminogen activator (Ad-uPA) (5 x 10^7 pfu/g

body weight) to improve trapping of small diameter donor cells. Virus was given 48 hours prior to cell transplantation by retroorbital or tail vein injection under isofluorane anesthesia. Animals were cycled back on NTBC once during a 5-week selection period.

Cryopreserved human hepatocytes (Life Technologies, Inc) were thawed and washed. The hepatoyctes were centrifuged at 100 x g for 5 minutes at 4˚C and reconstituted at 1 x 10^6 cells/mL. 4 x 10^5 live cells were injected to the spleen of recipient *Fah*$^{-/-}$ *Rag2*$^{-/-}$ *Il2rg*$^{-/-}$ (FRG-NOD) mice (Yecuris, Inc). FRG-NOD mice received (Ad-uPA) 48 hours prior to transplantation. Post-transplant, a standard NTBC cycling protocol was followed to promote human hepatocyte selection. Sulfamethoxazole-trimethoprim was included in the drinking water in a subset of animals as an antimicrobial prophylactic. All procedures and protocols with vertebrate animals were approved by the Oregon Health & Science University IACUC.

FACS analysis

Liver NPCs were isolated by a multi-step collagenase (type IV, type D) perfusion and labeled with antibodies MIC1-1C3, Cd31, Cd45, Cd11b, and Cd26 as previously described(44,61). Cells were sorted on an inFlux cytometer (BD Biosciences) equipped with 405, 488, 561 and 640nm excitation lasers. Double positive events were visually inspected to exclude the possibility of two cells stuck together.

Cell culture

Crude non-parenchymal cell fractions were enriched by gravity or FACS. 500 to 20,000 cells were seeded into 60µL matrigel droplets. Growth media included B27 supplement, N2 supplement, Wnt3a, Egf, Hgf, and Rspo1-Fc; differentiation media included dexamethasone and OSM as previously described.(41)

Gene expression analysis

FACS sorted mouse cells were lysed in Trizol (Life Technologies) and treated with chloroform. Whole human-mouse chimeric livers were directly homogenized without cell fractionation. The aqueous layer was precipitated with ethanol and applied to silica columns for purification and DNAse digestion (Qiagen RNAeasy Mini or Micro). The organic layer was saved for later DNA isolation. Samples meeting quality control thresholds (>20,000 cells, RNA integrity RIN >8.5, total RNA > 75ng) were prepared into barcoded libraries with the Truseq RNA Sample Prep Kit v2 according to the manufacturer's instructions (Illumina, Inc). Samples were sequenced on a HiSeq2000 (3-4 samples per lane, single end 50bp reads) to yield an average of 33.1 million exon-mapped tags per FACS sorted sample.

RNA-seq data analysis

The first 4 bases from each read were trimmed and the subsequent 44 bases were aligned to the *Mus muscularis* genome (UCSC mm9) using Bowtie version 0.12.7. Tag alignment was implemented using custom R scripts (http://www.R-project.org/) according to UCSC Refseq gene models. Only reads that uniquely aligned to the genome were counted. Gene expression levels were measured by RPKM (reads per

kilobase of exon per million reads). For comparative gene expression analysis, we used the edgeR package with general linear model (Bioconductor 3.2.4)(140). Significant genes were selected based on a false-discovery corrected p-value (q-value) cutoff of 0.01, a fold change >2, and RPKM > 1 in either group. Gene ontology analysis was performed using GSEA software (Broad Institute) using the canonical pathway KEGG modules. Unsupervised clustering was performed using Ward's method with log2 RPKM values for each gene.

Human-mouse chimeric liver samples were aligned to custom transcriptome index comprising 21 mouse and matched human Refseq RNA sequences (see Supplemental Table 4) with Bowtie version 0.12.7 set to allow no mismatches. Only tags that uniquely aligned to a single transcript were counted. Tags counts were compiled into a matrix using custom R-scripts, which are available upon request. Tag alignment was outputted to wiggle track format to examine the distributions of tags across each gene model as quality control. Expression levels were normalized to various housekeeping genes including GUSB, GAPDH, LMNA, and BACT. RNA-seq fastq files and RPKM matrix were deposited into the NCBI database (http://www.ncbi.nlm.nih.gov/geo/) under accession numbers GSE55552 and GSE58679.

Immunohistochemistry & microscopy

For transmission electron microscopy, 5 x 10^4 FACS sorted cells were pelleted and fixed in 3% gluteraldehyde at room temperature immediately after isolation. Cell pellets were osmicated, dehydrated, and embedded in araldite resin. Thin sections

were stained with uranyl acetate and lead citrate. Then cells were processed with high-pressure freezing and imaged. FACS isolated cells were fixed for 15 minutes in 4% paraformaldehyde (PFA) and cytospun onto charged slides (5' x 200g). Cells subsequently processed for immunohistochemistry or hemotoxylin and eosin staining. Liver tissues were fixed in 4% paraformaldehyde and cryopreserved in 30% sucrose prior to freezing in OCT tissue blocks. When possible, tissues were fixed with PFA perfusion into the portal vein. Otherwise resected tissues (ie partial hepatectomy) were submerged directly in PFA and fixed for >4 hours. Up to four-color images were captured on an Axio Imager M2 with color MRm and monochrome MRc 5 cameras (Carl Zeiss) running Xen Blue 2011. Large area images were acquired with the Tiles module and stitched. This system is part of the Advanced Light Microscopy Core at the Jungers Center, OHSU Portland, Oregon.

Immunohistochemistry

Antibody or antigen	IgG Type	Dilution factor	Use	Product	Source
MIC1-1C3	Rat mAB	100	FACS	NBP1-18961	Novus Biologics
OC2-2F8	Rat mAB	20	FACS	Gift	Craig Dorrell, OHSU
Cd31	Rat mAB	100	FACS	561410	BD Biosciences
Cd45	Rat mAB	100	FACS, IF	552848	BD Biosciences
Cd11b	Rat mAB	100	FACS, IF	552850	BD Biosciences
Fah	Rabbit pAB	500	IF	Custom	Grompe Lab
Ostepontin	Goat pAB	100	IF	AF808	R&D systems
A6	Rat mAB	50	IF	Gift	Valentina Factor, NCI
Krt19	Rabbit pAB	500	IF	Gift	Xin Wang, U. Minn.
Sox9	Rabbit pAB	500	IF	AB5535	Millipore, Inc
Hnf4a	Rabbit pAB	100	IF	sc-8987	Santa Cruz Bio
CD44	Mouse mAB	100	FACS	560533	BD Biosciences
EPCAM	Mouse mAB	50	FACS, IF	F0860	Dako

PFA-fixed tissues were cut into 8µm sections on a freezing microtome (Cryostat, Leica), washed 2 x 15' in PBS, permeablized in 0.2-0.5% Triton-X 100 and blocked in

5% normal donkey serum for 2 hours to overnight. Primary antibodies were applied for 1 hour at room temperature or overnight at 4 degrees in a humidity chamber. Secondary antibodies (Donkey) and conjugated to AlexaFluor 488 or AlexaFluor 647 were used (Jackson Immunoresearch). Tissues were counterstained with Hoechst 33342 and mounted in Prolong Gold Antifade mounting media (Life Technologies). For EdU analysis, a 100mg/kg pulse was given by intraperitoneal injection 6 hours prior to sacrifice. The Click-iT labeling protocol was used according to the manufacturer instructions (Life Technologies) followed by co-immunohistochemistry. mTomato and mGFP fluorophores were directly observed without secondary antibody detection.

Image analysis

Images were quantified and analyzed using ImageJ software (www.fiji.sc). For serial transplantation experiments fluorescent images were capture immediately before transplantation on a hemocytometer. For analysis of engrafted livers nodule diameter was measured in tiled sections. To correct for differential probability of identifying large spherical nodules in 2-dimension sections, a correction factor was applied as previously described (141).

RT-PCR

RT-PCR was performed as previously described(44). Mouse primers were used at 60 °C annealing,

Alb1 F- GCG CAGA TGA CAG GGC GGA A
Alb1 R – GTG CCG TAG CAT GCG GGA GG
Gapdh F – AAG GTC GGT GTG AAC GGA TTT GG
Gapdh R – CGT TGA ATT TGC CGT GAG TGG AG

Human specific primers were used at 66 °C annealing
LMNA F – CCT CCT CGC CCT CCA AGA GC
LMNA R – AGA TGC GGG CAA GGA TGC AG
KRT19 F – CCT CCC GCG ACT ACA GCC ACT A
KRT19 R – CCA CTT GGC CCC TCA GCG TA.

Semiquantiative *Fah* genotyping PCR was performed at 62 °C with 3 primers
Wt – GGA TTG GGA AGA CAA TAG CAG GC
Mut – TGA GAG GAG GGT ACT GGC AGC TAC
Com. – TTG CCT CTG AAC ATA ATG CCA AC

Statistics

Calculations were performed with the Prism 6.0 statistical software package (Graphpad, Inc). Parametric pairwise or paired t-tests were performed where appropriate for image analysis data. Significance levels were defined as $p< 0.05$, $p<0.01$*, or $p<0.001$***.

Results

Hepatocytes contribute to the oval cell response after extended injury

To specifically track the fate of mature hepatocytes in liver injury, we generated mice with chimeric livers by transplanting ROSA-mTmG hepatocytes into *Fah*$^{-/-}$ mice (**Fig. 5-1A**). After 10 weeks of repopulation the hepatocyte compartment, but not other cell types, were replaced by donor mTomato+ cells in agreement with previous detailed analyses in our lab (44,121,142).

Next, we induced a prototypical oval cell injury(143) by feeding mice a 0.1% 3,5-diethoxycarbonyl-1,4-dihydrocollidine (DDC) diet(39,41,61,112,133,144). As

expected from previous work, 2-weeks of DDC injury induced host-derived Opn+ Krt19+ ductal proliferation in ROSA-mTmG marked hepatocytes (**Fig. 5-1B**).

Following 6-weeks of DDC injury, however, cords of donor hepatocyte-derived mTomato+ cells were prominently observed in the periportal region and co-localized with progenitor markers Opn (**Fig. 5-1**) and Sox9 (not shown) in agreement with Yanger et. al(112). Opn+ mTomato+ cells had ductal morphology with oval-shaped nuclei. The induction of Opn in mTomato+ hepatocyte-derived ductal cells corresponded with a downregulation of the hepatocyte-marker Fah (**Fig. 5-1C**). hLPCs were proliferative and incorporated EdU (**Fig. 5-1D**). We then administered a low dose of a hepatocyte-specific rAAV8-TTR-Cre to adult ROSA-Confetti reporter mice as a second, independent method of marking mature hepatocytes (45,112). The findings after 6-weeks of DDC injury were similar to the chimera-based tracing results (n=3). Single clonally marked hepatocytes delineated by a single color of the reporter transgene expanded to cords of 10-40 cells with biliary morphology, indicating hepatocyte-derived duct-like cells were proliferative (**Fig. 5-9**).

Isolation of hepatocyte-derived liver progenitors cells with surface marker MIC1-1C3

To further study hepatocyte-derived liver progenitors cells (hLPCs) we adapted a FACS-based assay developed by Dorrell et al (61) to isolate antigenically defined progenitors based on cell surface phenotype (**Fig. 5-2A**).

Hepatocyte chimeric ROSA-*mTmG* / *Fah*$^{-/-}$ mice were treated for 1 to 8 weeks with DDC to induce oval cell activation. Livers were dissociated into single cells and MIC1-1C3^{+} CD45^{-} CD31^{-} Cd11b^{-} CD26^{-} PI^{-} cells ("MIC1-1C3^{+} cells") were FACS sorted by mTomato-fluorescence status (**Fig. 5-2B**). Without injury, less than 0.1% of MIC1-1C3^{+} cells were mTomato+ (median 0.067% n=4). Visual inspection of FACS-positive cells from uninjured mice confirmed that most mTomato+ ductal cells had small portions of adjacent membrane-localized fluorescent protein likely from an adjacent hepatocyte (**Fig. 5-10A**). In contrast, 8.7 - 39.3% of MIC1-1C3^{+} oval cells were mTomato+ after 4-8 weeks of injury, and thus determined to be of donor hepatocyte origin (n = 14) (**Fig. 5-2B**). Hepatocyte-to-oval cell conversion was rare before 14 days of injury and moderately correlated with the duration of injury (linear regression $r^2 = 0.63$). Again, our secondary marking strategy using low dose rAAV8-Ttr-Cre in non-chimeric reporter animals followed by DDC injury yielded analogous results when FACS phenotyping was used to detect hepatocyte to duct metaplasia (**Fig. 5-9**).

To further characterize the different populations of ductal progenitors, FACS isolated cells were fixed and analyzed by light and transmission electron microscopy (**Fig. 5-2C-F**). Consistent with historical descriptions of "oval cells", hepatocyte-derived liver progenitor cells hLPCs were highly similar to cholangiocytes by H&E or Hoechst 33342 staining. Compared with hepatocytes, hLPCs were significantly smaller in cell diameter (mean 14.6μm ± s.d. 3.2 versus 33.1μm ± 4.1; $p < 0.0001$) and the nucleus represented a greater fraction of total cell

area (0.417 ± 0.085 versus 0.138 ± .035 versus; p<0.0001). cLPCs were smaller in diameter compared with hLPCs (11.3μm ± 0.9 versus 1.46 ± 3.2; p<0.0001) and had significantly greater fractional nucleus size (0.489 ± 0.054 versus 0.417±0.085; p<0.001). Rare binucleated hLPCs were observed, however, no binucleated cholangiocytes were found (not shown).

hLPCs exhibited additional ultrastructual differences including a greater abundance of mitochondria and rough endoplasmic reticulum as well as decreased heterochromatin compared with cLPCs. Lysosomal contents in hLPCs were suggestive of autophagy (arrow) as a potential mechanism for organelle and cytoplasm volume reduction. Glycogen granules were found in mature hepatocytes but were largely absent in oval cells (**Fig. 5-10**).

Hepatocyte-derived MIC1-1C3^{+} cells express progenitor-associated genes

To determine whether the morphological differences between donor-derived hLPCs and host-derived cLPCs corresponded to changes in gene expression, mRNA was extracted from FACS-sorted hepatocytes, host-derived MIC1-1C3^{+} cells, and hepatocyte-derived mTomato^{+} MIC1-1C3^{+} cells for global expression analysis. RNA-sequencing indicated that 98.4 – 99.2% of mTomato tags were derived from FACS sorted MIC1-1C3^{+} mTomato+ cells, within the expected accuracy of FACS isolation (**Fig 5-3A,** n=4 paired samples, normalized to reads per million). Genotyping for *Fah* confirmed that FACS-sorting based on the mTomato+ phenotype effectively separated genetically distinct host from donor-derived progenitor cells (**Fig. 5-11**).

FACS-isolated hepatocyte-derived MIC1-1C3$^+$ cells from 5 independent experiments showed a unique gene expression phenotype according to unsupervised clustering (**Fig 5-3B**) and principle component analyses (**Fig. 5-11**). Hepatocyte-derived ducts were more similar to cholangiocyte-derived ducts than the corresponding parental hepatocytes isolated from DDC injured chimeras. Nevertheless, more than 2,010 genes were significantly differentially expressed (>2-fold, q<0.01, RPKM>1 in either group) between the two duct progenitor subtypes. 4,714 genes were differentially expressed between hLPCs and parental hepatocytes.

Next we examined expression of genes previously used as lineage tracing promoters to study ductal liver progenitors in mice, including *Sox9*, *Spp1 (*also called *Opn)*, and *Hnf1b* (**Fig. 5-3C**) (38,39,144). Expression levels of these genes were highly enriched in both progenitor cell types compared with hepatocyes, but hLPCs and cLPCs did not express significantly different levels of *Sox9* (92.44 ± 15.41 mean RPKM ± s.d. v. 102.56 ± 29.11; FDR q-value = 0.87), *Spp1* (17759.8 ± 1095.5 v. 18618.3 ± 587.6; q = 0.84), or *Hnf1b* (158.9 ± 12.9 v. 176.4 ± 21.4; q = 0.72). Thus, conversion of hepatocytes was associated with increased expression of ductal markers. Notably, not all ductal marker genes were highly induced. *Krt19* and EpCam were expressed at intermediate levels in hLPCs. For example, *Krt19* levels in hLPCs were 119-fold higher than in hepatocytes (42.53 ± 23.45 RPKM mean ± s.d., n=5 versus 0.36 ± 0.29; n=3, q< 1e-31) but 15-fold lower compared with cLPCs (657.89 ± 65.25; n=5, q <1e-44). Interestingly, FACS-sorted hepatocytes expressed

the highest levels of the putative progenitor marker *Lgr5* when compared with either progenitor subtype (5.5 or 13.4-fold higher, q < 8e-15).

Compared to the parental mature hepatocytes from which they derive, hLPCs expressed significantly lower levels of hepatocyte-associated genes such as albumin (*Alb*), homogentisic acid dehydrogenase (*Hgd*), *Cyp7a1,* the rate limiting enzyme in bile acid biosynthesis, coagulation factor IX (*F9*), and hepatocyte-nuclear factor 4 (*Hnf4a*). Importantly, expression of a subset of hepatocyte-associated genes in hLPCs was similar to cLPCs (e.g. *Alb, Hgd, Cyp7a1*) whereas others were intermediate between hepatocytes and cLPCs (e.g. *Hnf4a, F9*). The fact that mature hepatocyte genes were expressed at ratios different from hepatocytes themselves argues against hepatocyte contamination as the source of these transcripts.

Hepatocyte-to-ductal transition correlates with induction of EMT genes

Gene set enrichment analysis (GSEA) was performed to identify pathways that were differentially active between cell subpopulations. Although hLPCs expressed many ductal progenitor markers at levels similar to cholangiocyte-derived cells, they also retained patterns of gene expression closely associated with hepatocyte function, albeit at a low levels. Compared with cLPCs, hLPCs showed strong enrichment (FDR q-value < 0.05) of gene sets for hepatocyte functions including fatty acid metabolism, complement and coagulation cascades, drug metabolism & cytochrome P450, and branched amino acid degradation. Thus, hepatocyte-derived progenitors retained basal levels of transcription for genes encoding mature hepatocyte functions.

To understand what pathways were driving the hLPC conversion, we compared hLPCs to the parental hepatocyte population. Gene sets for notch signaling pathway, hedgehog signaling pathway, and the wnt signaling pathway were significantly induced ($q < 0.2$). Additional gene sets enriched in hLPCs included axon guidance, melanogenesis, tight junctions, and Tgf-β signaling gene sets ($q < 0.25$).

178 genes were significantly upregulated in hLPCs in pairwise comparisons with both hepatocytes and cLPCs. This finding again shows that the gene expression signature of hLPCs could not be explained by simple hepatocyte contamination. Notably, the transcription factor *Zeb1*, a master regulator epithelial-to-mesenchymal transition(145) (EMT) was overexpressed in hLPCs compared with cLPCs (3.6-fold, $q < 9e\text{-}36$) and hepatocytes (3.3-fold, $q < 2e\text{-}8$). Additional genes in this group associated with EMT included *Vim*(26,146)*, Mst1r, Fzd10* and *c-Kit*(66,96,147,148)*.* Hepatocyte-derived progenitors also showed enrichment of genes expressed in neuronal-progenitors that were previously identified in human ductular reactions or experimentally induced oval cells, including *Nes*(149), Neuronal-cadherin (also called *Cdh2*)(150), and *Ncam1*(27,60,151,152). *Smo*, an intermediate in the hedgehog pathway proposed to regulate epithelial-mesenchymal transitions in the liver(153), was highly upregulated in hLPCs compared with hepatocytes (36-fold increased, $q < 1e\text{-}16$) but similar to cLPCs ($q = 0.46$). A complete list of enriched gene sets and differentially expressed genes can be found in the **Tables 5-1, 5-2 and 5-3**.

Hepatocyte and cholangiocyte-derived oval cells are functionally distinct *in vitro*

Given that hepatocyte-derived progenitor cells were distinct from cholangiocytes with respect to gene expression patterns and ultrastructural features, we hypothesized they were also functionally distinct. After 6 weeks of DDC injury, chimeric livers were dissociated into single cells and seeded into our previously published organoid forming assay for liver progenitor activity(41). Organoid formation was robust. Despite the fact that hepatocyte-derived progenitors expressed *Sox9*, *Hnf1b*, and *Lgr5*, we found that organoids were universally negative for fluorescent protein mTomato (**Fig. 5-4A**). When FACS sorted MIC1-1C3 cells from injured chimeras were seeded into matrigel (500 – 2000 cells/animal), only mTomato-negative host cholangiocyte derived cells formed organoids, hollow structures >20 cells that could be passaged multiple times (n=6 animals, 50-200 organoids scored/animal). Interestingly, a third of hLPCs and ~1% host MIC1-1C3^{+} cells seeded into matrigel formed mesenchymal-like structures with fillipodia projections (**Fig. 5-4D-E**). When cultured cells were exposed to hepatocyte-differentiation medium containing dexamethasone and oncostatin-M, hLPCs showed an enhanced ability to upregulate albumin mRNA (**Fig 5-4F**) compared with Rspo-1 containing expansion medium. The ability of hepatocyte-derived progenitors to reactivate hepatocyte gene expression *in vitro* is in agreement with a recent publication(67).

To confirm that the fluorescent reporter protein was not preventing organoid formation, we switched the reporter to the host by generating *Fah*$^{-/-}$ ROSA-*mTmG* mice. We then transplanted these mice with unmarked wildtype hepatocytes. After 6 weeks DDC injury, >10% of MIC1-1C3^{+} cells were hepatocyte-derived by FACS (n=2, **Fig. 5-12**). Only host-derived mTomato+ cholangiocytes formed organoids, and donor-derived MIC1-1C3 cells (mTomato negative) accounted for nearly all cells with mesenchymal filipodia. This finding confirms our previous work showing that ductal progenitors are not simply transferred into recipient *Fah*$^{-/-}$ livers in the chimerization process(44,77,121). Given that hLPCs expressed an EMT signature and basal levels of hepatocyte-associated genes, we hypothesized that the conversion could be reversed through a mesenchymal-to-epithelial transition (MET) (96,154).

Sox9+ hepatocyte-derived progenitor cells revert back to hepatocytes *in vivo* after injury subsides

Continuous DDC injury induced the conversion of some hepatocytes to a highly ductal phenotype. We therefore wondered whether this fate conversion was highly stable as previously suggested(112) or whether the cells retained the ability to revert to their cell of origin upon cessation of the injury. To ask this question, we performed lineage tracing with a tamoxifen inducible Sox9 reporter. Our RNA-seq expression data (**Fig. 5-3**) indicated that Sox9 was expressed at high levels in hLPCs; therefore, we reasoned that a Sox9-CreERT2 allele could be used to specifically track the fate of hepatocyte-derived progenitor cells during an injury recovery period.

Chimeric mice were generated by transplanting gravity-purified Sox9-CreERT2 ROSA-mTmG hepatocytes into *Fah*$^{-/-}$ recipient mice. We allowed 8-10 weeks for repopulation. Next, we induced oval cell injury in chimeric mice by feeding 0.1% DDC. After 4 weeks a low-dose pulse of tamoxifen (15mg/kg) was given to induce recombination in Sox9+ hepatocyte-derived cells, converting their baseline red color to green. DDC was continued for two additional weeks to allow tamoxifen to wash out and residual mTomato protein to degrade in recombined cells. At the end of the DDC injury 1/3 partial hepatectomy was performed to measure the post-injury frequency of hepatocyte-derived duct cells. Following hepatectomy, animals were placed on a regular diet to allow healing and *in vivo* tracing of hepatocyte-derived liver progenitors in a 4-week recovery period (**Fig. 5-5A**). Thus, we were able to monitor the phenotype of Sox9-CreERT2 marked hepatocyte derived progenitor cells within the same animals before and after injury recovery.

At the peak of injury, the majority of Sox9-marked cells expressed the classic oval cell marker A6 and were arranged in ductal cords (**Fig. 5-5B**). At this injury baseline, only a small percentage (6.6%, range 3.5% to 10.5%, n = 4) of Sox9-CreERT2 marked cells co-expressed the hepatocyte-marker Fah (**Fig. 5C, D**). Importantly, the frequency of Sox9-marked hepatocytes was markedly increased after a 4 week injury recovery period in all animals tested (**Fig. 5-5E,F**). The average increase was ~5-fold from the immediate post-injury benchmark: 33.5% (range 22.9% to 38.96%; n=4, paired t-test p = 0.0067, **Fig. 5-5G**). This notable shift in the ratio of ductal progenitors:hepatocytes strongly suggested that a significant fraction

of hLPCs had redifferentiated back into hepatocytes once the injury subsided. It is worth noting that many hepatocyte-derived ducts had not reactivated the hepatocyte program at the 4-week recovery time point. This may be explained by the fact that signs of liver damage persist for many weeks after reinstitution of a normal diet (**Fig. 5-13**).

Clonal analysis of hepatocyte-derived progenitors in a new microenvironment

To further determine whether hepatocyte-derived ducts could revert to functional hepatocytes in the absence of ongoing injury, we performed serial transplantation of marked cells from chimeric mice treated with DDC for 6 weeks. This experiment differs from the lineage tracing after stopping the DDC injury in that the cells were transferred into a liver not undergoing oval cell injury. In this experiment, donor hepatocytes that had not undergone ductal metaplasia retained their original mTomato red color, whereas cells that transdifferentiated were marked mGFP because of their Sox9 expression. The two populations competed with each other for engraftment and repopulation of a secondary host.

We used low-speed gravity centrifugation to enrich ductal cells for transplantation. Before transplantation 6.3% of ROSA-mTmG cells were mGFP+ (22/333 in 5 random fields, **Fig 5-6B**). Over 90% of these had a highly ductal phenotype and did not express mature hepatocyte markers. 2 million total cells were then transplanted into *Fah*$^{-/-}$ recipient mice and harvested after 5 weeks for analysis. We found that mGFP marked donor cells were nearly as efficient as mTomato marked hepatocytes at engrafting in a new microenvironment: 2.3 – 4.1% of grafts were mGFP+

compared with 6.3% prior to transplant. Importantly, over 60% of the engrafted clones from green marked cells were clearly hepatocytic (range 62% to 81%). They expressed Fah, had hepatocyte morphology in terms of size and cell shape and most importantly formed repopulation nodules in the *Fah*$^{-/-}$ liver (**Fig 5-6D**, E)(77). This shows that a large fraction of hepatocyte-derived ducts converted back to the hepatocyte-fate despite their highly ductal phenotype and gene expression profile. This is in contrast to normal ductal progenitors that lack the ability to produce hepatocytes unless they are expanded and manipulated *in vitro* prior to transplantation (Huch et al 2013).

Human hepatocytes morph into oval cells following sustained injury

Finally, we asked whether the hepatocyte-ductal metaplasia mechanism might be conserved in human hepatocytes. To test the potential of human hepatocytes to undergo ductal metaplasia *in vivo*, we humanized the hepatocyte compartment of *Fah*$^{-/-}$ *Rag2*$^{-/-}$ *Il2rg*$^{-/-}$ (FRG) triple knockout mice by human hepatocyte transplantation(92). Moderately-humanized (>1500ug/mL human serum albumin (HSA)=~30% repopulation) or highly humanized (>4500ug/mL HSA =~90%) FRG mice were administered 0.1% DDC diet for several weeks. The diet was well tolerated and produced hepatomegaly, dramatic darkening of the liver, and ductal proliferation. In 3/6 mice treated with DDC human hepatocytes expressed EpCAM and morphed into duct-like cords with oval-shaped nuclei and scant cytoplasm (**Fig. 5-7B**). As a control for antibody specificity, hEpCAM+ ductal cords were observed in cirrhotic human liver but not in humanized mice maintained on NTBC or DDC injured mouse hepatocyte chimeras (**Fig. 5-14**). EpCAM+ cells co-expressed low

levels of Fah, confirming their donor origin. Fah-low ductal cords were negative for mouse-osteopontin, but were often adjacent to or intertwined with the mouse biliary cells (**Fig. 5-14**).

Next, whole chimeric livers were homogenized to assess levels of human specific mRNAs. Human KRT19 mRNA was detected in human liver surgical biopsies but not mouse liver control samples by qRT-PCR (**Fig. 5-7C,D**). No humanized animals maintained on normal chow expressed KRT19 mRNA (n = 0/11). In contrast, robust induction of KRT19 was observed in 3 of 6 chimeric mice treated with DDC. KRT19+ chimeric animals represented 3 different human hepatocyte donors. KRT19 levels, normalized to human LAMIN A/C, ranged from 9-to-285-times lower than normal human liver.

Finally, we wished to determine whether DDC oval cell injury would induce the expression of a range of duct progenitor-associated genes as it does in mouse hepatocytes. We performed RNA-seq on whole liver homogenates and used a custom transcriptome-based index (see Methods) to achieve highly species-specific gene alignment of tags (0.01% - 0.2% erroneous assignment with known single species controls) (**Fig. 5-7E**). Compared with humanized mice on normal chow, DDC-fed chimeric mice had increases in multiple biliary or oval cell associated genes, including SPP1, SOX9, KRT7 ($p<0.001$); CD44 ($p<0.01$); and VIM ($p<0.05$) (**Fig. 5-7F**). Together, these data are consistent with the direct conversion of human hepatocytes into biliary-like progenitor cells during oval cell liver injury.

Discussion

Until recently, the adult mouse liver was thought to harbor facultative stem cells residing in the biliary duct system and capable of producing both ducts and hepatocytes(32,33,41,47,105,155). Recent work, however, has challenged this traditional view and shown that biliary progenitors are inefficient at producing hepatocytes *in vivo* and do not contribute significantly to the restoration of hepatocyte mass during chronic damage(44,45). Our data herein provide an alternative and novel model explaining the existence of bipotential oval cells in chronic hepatic injury. We show that conversion of mature hepatocytes into biliary-like progenitor cells is a reversible process. These hepatocyte-derived progenitors display the properties previously ascribed to classic oval cells. They proliferate as ducts in the periportal region of the hepatic lobule and can also produce hepatocyte progeny. Our serial transplantation experiments indicate that hepatocyte-derived progenitors give rise to hepatocytes at a much higher efficiency (>60%) than clonogenic progenitors derived from biliary system (<1%(41,44)).

Our data confirm that mature hepatocytes possess significant phenotypic plasticity and reinforce previous studies by Michalopoulos(113), Yanger(112), and the recent report from Yimlamai(137). Our new observations that hLPC are distinct from cLPCs based on genome-wide expression profiling, electron microscopy, and functional characterization provides a more complete understanding of their unique properties. Interestingly, quantitative RNA-sequencing indicated that hepatocyte-derived progenitor cells express 119-fold higher levels of Krt19 than hepatocytes

but 15-fold lower levels than cholangiocytes. This intermediate level of expression could be interpreted either as Krt19-negative (45) or Krt19-positive(108,112) depending on the technical parameters of the immunohistochemistry assay. Our results therefore resolve an apparent contradiction between these previous reports.

Despite the equal expression of "progenitor markers" (ie MIC1-1C3, Sox9, Hnf1b, etc) and similar ductal morphology by light microscopy, hLPCs and cLPCs were derived from different lineages and were functionally distinct. For these reasons, we propose the general term "metaplasia" is more appropriate than transdifferentiation to describe the plasticity of hepatocytes in liver injury models. Transdifferentiation is a specific type of metaplasia where a cell irreversibly switches from one differentiated cell type into another fully differentiated cell type(156). It appears unlikely that there would be a physiologic requirement for hepatocyte to duct transdifferentiation in oval cell injury. The proliferation of host ducts is robust in DDC induced oval cell injury and all ductal proliferation is of non-hepatocyte origin for the first 2 weeks. Hepatocytes are not needed as a source of new ducts. On the other hand, severe hepatocellular injury has been associated with metaplasia towards numerous endodermal lineages including intestinal crypts (complete with goblet and neuroendocrine cells)(146,157) or pancreatic acinar-like cells(158). Additionally, chronic injury-associated metaplasia is widely reported to occur in endoderm-derived epithelial cell types in other organs(156).

We also demonstrated that human hepatocytes possessed similar phenotypic plasticity *in vivo* following liver injury. While classic lineage tracing is not possible in human patients, our study provides the first evidence that normal human hepatocytes can induce ductal progenitor genes during chronic injury *in vivo*. This suggests that hepatocyte-metaplasia may also occur in human cirrhosis and that hepatocytes may be the source of ductular reaction in long-term injury. Our dataset provides a specific gene-expression signature of both human and mouse hepatocyte-derived progenitors that may serve as a resource for future investigations (Supplemental Information). We hypothesize that hepatocyte-derived human progenitors would express similar EMT-associated markers, intermediate levels of Krt19, and exhibit unique characteristics in functional assays.

Hepatocytes were until recently considered a terminally differentiated cell that could replicate in acute hepatectomy but not chronic injuries(47). More broadly, the concept of terminal differentiation of mature cell types has been challenged by numerous demonstrations that cells can change their phenotype during both development and adulthood(159). Cellular plasticity induced by the epithelial-to-mesenchymal transition (EMT) program has been found to generate cells that exhibit stem-like properties, particularly in tissue repair, chronic inflammation, and neoplasia (145). The acquisition of mesenchymal features is associated with increased migration, resistance to apoptosis, degradation of the basement membrane, increased production of extracellular matrix, and expression of stem/progenitor markers—all which are associated with oval cell activation in

chronic liver injury models. In our study, the conversion of mature hepatocytes into biliary-like progenitors is marked by induction of mesenchymal markers *Vim*, *Zeb1*, *Cdh2* as well as stem/progenitor markers like *Sox9*, *c-kit*, *Tnfrsf12a* (also called *Fn14*), and *Cd44*. Various signaling pathways activate and maintain the EMT program including the Wnt/β-catenin and Tgf-β pathways (145). Our gene-set analysis identified Wnt and Tgf-βfamily signaling in addition to Notch(136) and hedgehog(153) signaling associated with hepatocyte-to-progenitor conversion. These data suggest multiple signaling events are responsible for the direct conversion of mature hepatocytes to progenitor cells and are consistent with an EMT process. Although genetic experiments have clearly shown a role for the Hippo signaling pathway in maintenance of the hepatocyte phenotype(137), its significance in oval cell injury induced metaplasia remains uncertain.

Hepatocyte-ductal metaplasia observed here follows the same pattern of epithelial-to-mesenchymal transition where transitioning cells later revert to their original state through mesenchymal-to-epithelial transition (MET)(145). Thus, the acquisition of mesenchymal attributes can be transient. In fact, fetal liver stem cells downregulate vimentin and other mesencymal markers as they differentiate into parenchymal epithelial cells(154). Additionally, the classic 2-AAF/partial hepatectomy model of oval cell activation is characterized by the reversible induction of mesenchymal markers including Vimentin, Tnfrsf12a (Fn14) and Bmp7(96,146).

We currently do not know whether ductal-metaplasia is an adaptive or maladaptive process. Two studies showed that ductal proliferation was required for adaptation to DDC injury and blocking ductal proliferation resulted in increased liver damage and decreased survival(133,135). On the other hand, our group recently showed that that cholangiocyte-progenitors were not producing a physiologically significant numbers of new hepatocytes (44). We now propose that hepatocyte-ductal-metaplasia is an injury evasion strategy that is facilitated by cholangiocyte proliferation. Metaplasia provides a mechanism to shut down the hepatocyte-gene expression program in order to avoid insults that are specifically toxic to hepatocytes but harm few other cell types (i.e. hepatitis virus, Cyp450-activated toxins, etc). This permits individual cells to improve their fitness. In our "decoy metaplasia" model, the hLPC pool expands in the presence of a regenerative stimulus (see Fig. 5-8, Graphical Abstract). If the injury is transient and eventually regresses, these hLPCs can revert back to their original fate: a mature hepatocyte.

Improving the efficiency of progenitor-to-hepatocyte reversion, or the mesenchymal-to-epithelial transition, with pharmacologic agents may represent a future strategy to improve hepatic function and outcomes in decompensated liver failure. Additionally, the propagation of hepatocyte-derived progenitor cells *in vitro* may provide an opportunity for autologous cell therapy in regenerative medicine applications. We speculate that a better understanding of the epigenetic mechanisms of "decoy metaplasia" in injury models may provide an opportunity for targeted therapies to provide a bridge to liver transplantation.

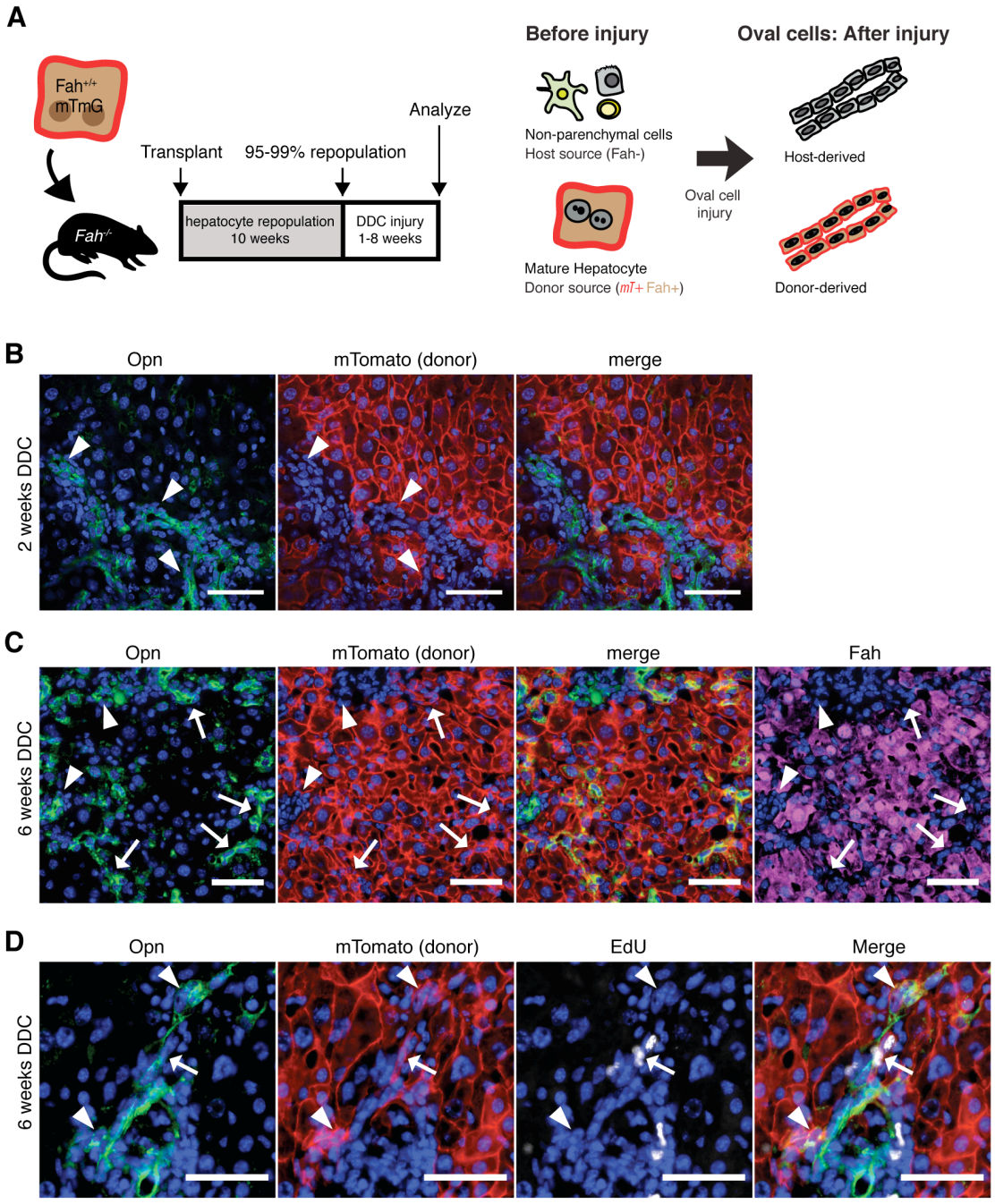

Figure 5-1: Hepatocyte-derived oval cells appear after extended injury.
A) Purified hepatocytes fluorescently marked hepatocytes were transplanted into the spleen of Fah-/- animals. After 10 weeks repopulation, DDC injury was given for 1 to 8 weeks. Since only hepatocytes were marked at baseline, any fluorescent marked ductal cells observed after injury were inferred to be hepatocytes-derived. B) Opn+ ductal proliferation did not colocalize with hepatocyte marker mTomato after 2 weeks injury (arrowhead), bar = 50µm. C) After 6 weeks of continuous injury, a fraction of Opn+ ductal cells co-localized with hepatocyte derived mTomato marked cells (arrow), however, the majority of ductal proliferation was still host-derived (arrowhead). Induction of ductal marker Opn was associated with the loss of Fah (arrows), bar = 50µm. D) Hepatocyte-derived progenitors (mTomato+ Opn+) incorporated EdU 6 hours after a pulse after 6 weeks of injury.

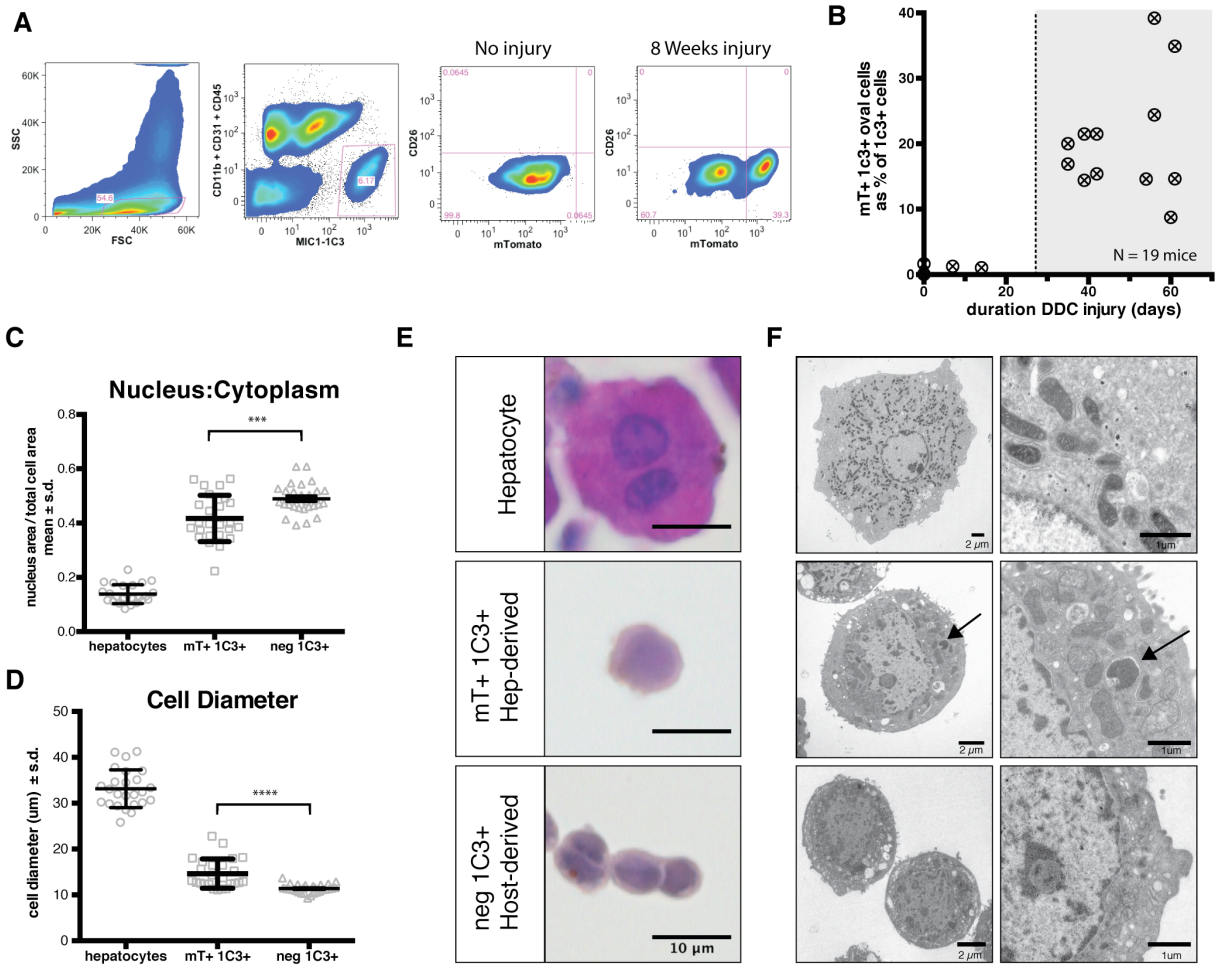

Figure 5-2: Hepatocyte-derived liver progenitors cells are isolated with MIC1-1C3 antibody
A) Non-parenchymal cells from dissociated livers were FACS sorted. Gates were applied for FSC/SSC, pulse width (not shown), PI- (not shown), and MIC1-1C3+ CD11b- CD31- CD45-. MIC1-1C3+ cell were then separated based on mTomato fluorescence as a marker of mature hepatocyte origin. Without injury mTomato+ cells were a trace component of MIC1-1C3+ population but increased with injury. B) The percentage of ductal cells derived from mTomato-marked hepatocytes is plotted against the number of days of DDC injury. Hepatocye-derived MIC1-1C3+ ductal progenitors emerged after approximately 4 weeks injury. C) FACS isolated populations were fixed and nucleus to cytoplasmic ratios and D) cell diameter and were examined for each population (pairwise t-test, $p<0.001$ ***, $p<0.0001$****). E) Representative H&E staining (bars = 10µm) and F) transmission electron microscopy from directly isolated cells from each population (bar size indicated). The arrow indicates a membrane bound structure in a lysosome adjacent to mitochondria.

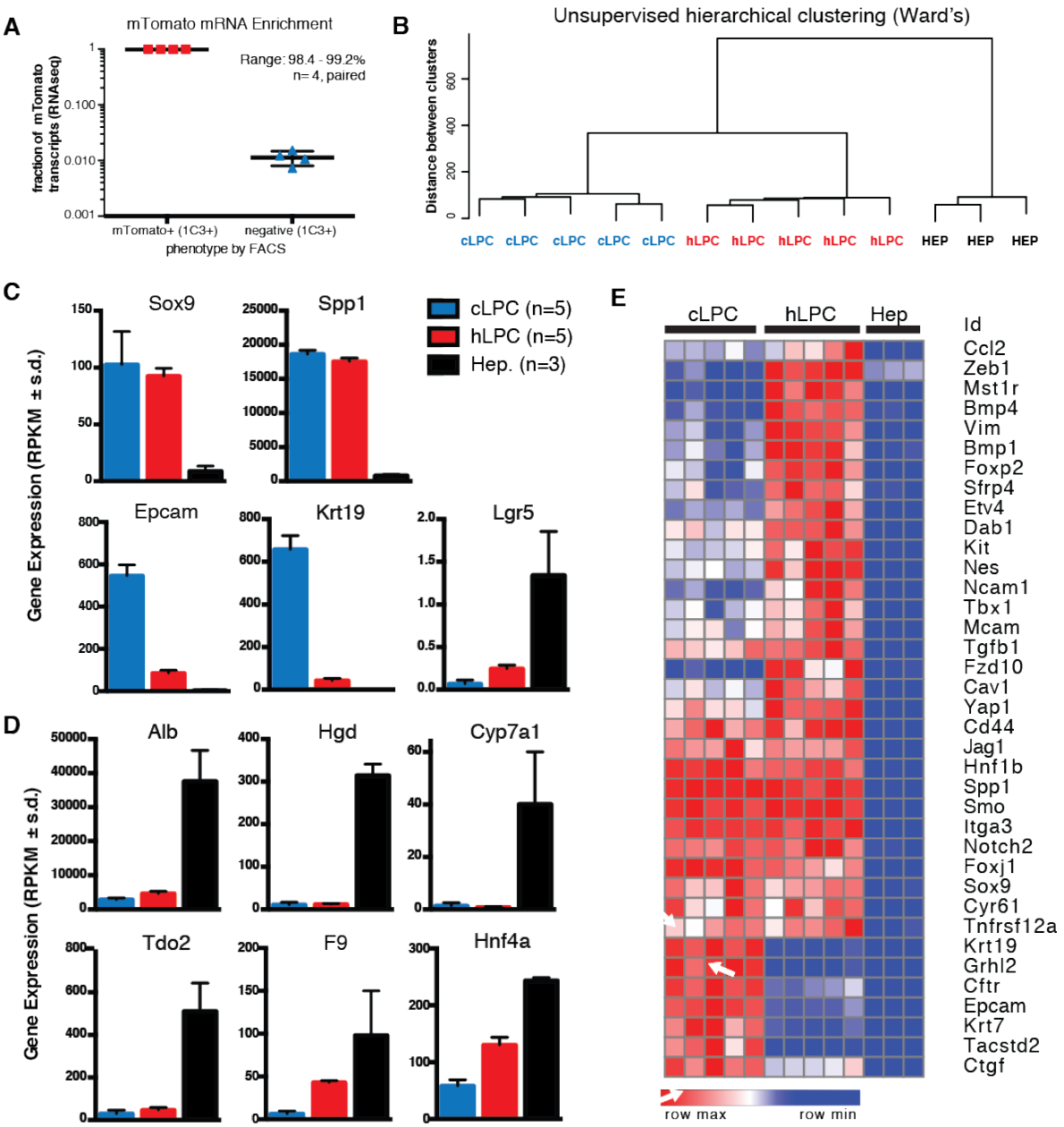

Figure 5-3: Hepatocyte-derived oval cells are transcriptional distinct from cholangiocytes. A) FACS separation of MIC1-1C3 cells based on ROSA-mTomato resulted in 98.4-99.2% enrichment in mTomato+ cells relative to mTomato- cells (paired analysis, n=4 animals). B) Unsupervised hierarchical clustering (Ward's method) showed that hepatocyte-derived liver progenitor cells (hLPCs) reproducibly clustered together and were distinct in phenotype from parental hepatocytes and cholangiocyte-derived liver progenitors (cLPCs). C) Gene expression in reads per kilobase per million exon mapped reads (RPKM) for progenitor associated genes and D) Hepatocyte-associated genes (mean ± s.d.) cLPCs (n=5), hLPCs (n=5), and hepatocytes (n=3). E) Cluster analysis shows hLPCs express biliary progenitor associated genes and a distinctive mesenchymal signature.

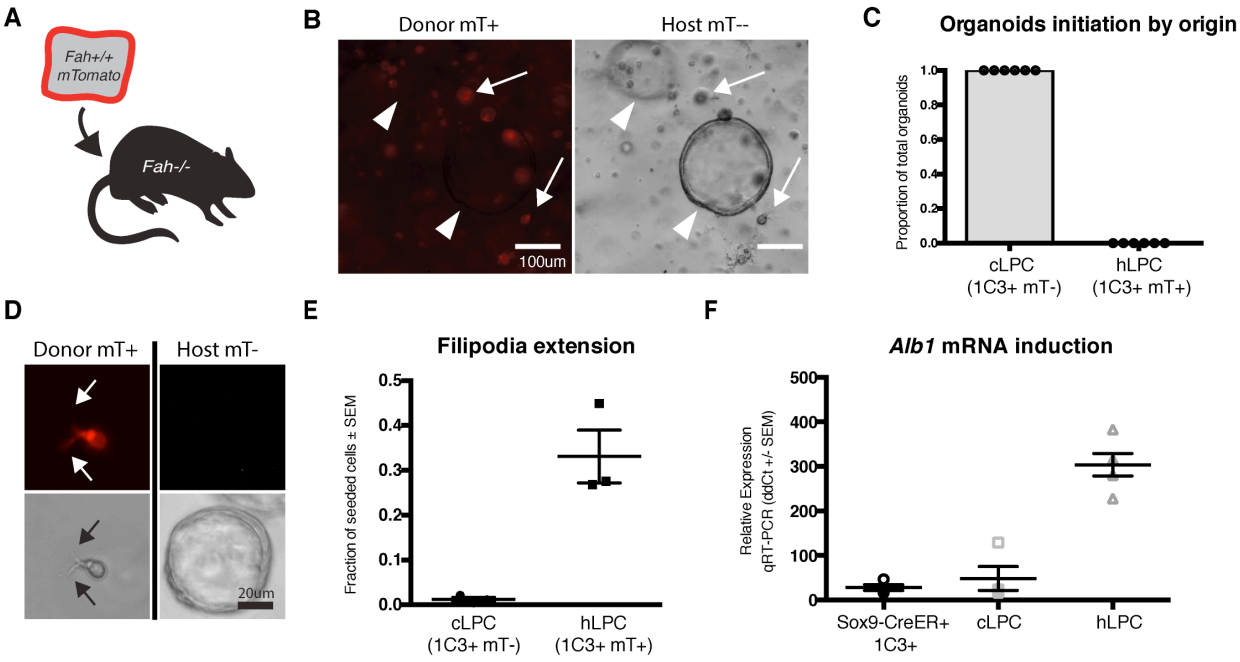

Figure 5-4: hLPCs are functionally distinct *in vitro*.
A) Fah$^{-/-}$ mice were repopulated with Fah$^{+/+}$ Rosa-mTomato+ hepatocytes and subsequently injured with DDC. B) Organoids derived from crude non-parenchymal preps from DDC injured chimeric liver were seeded in matrigel / Rspo1 conditions for organoid formation. Hepatocyte-derived mTomato+ cells (arrows) did not initiate organoids. All organoids were mTomato- (arrowhead).
C) MIC1-1C3+ mTomato+ and mTomato- cells were seeded into matrigel for organoid formation. All organoids were host-derived (50-200 counted/animal, n=6 animals). D) hLPCs formed fillipodia in matrigel (left) while mTomato- cholangiocyte-derived MIC1-1C3+ cells formed spherical organoids (right). E) Fillipodia formation was quantified as a fraction of seeded cells. F) hLPCs cultured in hepatic differentiation medium induced albumin mRNA with 10.8-fold greater efficiency than cLPCs or MIC1-1C3+ cells from uninjured Sox9-CreERT2 reporter mice (unpaired t-test, $p<0.001$***).

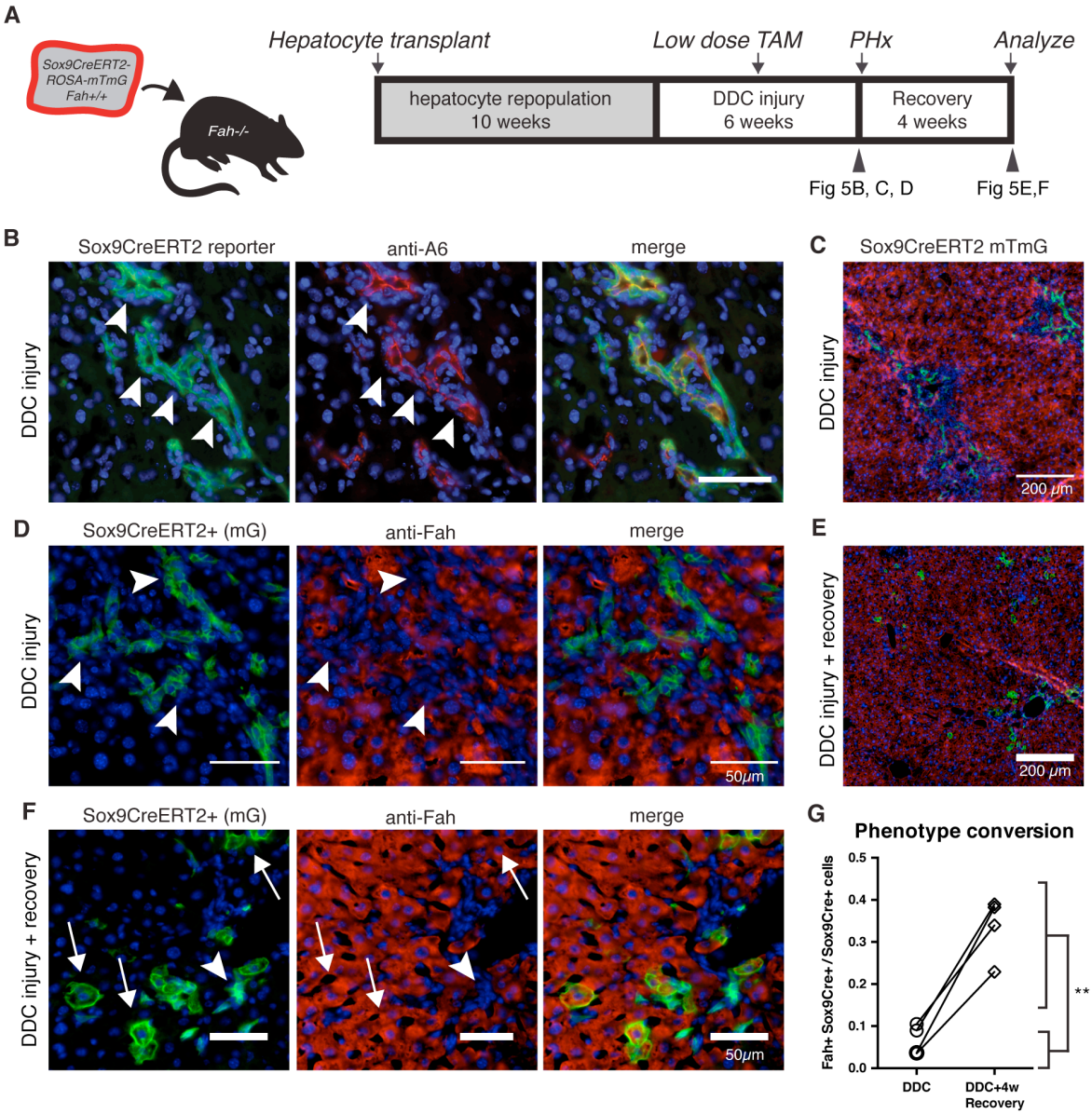

Figure 5-5: Hepatocyte-derived progenitors revert back to hepatocyctes *in vivo*.
A) Fah+/+ ROSA-mTmG Sox9-CreERT2 hepatocytes were transplanted into Fah-/- recipients to generate chimeras for lineage tracing. After 10 weeks repopulation DDC injury was given to repopulated chimeras for 4 weeks, a low dose pulse of tamoxifen was given (15mg/kg), and injury was continued for 2 additional weeks. B) Tissue harvested by 1/3 partial hepatectomy showed most Sox9-CreERT2 marked (mGFP+) cells co-localized with A6 antigen (arrowhead). C) Low-power view shows ductal cells in periportal zone with D) biliary morphology that do not co-localize with hepatocyte antigen FAH. E) Following a 4-week recovery period, mGFP+ hepatocytes localized in the portal area. F) Upon healing Sox9-Cre marked cells assumed hepatocyte morphology co-localized with Fah (arrow). G) Within animal comparison indicated that recovery from DDC injury was associated with a 5-fold increase in marked hepatocytes (6.6% versus 33.5%, $p < 0.01$**, paired t-test, n=4).

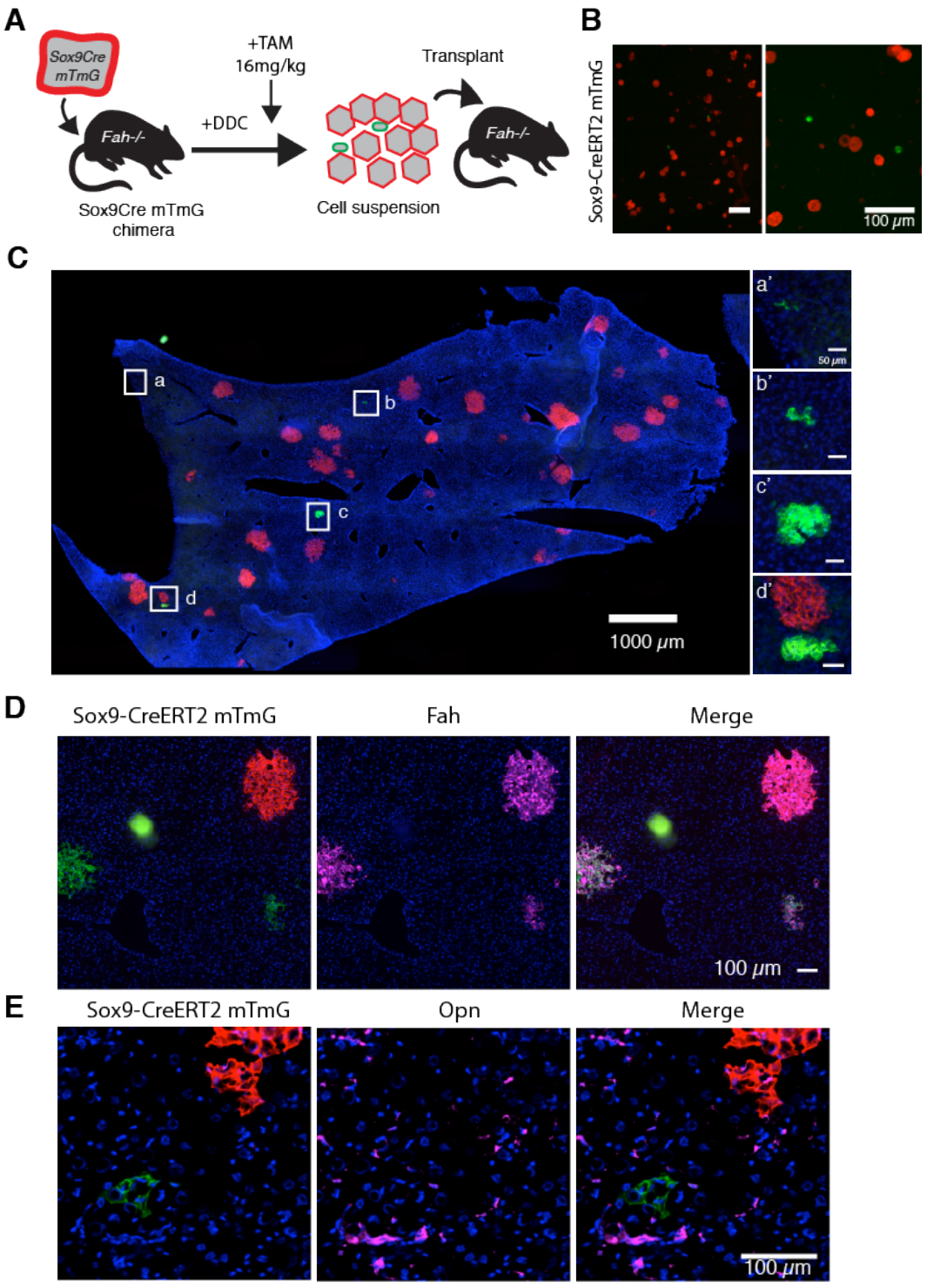

Figure 5-6: hLPCs differentiate back into hepatocytes upon serial transplantation
A) mGFP+ hLPC and mTomato+ hepatocytes were dissociated as single cells from DDC-injured chimeric mice for intrasplenic transplantation into Fah-/- mice. B) Sox9-CreERT2+ mGFP+ cells were smaller than hepatocytes and represented 6.3% of mTmG cells scored in 5 random fields before transplantation. C) After 5-weeks NTBC cycling, we assessed the rate at which mGFP+ hLPCs contributed to repopulation. mGFP+ clones were smaller than mTomato+ clones D) Hepatocyte-nodules expressed hepatocyte marker Fah but E) not biliary/progenitor marker Opn.

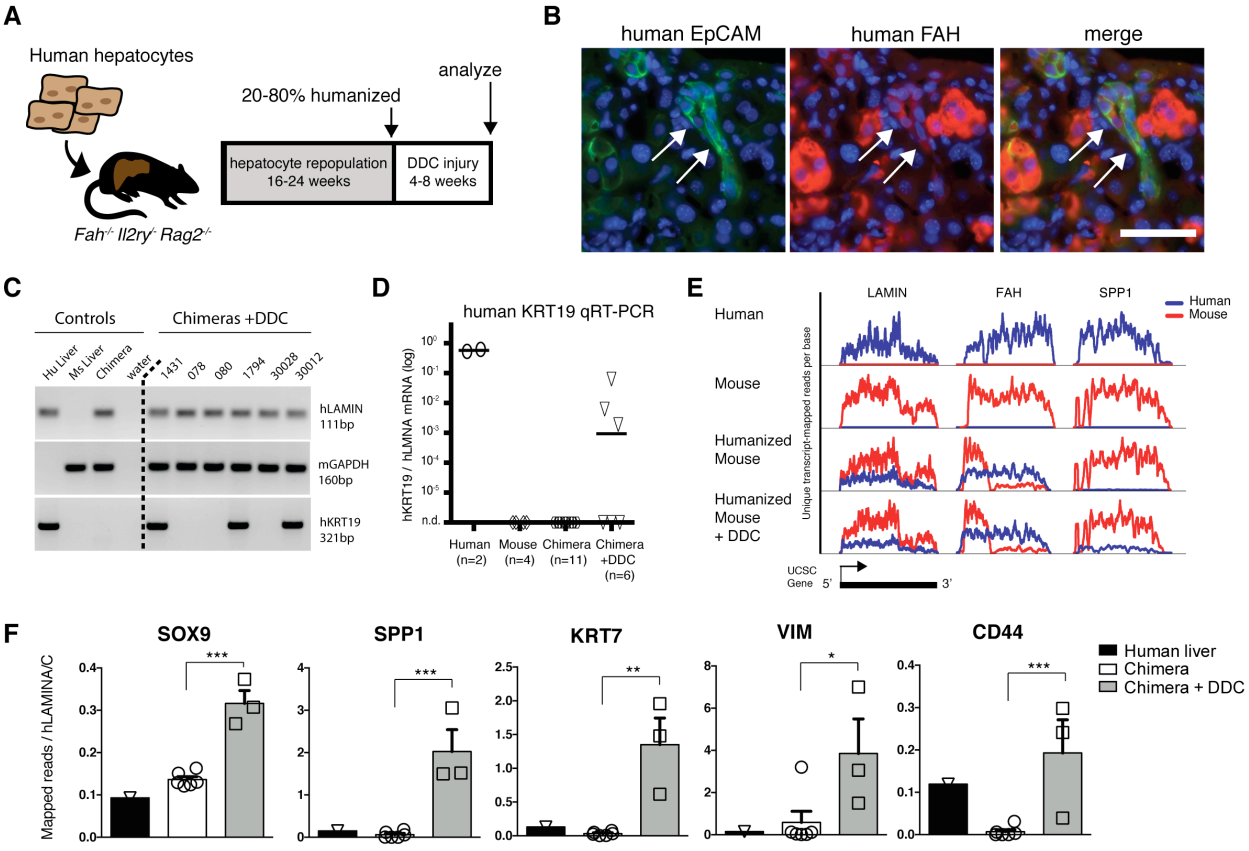

Figure 5-7: Human hepatocytes are directly converted into biliary-like cells *in vivo*.
A) Humanized livers were generated by human hepatocyte transplantation into FRG mice. After 16-24 weeks repopulation, animals were fed 0.1% DDC diet for 4-8 weeks. B) After injury, human EpCAM+ FAH^{low} cells with ductal morphology emerged. C) KRT19 qRT-PCR assay on whole liver specifically amplified human KRT19. 3/6 DDC-treated chimeric mice showed robust KRT19 induction. D) KRT19 levels relative to human LMNA were only 9-to-285 fold lower (n=3) than whole human liver reference samples (n=2). E) RNA-sequencing of whole chimeric livers effectively separated human (blue) from mouse (red) transcripts, graphed as unique transcript-mapped reads per position across each UCSC gene model (3 examples shown). The FAH transcript in chimeric livers shows expected truncation of mouse *Fah$^{\Delta exon5}$* and non-sense mediated decay but full length human FAH. F) Human mRNA levels of ductal progenitor genes were quantified relative to housekeeping gene LMNA in normal human liver (n=1), chimeric livers (n=6), and DDC injured chimeric livers (n=3)(mean ± SEM, *p <0.05, **p < 0.01, *** p<0.001).

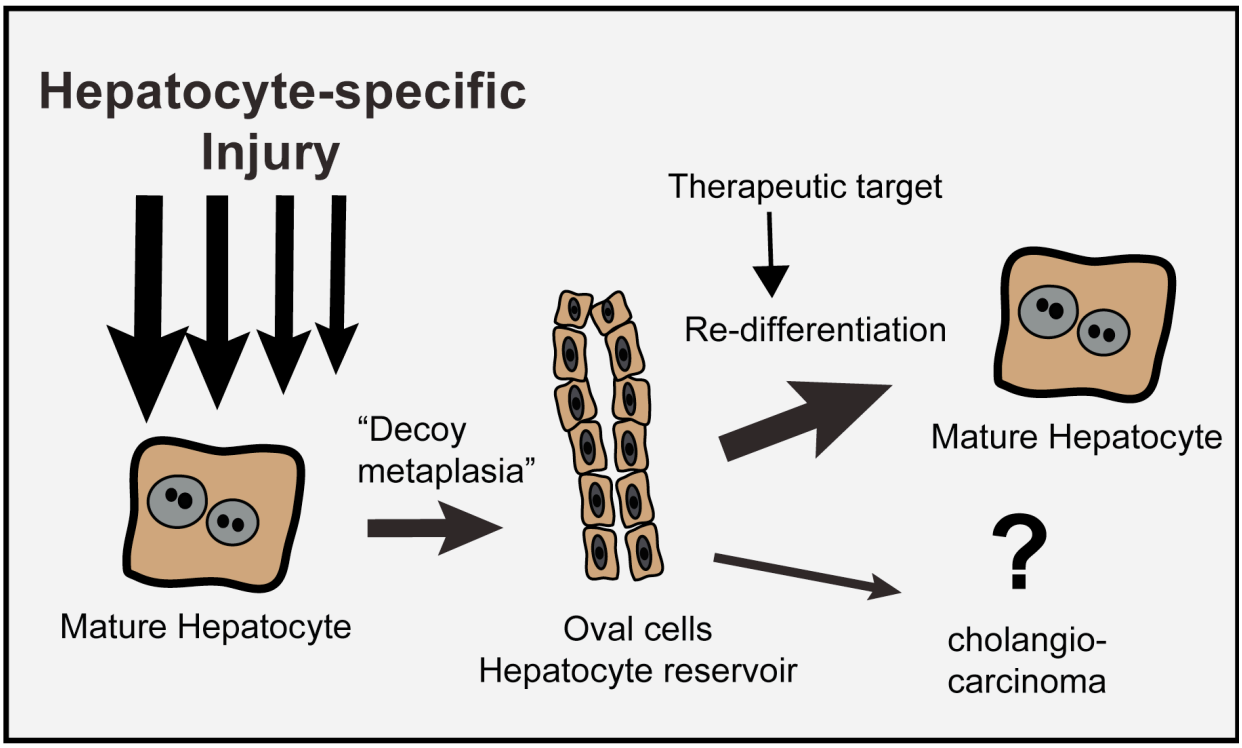

Figure 5-8: Decoy metaplasia hypothesis
Hepatocyte-specific injuries specifically target mature hepatocytes, causing cellular injury and death due to their phenotype. But loss of hepatic gene expression increases the fitness of the cell and reduces susceptible to hepatocellular injury. The ductal phenotype serves as a disguise or decoy. Hepatocyte-derived progenitors proliferate in the presence of a regenerative response. They cells may differentiate back into hepatocytes if injury is stopped or become transformed with continued injury.

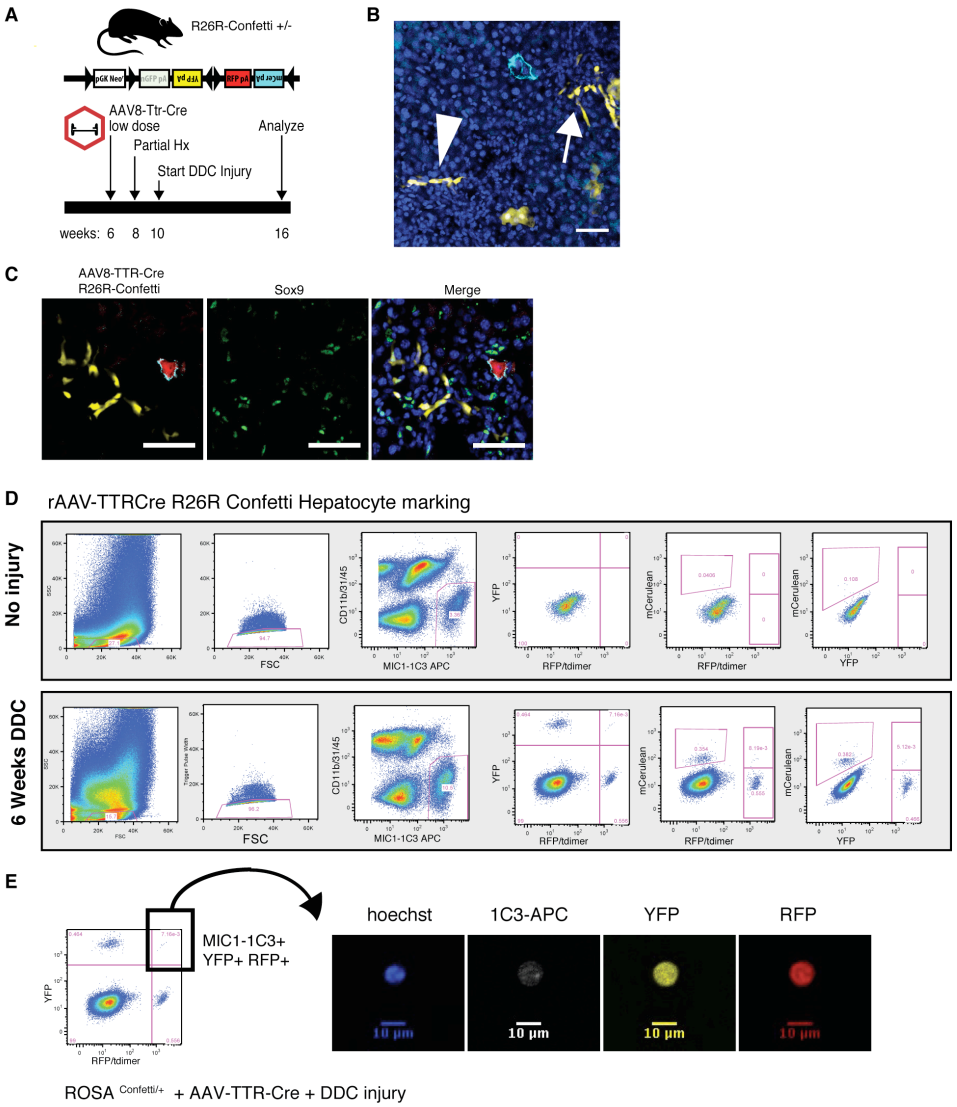

Figure 5-9: Hepatocytes labeled with rAAV8 clonally expand and undergo ductal metaplasia. A) Animals were given low dose rAAV8-Ttr-Cre (2e10 vg), administered partial hepatectomy to deplete rAAV particles, and 6 weeks 0.1% DDC to initiate an oval cell response. B) Confocal analysis of thick sections indicated single hepatocytes proliferated into clusters of 20-40 cells. Clusters of 24 cells (arrowhead) and >31 cells (arrow) are shown. C) Hepatocyte-derived ductal cells co-expressed Sox9 and Opn(not shown), bars = 50 µm. D) FACS based analysis indicated that rAAV-Ttr-Cre did not mark MIC1-1C3 cells without injury (top) but 2% of hepatocytes were marked in this animal (not shown). Following 6 weeks DDC injury (bottom) Cre-marked MIC1-1C3 cells were detected. E) Approximately 1% of hepatocyte-derived progenitors in R26R-Confetti heterozygous mice expressed 2 colors of the Confetti reporter. R26R-Confetti is present at 1 copy per diploid genome, suggesting that double-positive cells hepatocyte-derived progenitor cells were polyploidy. Microscopy confirmed that cells were not doublets.

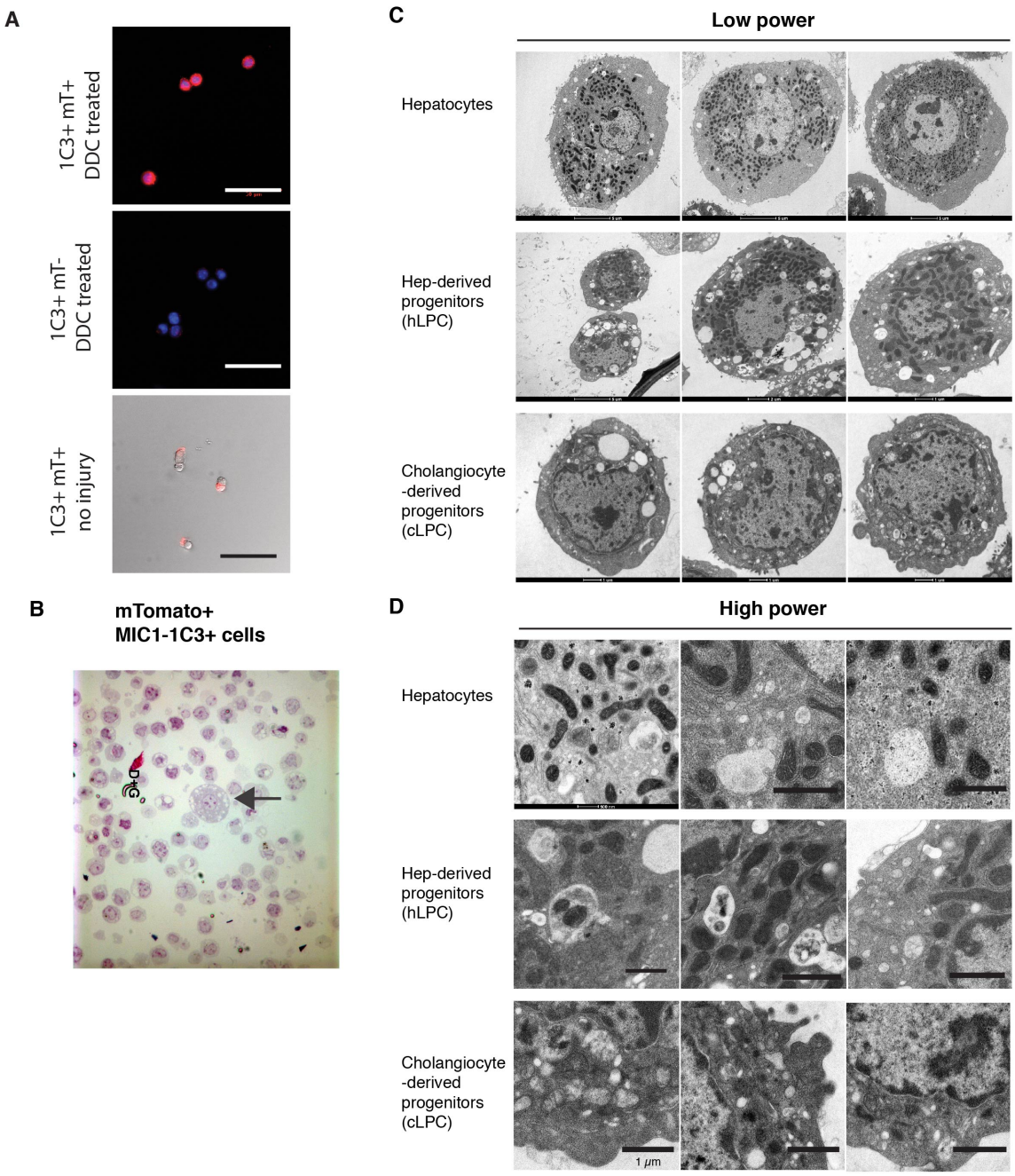

Figure 5-10: Additional microscopy images of sorted liver cells.
A) mTomato+ MIC1-1C3+ (top) or mTomato—MIC1-1C3+ (middle) from a DDC treated chimeric mouse were fixed and counterstained with Hoechst 33342. Rare MIC1-1C3+ mTomato+ trigger-pulse-width low FACS events (bottom) from an uninjured chimera (unfixed) had mTomato+ membrane fragments and adherent cells. B) Plastic section of hLPCs with a single contaminating hepatocytes present (arrow) shown for comparison. C) Low power TEM images of FACS sorted hepatocytes, hLPCs, and cLPCs and D) high power (bar length 1μm, or as indicated).

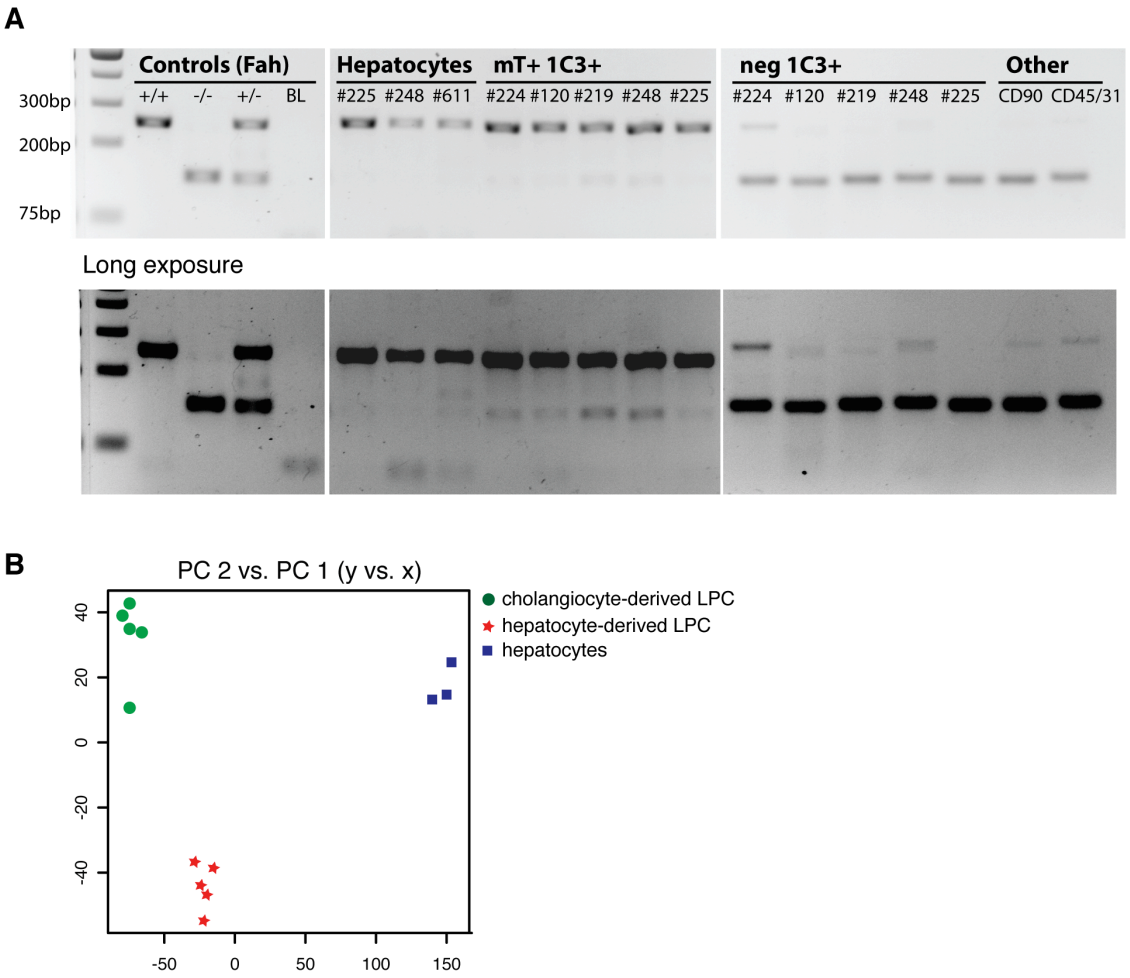

Figure 5-11: FACS-isolation based isolation of MIC1-1C3 by mTomato-status separates cells by origin and phenotype.
A) 3-primer DNA genotyping assay for *Fah* on FACS isolated MIC1-1C3+ cells confirms that mTomato was a reliable marker of cell origin. All samples were run on the same multi-row gel. Long exposure shows trace level cross contamination in FACS samples but not PCR controls. B) Principle-component analysis of RNAseq data separates three FACS sorted populations by gene expression.

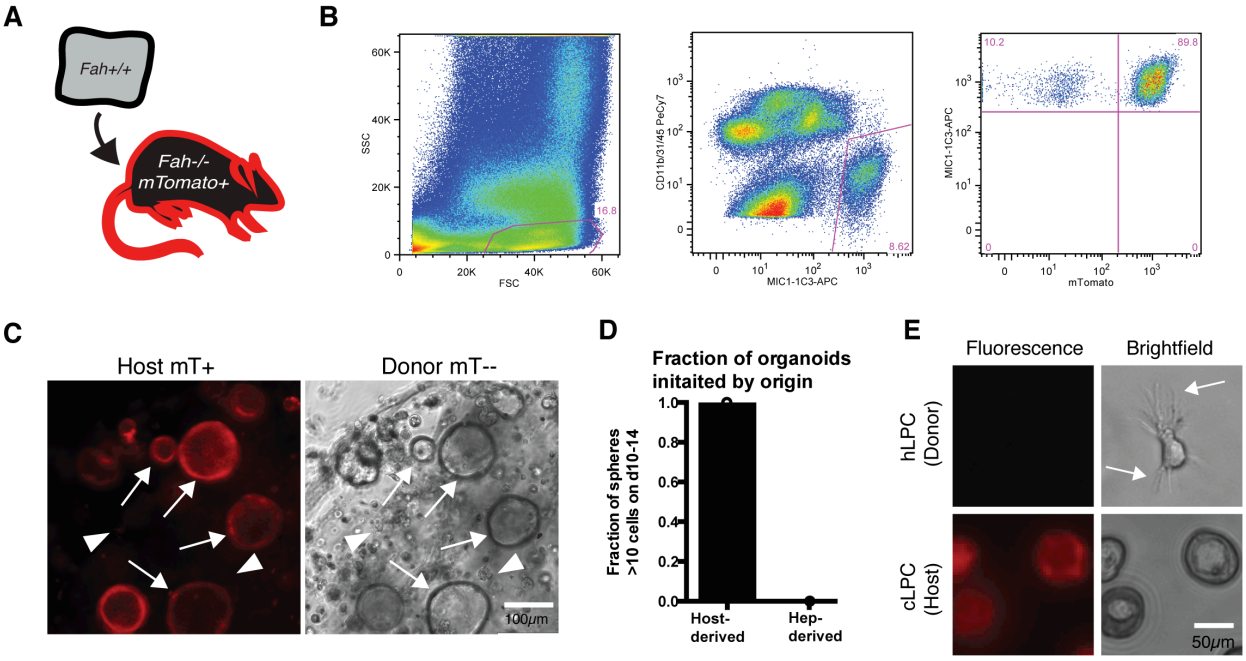

Figure 5-12: Color swap: *in vitro* differences are not an artifact of the mTomato fluorescent protein.

A) Wildtype hepatocytes were transplanted into ROSA-mTomato Fah$^{-/-}$ mice, allowed to repopulate for 10 weeks, and given DDC for 6 weeks. B) CD31- CD45- CD11b- MIC1-1C3+ cells were analyzed for mTomato status following DDC injury. C) Unsorted non-parenchymal cells were seeded into matrigel for organoid formation assay. mTomato+ cells formed organoids (arrowhead) but mTomato-negative cells did not (arrow). D) all organoids were mTomato+, indicating a cholangiocyte/host source. E) FACS sorted hLPCs (mTomato --) did not form organoids but extended filipoida, while host-derived cLPCs (mTomato+) initiated self-renewing organoid.

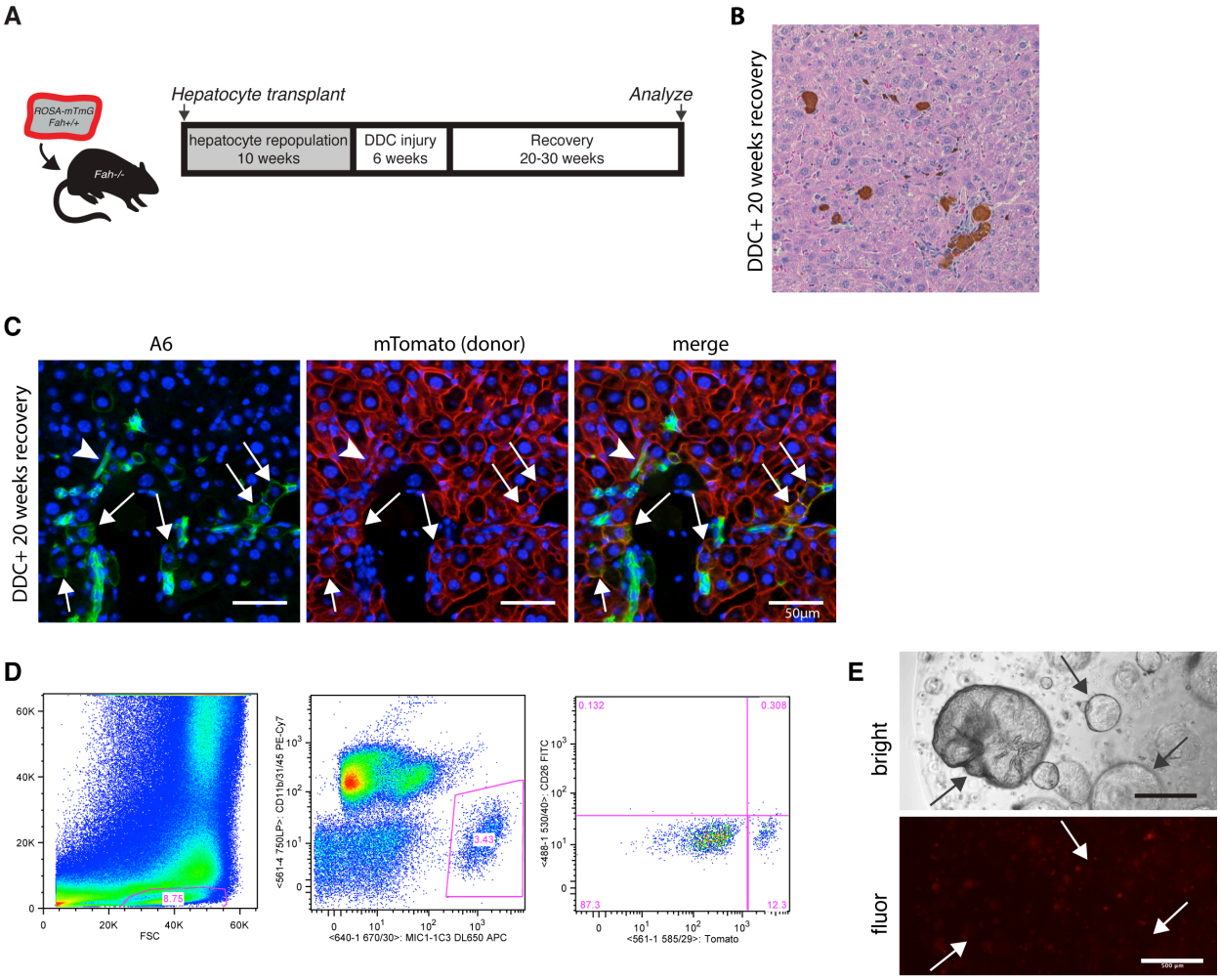

Figure 5-13: Fate of hLPCs in long-term recovery from DDC injury.
A) mTomato+ hepatocyte chimeric mice were allowed to recovery from DDC injury for 20-30 weeks (n=3). B) After 20 weeks on normal diet, livers showed residual cholestasis, inflammation, and porphyrin accumulation by H&E (bar = 50µm). C) A6-low hepatocytes (arrow) adjacent to biliary structures colocalized with ROSA-mTomato+ indicating they were hepatocyte-derived. Residual A6-high mTomato+ hLPCs were still present (arrowhead). D) Greater than 10% of MIC1-1C3+ cells were hepatocyte-derived by FACS-based analysis (n=3). E) All organoids were still host-derived (mTomato-negative) indicating that hepatocytes did not transdifferentiate into organoid forming progenitors after 20 weeks of recovery (bar = 500µm, representative image, n=2 animals).

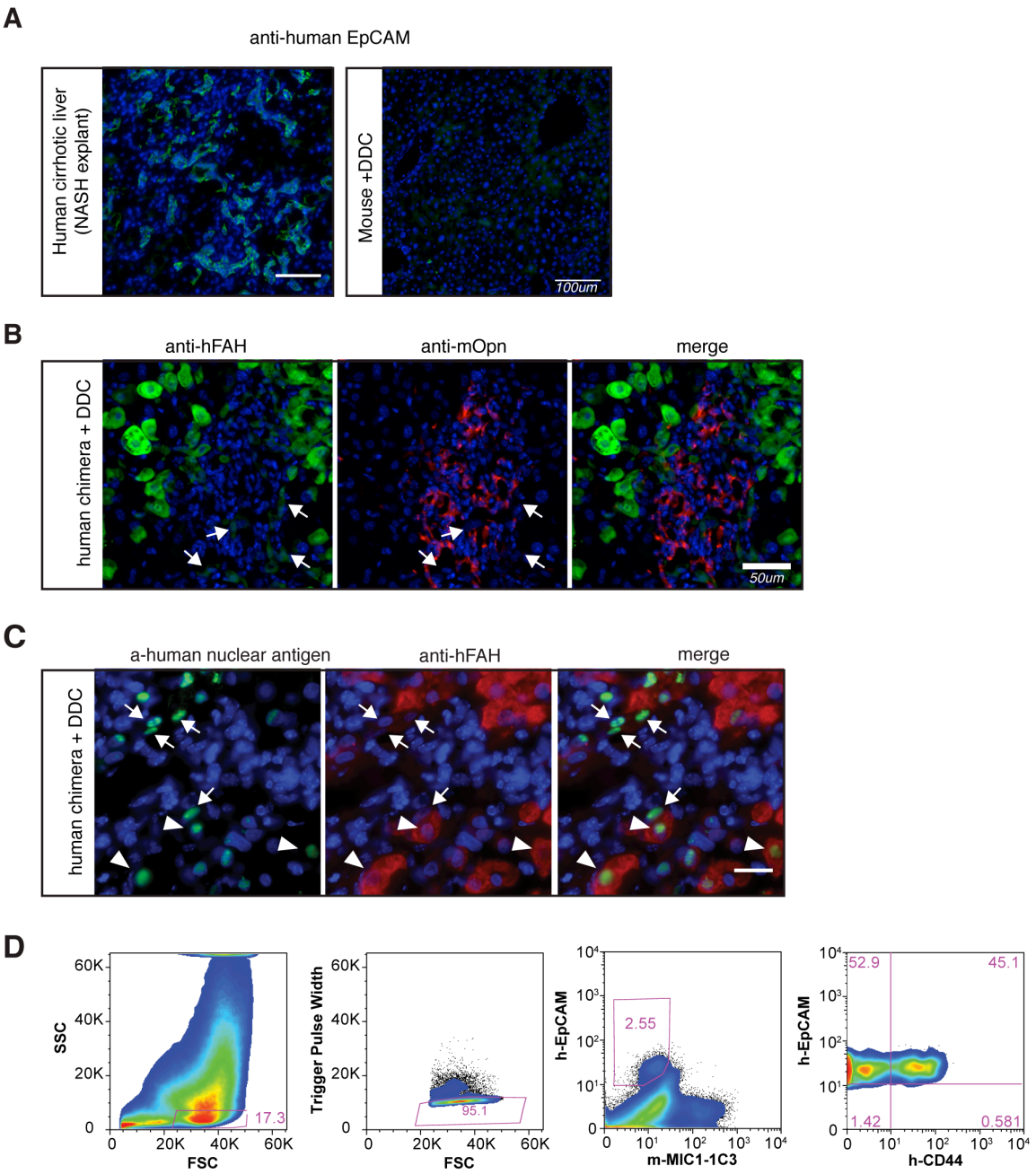

Figure 5-14: Identification of human hepatocyte-derived cells in chimeric livers with additional markers.

A) Anti-human EpCAM identified ductal reactions in cirrhotic human liver (non-alcoholic steatohepatitis explant) but not DDC-injured mouse liver tissue. B) Human hepatocyte-derived progenitors assume a ductal morphology (arrow), express low levels of FAH (FAH is overexposed in hepatocytes here), and are in close contact with mouse-Opn+ cells. C) Human hLPCs (arrows) are positive for human nuclear antigen, have ovoid nuclei and scant cytoplasm, and downregulate hepatocyte gene FAH. Hepatocytes (arrowhead) express high levels of FAH, have round nuclei and abundant cytoplasm. D) Livers from DDC treated humanized mice were dissociated into single cells and analyzed by flow cytometry. After injury, human EpCAM+ mouse MIC1-1C3-negative CD45-CD31- were identified. A subset of EpCAM+ cells were CD44+ in injured but not uninjured chimeras or cells from DDC treated mice analyzed in parallel (not shown).

Table 5-1: Gene expression of selected genes between cell types in DDC injury

Gene symbol	Hepatocytes(n=3) (RPKM)	s.d.	hep-derived LPC (n=5) (RPKM)	s.d.	chol-derived LPC (n=5) (RPKM)	s.d.	Fold diff: hLPC / Hep	hLPC / cLPC
Hepatocyte								
Alb	37559.47	9091.36	4653.57	1406.89	2872.78	489.03	**0.12**	**1.62**
Hgd	314.05	26.73	11.76	4.89	10.71	5.80	**0.04**	**1.10**
Cyp7a1	40.12	19.99	0.84	0.65	1.34	1.20	**0.02**	**0.63**
Ttr	3108.40	351.13	705.55	149.94	463.34	38.86	**0.23**	**1.52**
F9	135.63	11.16	43.14	4.85	6.54	3.31	**0.32**	**2.52**
Fah	292.62	57.61	58.87	7.36	14.014*	4.37	**0.20**	**N/A**
Tdo2	510.59	132.18	47.25	25.76	29.44	17.16	**0.09**	**1.61**
Hnf4a	243.50	5.19	130.29	30.12	58.34	10.81	**0.54**	**2.23**
Progenitor/cholangiocyte								
Sox9	8.84	4.48	92.45	15.41	102.56	29.11	**10.46**	**0.90**
Spp1 (Opn)	796.50	198.50	17559.80	1095.90	18618.33	587.62	**22.05**	**0.94**
Hnf1b	12.77	1.17	158.86	12.92	176.43	21.44	**12.44**	**0.90**
Krt19	0.36	0.29	42.54	23.45	657.89	65.25	**119.27**	**0.06**
Lgr5	1.34	0.52	0.24	0.10	0.07	0.05	**0.18**	**3.70**
Cd44	11.24	2.97	178.73	37.13	150.82	35.34	**15.90**	**1.19**
Cd24	2.02	0.84	481.16	61.65	676.05	85.61	**238.59**	**0.71**
Nes	0.04	0.03	8.54	2.06	2.94	0.47	**213.60**	**2.91**
Kit	0.14	0.06	7.22	2.06	2.94	0.51	**52.83**	**2.46**
Epcam	0.83	0.14	85.30	29.48	545.47	51.95	**103.19**	**0.16**
Itga3 (MIC1-1C3)	6.79	0.71	157.60	15.29	154.36	6.57	**23.20**	**1.02**
Cftr	0.02	0.03	11.50	3.61	49.78	5.23	**492.86**	**0.23**
Tacstd2 (Trop2)	0.02	0.02	1.16	0.57	38.75	11.30	**57.90**	**0.03**
Tnfrsf12a (Fn14)	116.01	13.28	314.77	63.33	278.23	45.34	**2.71**	**1.13**
Prom1 (Cd133)	10.96	15.11	26.59	9.19	139.14	17.75	**2.43**	**0.19**
Jag1	1.51	0.65	75.73	9.86	77.66	23.22	**50.15**	**0.98**
Notch2	14.43	1.46	56.36	8.42	51.75	4.03	**3.90**	**1.09**
EMT-related								
Zeb1	5.04	0.26	12.55	0.85	3.44	0.90	**2.49**	**3.65**
Vim	9.12	4.74	211.34	33.53	45.79	25.42	**23.16**	**4.62**
Cdh2	29.47	2.37	60.19	4.68	13.19	5.24	**2.04**	**4.56**
Ncam1	0.01	0.01	7.03	2.82	1.36	0.70	**1054.80**	**5.16**
Smo	1.38	0.46	36.47	2.16	35.23	2.65	**26.42**	**1.04**
Snai1	0.09	0.10	0.09	0.04	0.88	0.52	**1.02**	**0.10**
Snai2	3.86	1.37	1.52	0.33	0.50	0.23	**0.39**	**3.02**
Twist1	0.01	0.01	0.19	0.07	0.17	0.12	**27.90**	**1.12**
Cdh1	100.13	9.08	377.64	36.59	553.60	39.05	**3.77**	**0.68**
Other cell types								
Ptprc (Cd45)	0.22	0.18	1.46	0.98	2.89	1.97	**6.62**	**0.50**
Pecam1 (Cd31)	0.44	0.32	1.64	1.06	3.96	2.56	**3.76**	**0.42**
Gfap	0.00	0.01	0.08	0.04	0.30	0.07	**22.80**	**0.25**
Thy1	0.02	0.00	0.40	0.49	0.77	0.67	**20.10**	**0.52**
Col1a1	0.20	0.17	3.68	1.47	35.64	39.97	**18.41**	**0.10**
Desmin	0.05	0.02	0.30	0.13	1.55	1.11	**5.92**	**0.19**
Yap1	30.93	0.06	52.73	2.76	42.73	3.30	**1.70**	**1.23**
Ctgf	0.85	0.15	205.68	52.08	494.72	83.77	**241.98**	**0.42**
Cyr61	71.07	11.90	1037.55	326.93	1056.27	401.06	**14.60**	**0.98**
AmotL2	6.40	2.39	57.40	8.31	92.56	17.35	**8.96**	**0.62**
Rbfox3 (NeuN)	0.00	0.01	0.02	0.01	0.09	0.08	**4.80**	**2.52**
Afp	2.96	0.67	3.48	0.68	2.62	1.85	**1.18**	**2.52**

*Denotes gene deletion at exon5

Table 5-2: Genesets enriched in hLPCs versus Hepatocytes

Geneset DETAILS	SIZE	NES	NOM p-val	FDR q-val
KEGG_NOTCH_SIGNALING_PATHWAY	42	1.6	0.001	0.073
KEGG_BASAL_CELL_CARCINOMA	54	1.61	0.001	0.114
KEGG_MELANOGENESIS	93	1.48	0.001	0.144
KEGG_HYPERTROPHIC_CARDIOMYOPATHY_HCM	83	1.42	0.004	0.151
KEGG_ARRHYTHMOGENIC_RV_CARDIOMYOPATHY	74	1.49	0	0.151
KEGG_FOCAL_ADHESION	184	1.38	0.001	0.161
KEGG_PATHWAYS_IN_CANCER	304	1.39	0	0.162
KEGG_EPITHELIAL_CELL_SIGNALING_IN_H_PYLORI	63	1.42	0.005	0.162
KEGG_ECM_RECEPTOR_INTERACTION	80	1.4	0.009	0.169
KEGG_PHOSPHATIDYLINOSITOL_SIGNALING_SYSTEM	64	1.39	0.013	0.171
KEGG_DILATED_CARDIOMYOPATHY	89	1.42	0.008	0.172
KEGG_AXON_GUIDANCE	125	1.5	0	0.173
KEGG_SPLICEOSOME	94	1.39	0.002	0.174
KEGG_NEUROTROPHIN_SIGNALING_PATHWAY	116	1.42	0	0.178
KEGG_HEDGEHOG_SIGNALING_PATHWAY	54	1.51	0.004	0.187
KEGG_WNT_SIGNALING_PATHWAY	140	1.43	0.001	0.188
KEGG_COLORECTAL_CANCER	60	1.36	0.027	0.191
KEGG_TIGHT_JUNCTION	119	1.45	0.002	0.191
KEGG_MAPK_SIGNALING_PATHWAY	249	1.43	0	0.193
KEGG_LEISHMANIA_INFECTION	47	1.35	0.037	0.203
KEGG_RENAL_CELL_CARCINOMA	67	1.34	0.026	0.207
KEGG_OLFACTORY_TRANSDUCTION	28	1.34	0.069	0.211
KEGG_ENDOCYTOSIS	150	1.33	0.005	0.219
KEGG_T_CELL_RECEPTOR_SIGNALING_PATHWAY	104	1.32	0.01	0.22
KEGG_REGULATION_OF_ACTIN_CYTOSKELETON	192	1.33	0.001	0.223
KEGG_ERBB_SIGNALING_PATHWAY	83	1.3	0.034	0.224
KEGG_FC_GAMMA_R_MEDIATED_PHAGOCYTOSIS	84	1.3	0.038	0.226
KEGG_CELL_CYCLE	113	1.31	0.007	0.227
KEGG_CHRONIC_MYELOID_LEUKEMIA	70	1.3	0.043	0.233
KEGG_ENDOMETRIAL_CANCER	49	1.29	0.077	0.233
KEGG_TGF_BETA_SIGNALING_PATHWAY	84	1.29	0.037	0.234
KEGG_VEGF_SIGNALING_PATHWAY	69	1.31	0.043	0.235
KEGG_ADHERENS_JUNCTION	72	1.27	0.034	0.236
KEGG_SMALL_CELL_LUNG_CANCER	80	1.29	0.048	0.236
KEGG_GLYCOSAMINOGLYCAN_BIOSYNTHESIS_CHONDROITIN_SULFATE	15	1.31	0.111	0.236
KEGG_VASOPRESSIN_REGULATED_WATER_REABSORPTION	42	1.28	0.09	0.238
KEGG_DNA_REPLICATION	33	1.28	0.107	0.242
KEGG_GNRH_SIGNALING_PATHWAY	94	1.28	0.042	0.245

Table 5-3: Genesets enriched in hLPCs versus cLPCs

Geneset DETAILS	SIZE	NES	NOM p-val	FDR q-val
KEGG_TYROSINE_METABOLISM	36	2.35	0	0
KEGG_FATTY_ACID_METABOLISM	33	2.25	0	0.001
KEGG_BETA_ALANINE_METABOLISM	22	2.18	0	0.001
KEGG_TRYPTOPHAN_METABOLISM	37	2.15	0	0
KEGG_COMPLEMENT_AND_COAGULATION_CASCADES	48	2.13	0	0
KEGG_BUTANOATE_METABOLISM	30	2.11	0	0
KEGG_DRUG_METABOLISM_CYTOCHROME_P450	42	2.05	0	0.001
KEGG_VALINE_LEUCINE_AND_ISOLEUCINE_DEGRADATION	41	2.03	0	0.001
KEGG_PHENYLALANINE_METABOLISM	18	2	0	0.001
KEGG_CYSTEINE_AND_METHIONINE_METABOLISM	30	1.99	0	0.001
KEGG_BIOSYNTHESIS_OF_UNSATURATED_FATTY_ACIDS	18	1.93	0	0.002
KEGG_ASCORBATE_AND_ALDARATE_METABOLISM	13	1.92	0.003	0.002
KEGG_HISTIDINE_METABOLISM	27	1.92	0.004	0.002
KEGG_PEROXISOME	71	1.91	0	0.002
KEGG_PENTOSE_AND_GLUCURONATE_INTERCONVERSIONS	14	1.87	0	0.003
KEGG_DRUG_METABOLISM_OTHER_ENZYMES	27	1.85	0	0.005
KEGG_LIMONENE_AND_PINENE_DEGRADATION	10	1.81	0.003	0.007
KEGG_GLYCINE_SERINE_AND_THREONINE_METABOLISM	31	1.73	0.004	0.013
KEGG_FOLATE_BIOSYNTHESIS	10	1.71	0.011	0.014
KEGG_AMINOACYL_TRNA_BIOSYNTHESIS	32	1.7	0	0.016
KEGG_PROPANOATE_METABOLISM	30	1.67	0.004	0.021
KEGG_CITRATE_CYCLE_TCA_CYCLE	28	1.63	0	0.028
KEGG_PRIMARY_BILE_ACID_BIOSYNTHESIS	15	1.6	0.023	0.036
KEGG_ALANINE_ASPARTATE_AND_GLUTAMATE_METABOLISM	31	1.58	0.008	0.04
KEGG_ARGININE_AND_PROLINE_METABOLISM	50	1.55	0.005	0.048
KEGG_RETINOL_METABOLISM	31	1.54	0.021	0.049
KEGG_MATURITY_ONSET_DIABETES_OF_THE_YOUNG	19	1.54	0.038	0.048
KEGG_PORPHYRIN_AND_CHLOROPHYLL_METABOLISM	29	1.54	0.025	0.048
KEGG_NICOTINATE_AND_NICOTINAMIDE_METABOLISM	21	1.53	0.031	0.049
KEGG_PANTOTHENATE_AND_COA_BIOSYNTHESIS	15	1.52	0.038	0.051
KEGG_METABOLISM_OF_XENOBIOTICS_BY_CYTOCHROME_P450	39	1.48	0.028	0.067
KEGG_GLUTATHIONE_METABOLISM	45	1.47	0.052	0.069
KEGG_LYSINE_DEGRADATION	43	1.44	0.038	0.08
KEGG_ABC_TRANSPORTERS	40	1.43	0.049	0.083
KEGG_RIBOFLAVIN_METABOLISM	16	1.39	0.103	0.104
KEGG_PROTEASOME	43	1.38	0.045	0.105
KEGG_SELENOAMINO_ACID_METABOLISM	21	1.35	0.108	0.121
KEGG_PPAR_SIGNALING_PATHWAY	61	1.33	0.048	0.135
KEGG_GLYCOLYSIS_GLUCONEOGENESIS	54	1.26	0.087	0.194
KEGG_LYSOSOME	114	1.23	0.054	0.219
KEGG_PENTOSE_PHOSPHATE_PATHWAY	24	1.21	0.154	0.237
KEGG_STEROID_HORMONE_BIOSYNTHESIS	31	1.21	0.151	0.237
KEGG_REGULATION_OF_AUTOPHAGY	28	1.19	0.162	0.246

Table 5-4: Total transcript-mapped reads in 21 selected genes from DDC treated humanized mice and controls

Gene	30141_ Chimera	30154_ Chimera	1794_Chimera_DDC	30012_ Chimera	225_Mouse_Heps	225_Mouse_MIC11c3	Normal Human Liver	F19b1_ Chimera	F19b2_ Chimera	F19b3_ Chimera	Human Cholang-iocytes	1431_Chimera_DDC	3567_Chimera_DDC	Refseq ID	% identity (species-species)	% gaps
ACTB	847	900	7471	9280	27	151	6803	2667	1502	3817	74351	981	1692	NM_001101.3	90	1
ALB	484250	655243	691371	1325310	0	0	640934	760431	259616	433514	283474	162014	349546	NM_000477.5	77	1
CD24A	46	56	2280	200	0	0	244	47	11	16	17697	435	231	NM_001792.3	78	8
CD44	0	1	430	35	0	0	91	0	0	3	192	51	16	NM_013230.2	79	3
CDH2	145	257	887	1066	0	1	350	475	82	213	2970	151	216	NM_000610.3	88	1
FAH	642	792	1721	1994	0	0	564	767	275	822	242	231	537	NM_001454.3	85	0
FOXJ1	0	0	3	0	0	0	0	0	0	0	141	0	0	NM_007197.3	87	1
FZD10	0	0	0	0	0	0	0	0	0	0	0	0	0	NM_000137.2	86	1
GAPDH	1794	2397	9850	7841	1	1	3581	5210	3109	7165	9557	1451	2255	NM_000181.3	89	0
GUSB	176	248	1620	828	0	0	534	272	97	314	1158	115	411	NM_001289745.1	79	1
HNF1B	15	26	247	77	4	67	88	31	10	45	3355	38	44	NM_000458.2	86	2
JAG1	5	12	162	12	1	17	76	28	17	45	5597	31	26	NM_000214.2	89	1
KRT19	0	1	0	0	0	0	129	0	1	0	5702	4	0	NM_002276.4	84	1
KRT7	7	16	2826	88	0	0	99	1	4	3	16575	314	253	NM_005556.3	85	1
LMNA	221	315	1444	1133	0	0	764	325	177	489	18240	212	411	NM_170707.3	84	1
SMO	233	273	282	913	0	0	164	158	52	151	323	40	94	NM_000582.2	88	1
SOX9	36	39	538	146	0	0	71	49	23	59	8267	65	110	NM_005631.4	89	2
SPP1	26	57	4413	66	0	0	116	0	0	2	6501	322	616	NM_000346.3	80	1
TTR	9348	13098	12529	32752	0	0	21720	7799	2576	6200	898	1509	5176	NM_000371.3	81	0
VIM	1	4	262	10	0	0	752	0	4	0	11407	36	6	NM_003380.3	90	1
ZEB1	70	51	129	182	19	28	90	108	46	37	18	52	35	NM_001128128.2	86	1
mActb	222153	208173	193101	178538	107822	26466	0	182431	180821	211433	0	351304	178593	NM_007393.3		
mAlb	2079696	2490783	3465719	2514398	1969623	280099	0	2376240	1759517	1758750	0	4236799	2065659	NM_009654.3		
mCd24A	1725	1775	1229	1530	12501	3225	0	490	784	966	0	1842	1197	NM_007664.4		
mCd44	554	960	977	711	600	10937	0	869	700	884	0	975	696	NM_009846.2		
mCdh2	657	1080	805	840	945	13385	0	623	681	840	0	1131	712	NM_009851.2		
mFah	3828	37385	31513	9864	32438	637838	0	2063	2403	2266	0	98928	22385	NM_008240.3		
mFoxj1	62	95	529	276	3	1115	0	133	304	375	0	1454	767	NM_175284.3		
mFzd10	41	166	592	245	2	1102	11	80	67	119	307	794	470	NM_010176.4		
mGapdh	370	1229	503	329	172	10816	0	769	362	412	2	684	485	NM_010368.1		
mGusb	706	1233	1960	911	108	34171	0	1297	4621	4319	0	4774	1426	NM_001289726.1		
mHnf1B	182	482	682	297	172	5800	0	479	422	756	0	753	338	NM_001291268.1		
mJag1	32	334	310	90	18	4966	0	16	19	30	0	384	262	NM_013822.5		
mKrt19	1751	2025	3471	1679	2361	3460	0	2437	2291	3071	0	3311	1697	NM_008471.2		
mKrt7	2685	3004	4899	2843	5911	12193	0	7306	6218	8930	0	6034	3195	NM_033073.3		
mLmna	61817	59751	51286	47340	80796	44334	1	49978	76233	88338	11	69571	51227	NM_001002011.3		
mSmo	3101	3440	3211	2350	5879	14168	0	4049	4325	5069	1	4480	2625	NM_001204201.1		
mSox9	795	924	570	602	721	1901	1	1157	1202	1299	0	992	560	NM_176996.4		
mSpp1	1	0	4	0	17	329	0	6	2	0	0	3	3	NM_011448.4		
mTtr	1118	1448	5322	2720	469	11764	0	991	792	1032	5	7153	2479	NM_013697.5		
mVim	260	458	2790	883	2175	30612	0	758	399	400	0	3707	1388	NM_011701.4		
mZeb1	15081	12558	34180	16161	28419	64649	41	71139	82192	107686	527	47776	24449	NM_011546.3		
TOTAL	2,894,477	3,501,089	4,542,118	4,164,540	2,251,204	1,213,595	677,224	3,481,679	2,391,957	2,649,870	467,518	5,010,901	2,722,288			
Human	497,862	673,786	738,465	1,381,933	52	265	677,170	778,368	267,602	452,895	466,665	168,052	361,675			
Mouse	2,396,615	2,827,303	3,803,653	2,782,607	2,251,152	1,213,330	54	2,703,311	2,124,355	2,196,975	853	4,842,849	2,360,613			
% human tags	17.20%	19.25%	16.26%	33.18%	0.00%	0.02%	99.99%	22.36%	11.19%	17.09%	99.82%	3.35%	13.29%			
Erroneous alignment					0.0023%	0.0218%					0.1825%					

CHAPTER 6: THERAPEUTIC APPLICATIONS OF BASIC BIOLOGY

Chapter summary[§]

- *Patients with chronic liver disease need therapies to improve liver function & regeneration*
- *Cell therapy and bioengineering provide promising applications*
- *Extrahepatic cell therapy autologous hepatocyte cell therapy may be feasible for patients who are not transplantation candidates*

Treating liver failure: current approaches

Cirrhosis is a heterogeneous clinical syndrome associated with high mortality rates. It is estimated that up to 1% of the population in the United States is afflicted with some stage of the disease(2). Chronic liver disease or cirrhosis is the 12th leading cause of death for the total population in the United States and accounted for 31,903 deaths in 2010 according to the Center for Disease Control(1). Patients with decompensated cirrhosis, characterized by jaundice, ascites, and/or esophageal varices have a 20-57% one-year mortality rate without transplantation (5). Five-year mortality rates once cirrhosis has progressed are as high as 85% in patients who do not receive transplants(2). Orthotopic liver transplantation significantly improves the survival and quality of life of patients who receive new livers. But a large proportion of cirrhotic patients die on the transplantation list due to a severe

[§] This work is unpublished. The cirrhotic human hepatocyte work was done in collaboration with Bin Li, Scott Naugler, Matthew Taylor, and Annelise Haft. I procured livers from the operating room, performed some of the organ perfusions, some of the surgeries, and minority of the animal care work. I coordinated immunohistochemical work with Milton J. Finegold at Baylor College of Medicine

shortage of donor livers. Additional patients are never added to the transplantation list due to substance problems, lack of insurance, or a lack of support.

Medical management and supportive care have produced impressive improvements in both the survival and quality of life of patients with cirrhosis in the last few decades. The death rate for all patients with cirrhosis has dropped from 40 per 100,000 in 1975 to less than 15 per 100,000 in 2000(6). Treating the underlying disease is likely to blunt the progression of the disease. Abstinence treatment for alcoholic cirrhosis, antiviral therapy for hepatitis C-cirrhosis, corticosteroid treatment of autoimmune hepatitis, and nucleoside inhibitors for hepatitis B, and iron chelation therapy for hematochromatosis all improve outcomes for patients with cirrhosis. Some evidence suggests that treating the underlying cause of liver disease (i.e. anti HCV drugs) may even reverse fibrosis/cirrhosis(160), however, larger controlled studies are needed. Major advances have also occurred in treating the common complications from cirrhosis that include (but are not limited to) esophageal varicies, bleeding, encephalopathy, hepatorenal syndrome, hepatopulmonary syndrome, and bacterial infections. In short, these patients badly need more treatment options that improve underlying liver function.

The challenge for the field in the next 10 years is to capitalize upon recent basic science discoveries that have improved our mechanistic understanding of liver regeneration, hepatocyte biology, and the pathophysiology of cirrhosis. Here, I will

review several promising approaches that aim to reconstitute liver function and reverse cirrhosis.

The bioartificial liver

The liver is unique among major solid organs in that a machine cannot temporarily replace it. Kidney failure patients can be maintained on dialysis. Patients with fulminant lung failure (ie ARDS from influenza A) can be placed on extracorporeal membranous oxygenation (ECMO) to replace lung function until their own lungs can recover. Mechanical heart implants such as left-ventricle assist devices (LVAD) provide the pumping function of a failing heart. Yet no artificial system has achieved widespread acceptance for replacement of liver function. Supporting patients with acute liver or chronic liver failure may provide a bridge to liver transplantation or allow the endogenous liver to regenerate, potentially negating the need for a transplant(161).

In bioartificial liver systems (BAL), patient plasma is circulated outside the body through a bioreactor system that grows hepatocytes or hepatocyte-like cells on plates or hollow fibers. The hepatocytes detoxify the blood and secrete proteins such as clotting factors and albumin into the plasma. The detoxified plasma is then returned to the patient similar to kidney dialysis. A limitation of these devices is that they require as many as 10^{10} normal hepatocytes to achieve sufficient bioactivity. Hepatocytes are difficult to expand and maintain in long-term culture. Alternative cell sources such as immortalized cell lines, rabbit hepatocytes, or pig hepatocytes have been used as an alternative.

Multicenter clinical trials have demonstrated the safety and feasibility of operating BAL systems to treat more than 100 patients in a controlled clinical trial setting. But improved laboratory measures of liver function (ie bilirubin, albumin levels) in several controlled clinical trials only resulted in a significant survival benefit after post-hoc subgroup analysis(161,162). Further engineering advances may improve both the efficacy and ease of operating BAL systems in the future.

Pharmacological targets in chronic liver disease

Few treatments options currently exist to promote hepatic function in chronic liver disease. Corticosteroids and pentoxifylline, a TNF-a synthesis inhibitor have demonstrated modest success in reducing complications in acute-on-chronic disease but have had inconsistent effects on short term mortality(163). It follows that pharmacologic therapy in cirrhosis is focused on limiting complications such as bleeding and hepatorenal syndrome. But two emerging strategies aim to improve underlying function of the hepatocyte in chronic liver disease.

Anti-fibrinogenic therapy

Fibrosis is the excess accumulation of scar tissue or extracellular matrix that results from chronic injury and inflammation in the liver. An improved understanding of the cell types that contribute and molecular mechanisms governing matrix deposition has raised the prospect that anti-fibrotic therapies could improve outcomes in liver injury. A comprehensive review of hepatic fibrosis is beyond the

scope of this section, however, several excellent review articles provide a more complete discussion(160,164). The ductal reaction of cirrhosis is both spatially and temporally associated with the ductal reaction. In cirrhosis, nodules of hepatocytes become encapsulated in bands of extracellular matrix.

Interestingly, several drugs targeting the ductal progenitors cells have shown anti-fibrotic activity in rodent fibrosis models. Specifically, inhibitors to integrin αvβ6(165) and the hedgehog signaling pathway (166) effective in blocking fibrosis progression. Integrin αvβ6 and hedgehog signaling intermediate smoothened are expressed in proliferative ductal cells. These studies suggest that suppressing the ductal reaction of chronic liver injury may decrease the progression of fibrosis. Previously it was thought that blocking ductal progenitor proliferation would results in impaired regeneration of the hepatocyte mass. But recent lineage tracing studies have cast doubt on the hypothesis that the ductal reaction is activating a reserve stem cell that contributes to the hepatocyte mass(39,44,45). These studies remove a theoretical barrier to developing treatments that blunt injury-associated ductal proliferation.

Anti-fibrotic therapy relies on the fact that hepatocytes are not irreversibly damaged in cirrhosis and could regenerate themselves in a different context. In other words, anti-fibrotic treatment is conceptually linked with hepatocyte renewal. Therefore, rigorously testing the ability of cirrhotic hepatocytes to regenerate

themselves in a new microenvironment needs to be convincingly demonstrated to advance this line of therapy.

Strategies to promote hepatic fate and function

Chronic liver injury is associated with the loss of hepatocytic mass and simultaneous appearance of atypical ductal proliferations. In mouse lineage tracing models, activation of the Notch signaling pathway has been shown to be both necessary and sufficient for hepatocyte-to-ductal conversion(11,112,136,137). Our group has hypothesized that hepatocyte-derived ductal proliferations are likely to exist in multiple etiologies of chronic liver disease. We propose that hepatocyte-derived ducts are epigentically poised to differentiate back into hepatocytes given the correct cues or the correct microenvironment.

One strategy that may promote the differentiation of hepatocyte-derived ducts back into hepatocytes is Notch pathway inhibition. Multiple steps in the Notch signaling pathway may be targeted with existing therapeutic inhibitors to the ligand Jag1, individual notch receptors, or gamma-secretase enzyme that activates the notch intracellular signaling domain(167). While the Notch pathway clearly participates in the initial conversion(108,112), it is unknown whether persistent notch signaling activity is needed to stabilize and maintain the biliary fate. Further research is required to test this hypothesis in precise lineage tracing models that can differentiate hepatocytes from hepatocyte-derived ductal cells.

A pilot experiment in our laboratory to selectively block Notch2 (but Notch1) in a

healing period following mouse DDC injury failed to demonstrate activity in the liver. A surrogate biomarker (splenic marginal zone B-cell differentiation) indicated that Notch2 blockade was pharmacologically achieved in these negative experiments. Notch1 was not blocked. Interestingly, the inhibition of Notch-signaling with a gamma-secretase inhibitor (blocks all Notch signaling) was shown to attenuate ductal proliferation, decrease the injury-induced expression of EMT genes, and decrease the accumulation of fibrotic tissue in a rodent cirrhosis model(168).

Another strategy that may improve liver function in chronic liver disease involves reinforcing the hepatic differentiation program. *C/ebpa* is a transcription factor required for liver organogenesis and hepatocyte fate. *C/ebpa* expression can be increased by delivery of synthetic RNA-oligonucleotides. In a rodent model of liver disease, increased *C/ebpa* led to a statistically significant increase in albumin secretion and other liver functions(169). It remains to be tested whether expression of other essential transcription factors in impaired hepatocytes may give superior results.

Liver directed cell transplantation

Hepatocyte transplant has successfully corrected multiple rodent models of acute and chronic liver disease(77,170). Cell transplantation has several theoretical advantages over whole organ replacement. Specifically, it is less invasive, cells from a single donor could be given to multiple patients, cells can be cryopreserved, bioengineered cells (ie embryonic stem cell derived) could be given, genetically

manipulated autologous cells could be reinfused, and purified hepatocytes may be less immunogenic than whole organ transplantation(73).

Several case reports have demonstrated the feasibility of cell therapy with allogenic human hepatocytes. Of note, infusion of cryopreserved allogenic hepatocytes into a patient with Crigler-Najjar Syndrome, an inborn metabolic disorder characterized by severe unconjugated hyperbillirubinemia, showed evidence of biochemical correction. Infusion of 7.5×10^9 hepatocytes allowed the patient to reduce the duration of phototherapy, resulted in improved bilirubin levels, produced bilirubin conjugates, and provided a temporary partial correction of the disease. Nonetheless, the graft ultimately decreased in activity and the patient received a liver transplant. As of 2006, at least 78 patients had received hepatocyte transplants in a clinical setting for acute liver failure, inborn errors of metabolism, or chronic liver disease(7). Most trials were not controlled and results varied.

Improvement of hepatocyte transplantation protocols remains an active area of basic science research. A major obstacle to cell therapy is the engraftment of a sufficient number of cells to achieve a therapeutic response. Many researchers have focused on conditioning regimens that will allow expansion of donor cells at the expense of diseased cells. Single lobe external beam irradiation of single hepatic lobes allowed engraftment and expansion of wildtype hepatocytes in rodent models(171). The development of similar protocols for primate models and human clinical trials are underway and show considerable promise.

Additional barriers to hepatocyte transplantation include limited cell sources (cell isolation sometimes competes with orthotopic liver transplantation), appropriate immunosuppressive regimens, and methods to improve initial engraftment of the cells.

At present, hepatocyte transplantation remains a distant possibility for the treatment of chronic liver disease. Upcoming clinical trials are likely to focus on diseases that can be corrected with ~5% hepatocyte correction such as hemophilia, phenylketonuria, maple syrup urine disease and Crigler-Najjar syndrome. Another advantage of treating inborn errors of metabolism is that many genetics diseases are not associated with fibrosis. In contrast, even a small number of residual uncorrected hepatocytes in tyrosinemia type I or precancerous adenomas in a cirrhotic patient could put a hepatocyte-transplantation patient at increased risk for hepatocellular carcinoma. Additionally, clinical trials for the treatment of metabolic disorders are easier to evaluate because the function of the donor cells can be monitored with non-invasive biomarkers (i.e. Factor IX levels in hemophilia, conjugated bilirubin in Crigler-Najjar).

Extrahepatic cell transplantation

Most cell therapy approaches have focused on directly engrafting donor hepatocytes into the diseased liver. A limitation to this approach is that the cirrhotic liver is a fibrotic and inflammatory environment not conducive to normal hepatocyte

function. Thus, an alternative cell therapy approach is to build ectopic livers. Three different groups have produced promising strategies, which I discuss here.

Engineered biomaterials

Tissue engineering techniques have improved the long-term maintenance of functional hepatocytes *in vitro*. Bhatia and colleagues applied *in vivo* by printing arrays of human hepatocytes and supporting non-parenchymal cells onto thin polymer scaffolds that resemble a contact lens. These bioengineered "human ectopic artificial livers" or (HEALs) were then implanted into the mesentery of immunodeficient mice. The ectopic livers became vascularized in the host, produced human proteins, metabolized drugs, but only survived for several weeks. The levels of human albumin were approximately 50,000 times lower than what has been reported with the hepatocyte humanization of the $Fah^{-/-}$ mouse(92).

Ectopic liver buds from embryonic stem cells

Despite initial enthusiasm that embryonic stem cells (ES cells) or induced pluripotent stem cells (iPS cells) could represent a source of hepatocytes, real hepatocytes have been notoriously difficult to engineer. Differentiation protocols are time intensive and produce only partially functional cells called "hepatocyte-like cells"(71). Hepatocyte-like cells perform many of the functions of true hepatocytes but produce lower levels of albumin and do not efficiently engraft into the $Fah^{-/-}$ mouse.

Taniguichi and colleagues developed a multicellular organogenesis model by combining human-iPS cells with endothelial cells and mesenchymal cells(172). In organogenesis, normal mesenchymal and endothelial cells provide signaling cues that guide the differentiation of hepatocytes. Here, when researchers combined hepatic-endoderm specified iPS cells with endothelial cells and mesenchymal cells in a 2-dimension culture, they observed the spontaneous formation of 3-dimensional liver-like buds within 48 hours. When transplanted into the mesentery of an acute liver failure mouse model, the liver buds produced a functional rescue. The liver buds silenced expression of fetal liver stem cell marker *Afp* and produced 1983 ng/mL human serum albumin. This level of albumin is about 5,000-fold less than what is achieved with humanization of the $Fah^{-/-}$ mouse. Nevertheless, by imitating the steps of organogenesis, these iPS-derived liver buds show promise for autologous therapy in the setting of acute and chronic liver disease. Encapsulation of the liver buds in a biomaterial could improve their safety profile and allow transplantation into human hosts.

Ectopic livers in lymph nodes: not so far out

Lymph nodes support the growth of many cell types and are often the first site that cancer cells metastasize. Lagasse and colleagues exploited this observation by showing that normal lymph nodes supported the growth of normal hepatocytes. Hepatocytes transplanted into the lymph nodes were able to grow to nearly the same size as a normal liver and rescue mice from lethal liver failure(173). Ectopic lymph node livers appeared to conduct normal liver functions but cholangiocyte were completely absent, thus no traditional biliary drainage system developed.

Even so, the hepaticized lymph nodes produced bile acids but did not develop cholestasis or steatorrhea, which suggested that the lymphatic vasculature might have transported bile systemically. Further improvements in bile drainage could be achieved by surgically attaching ectopic livers to the small intestines to facilitate bile drainage from the ectopic liver. A similar procedure, named after Dr. Kasai, is commonly performed in infants with biliary atresia, a disease characterized by atrophy of the biliary system.

I recently found that ectopic hepatocyte buds, derived from hepatocytes injected into the spleen, could give rise to a system of ductal cells when treated mice were hepatocytes were injured with the compound DDC (**Fig. 6-1**). Hepatocytes that transitioned into a biliary phenotype were marked with Sox9-CreERT2 and appear green or mGFP+. The mGFP+ ductal cells arrange in cords, have little cytoplasm, and do not co-localize with hepatocyte marker Fah (**Fig. 6-1C**). These data are consistent with our findings that injured hepatocytes give rise to biliary-like cells in the liver (Chapter 5). Further work is ongoing that will determine whether these biliary like cells for patent lumens or improve the systemic trafficking of bile acids.

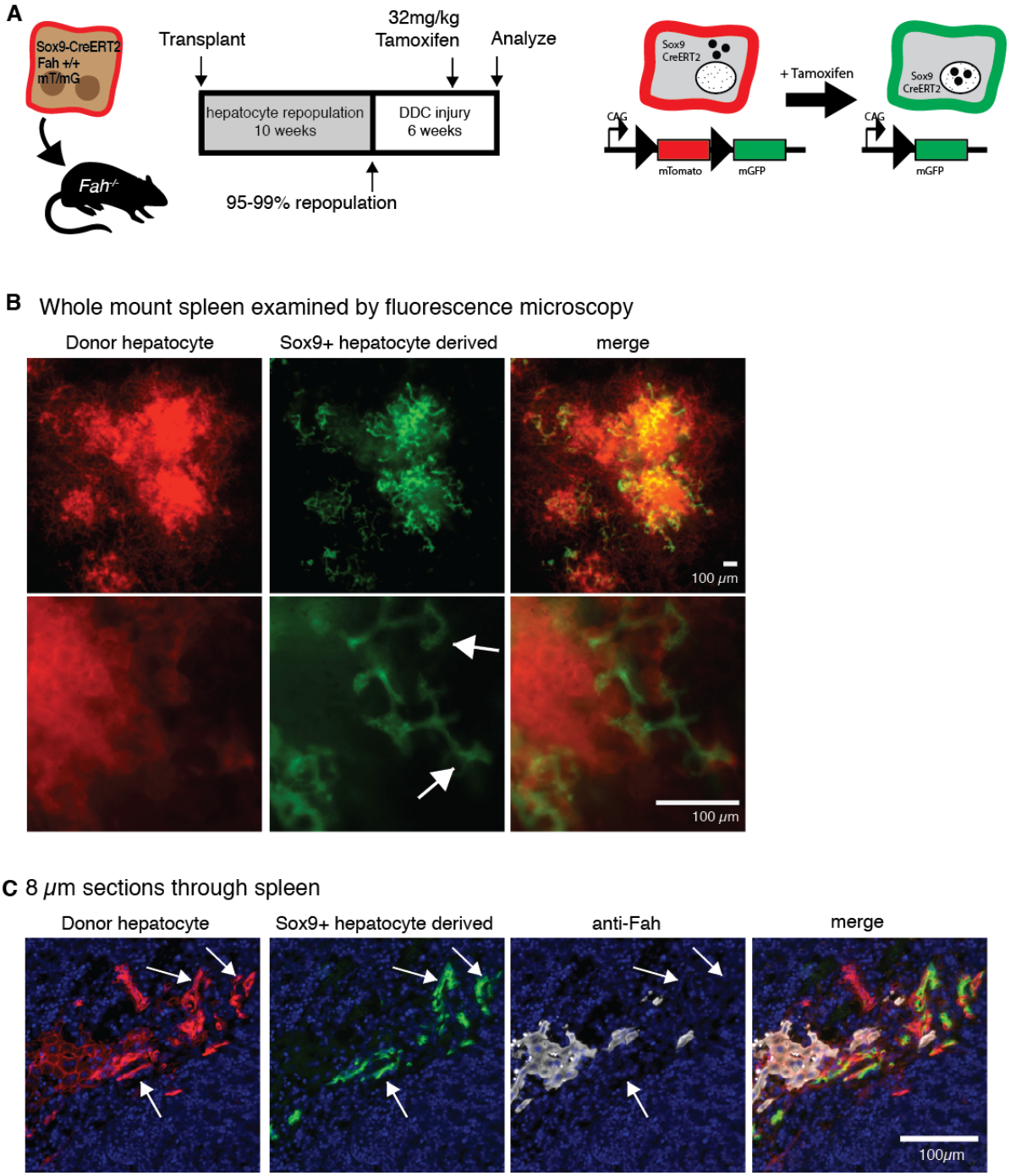

Figure 6-1: Ectopic hepatocyte nodes give rise to Sox9+ ductal cells upon chronic injury. A) Sox9-CreERT2 ROSA-mTmG hepatocytes were transplanted into the spleen of Fah mice. After repopulation, mice were treated with 0.1% DDC for 6 weeks. A pulse of tamoxfen was given to label Sox9+ biliary-like cells. Sox9+ cells irreversibly switched from mTomato red fluorescenct to mGFP green fluorescence. B) Spleens were isolated and examined by whole mount to visualization of the ductal architecture. C) Co-immunohistochemistry showed that a subset of donor cells assumed a ductal morphology, induced biliary marker Sox9, and downregulated hepatocyte marker Fah (arrows).

The Lagasse group has proposed to target allogenic hepatocyte transplant cell with hepatocytes isolated from blood type matched cadaveric human donors (*personal communication*). Due to the risk of immune rejection, these patients will likely require life-long immunosuppression. Allogenic hepatocyte transplant will also rely upon the same limited supply of cadaveric livers as a source of cells.

As an alternative approach, I have performed a series of pilot experiments in the Grompe laboratory that suggest autologous cell therapy may be a viable approach. These experiments justify further investigating whether transplanting autologous hepatocytes into the lymph node may improve outcomes in cirrhotic liver disease.

Contrary to dogma in the field(33,34), our group has found that cirrhotic hepatocytes do in fact retain the ability to replicate and form repopulation nodules when transferred into a new microenvironment. This is consistent with reports that cirrhotic rodent hepatocytes can repopulate a secondary recipient after a long latency period(174) and that replication in a new microenvironment can reverse hepatocyte senescence(175). Here, cirrhotic human hepatocytes were isolated from a 37-year old female with end-stage cirrhosis secondary to biliary atresia and a 51-year old male with end-stage cirrhosis secondary to primary sclerosing cholangitis. When transplanted into the spleen of immune-compromised *Fah*$^{-/-}$ mice, these cells formed repopulation nodules and secreted human serum albumin (**Fig6-2A,B**). Furthermore, as proof of concept, we found that viable human hepatocytes could be isolated from 18-G biopsies of explanted livers from patients with alcoholic

cirrhosis, end-stage non-alcoholic fatty liver disease (NASH), primary biliary cirrhosis, hepatitis-C virus cirrhosis, hepatitis B virus cirrhosis, and autoimmune hepatitis (**Fig 6-2C-G**). Cells were maintained for up to 1 week in culture and functional characterization was limited.

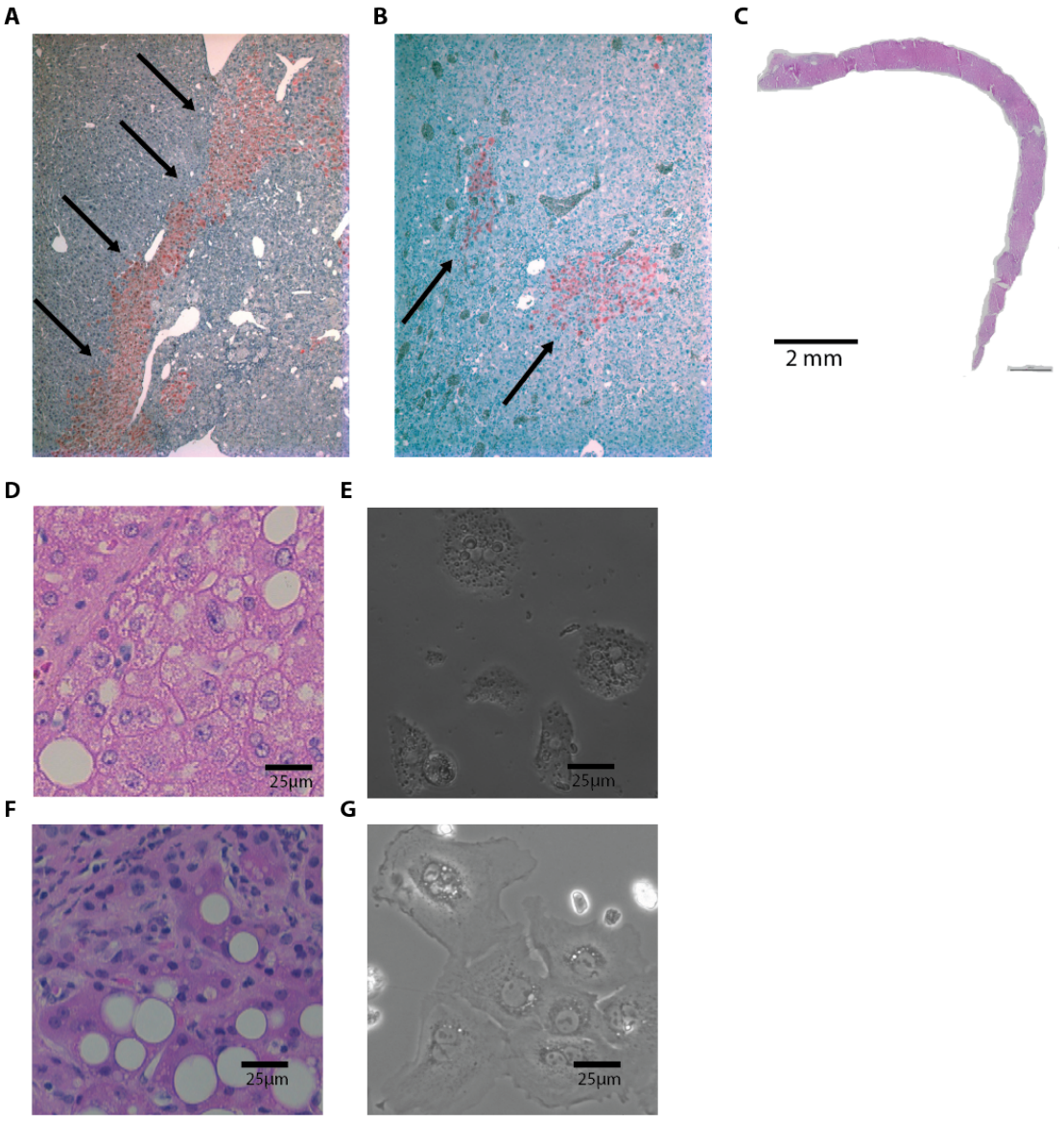

Figure 6-2: Cirrhotic human hepatocytes retain liver repopulating capacity.
A) Human hepatocytes engrafted (arrows, Fah$^+$ nodules) into FRG mice from patients with end-stage liver disease secondary to biliary atresia and B) primary sclerosing cholangitis. C) 18-gauge 34mm long biopsies were collected from explanted diseased livers. D) H&E image of a liver from patient with end-stage alcoholic cirrhosis contained E) viable human hepatocytes. F) Non-alcoholic steatohepatitis (NASH) end-stage liver histology and G) viable hepatocytes isolated from a biopsy of the same explanted liver.

Further work is needed to determine the growth properties of biopsy-derived hepatocytes. These results demonstrate that viable hepatocytes can be isolated with conventional techniques from even the sickest patients with end-stage cirrhosis. I speculate that a small number of hepatocytes liberated from the fibrotic liver and introduced into a protected ectopic site may be capable of expanding into a clinically significant hepatic mass. This is because chronic liver disease provides a strong hepatocyte regeneration stimulus but the fibrotic/inflammatory environment of the cirrhotic liver limits their normal function.

Conclusions & future directions

In 1964, J.W. Grisham summarized the views on the origin and fate of hepatic ductal cells(31) in liver injury that surprisingly fit the conclusions of this thesis. Based only on light microscopy and ultrastructural analyses of rat injury models and human pathological samples Grisham wrote:

> "Some investigators believe that ductular cells arise from affected hepatocytes by a process of dedifferentiation, whereas others believe that they can differentiate into hepatocytes and may serve as a replacement reservoir when the latter are destroyed . . . A view that combines aspects of the preceding two is that both types of cells are in a state of dynamic interchange or modulation."

Fifty-years later, this thesis uses Cre-recombinase-based lineage tracing, transgenic mice, cell transplantation, immunohistochemistry, confocal fluorescence microscopy, flow cytometry, cell culture with defined concentrations of recombinant proteins, and RNA-sequencing to reach similar conclusions. Here, I propose a slight but important modification of the *dynamic interchange* that Grisham discusses. I find that chronically injured mature hepatocytes do in fact give rise to or "dedifferentiate" into proliferative ductules. Additionally the data presented here show that conversion of mature hepatocytes into biliary-like progenitor cells is a reversible process, thus providing an explanation for the origin of bipotential oval cells. These hepatocyte-derived progenitors display the properties previously ascribed to classic oval cells but are functionally distinct from cholangiocytes. They proliferate as ducts in the periportal region of the hepatic lobule and revert back into hepatocytes at a low rate.

In contrast, clonal lineage tracing of the normal biliary compartment suggests that proliferative cholangiocytes rarely trans-differentiate into hepatocytes. This latter finding argues against the existence of a physiologically relevant reserve stem cell in the mouse liver and suggests limits on the dynamic phenotypic interchange of epithelial cells discussed by Grisham. Moreover, we find that hepatocytes continued to produce new hepatocytes in all mouse injury models that we examined; a non-hepatocyte precursor was not physiologically required for adaptation to model liver injuries.

A major limitation of this study is that the cell tracing experiments were performed in mice with chemical injuries that model only some features of human liver disease. Our current lineage tracing capabilities cannot be applied to study the origin of rat oval cells in the classic liver injury models because the injury models are different. But the goal of the field is not to understand the intricacies of an otherwise obscure chemical like 2-AAF, but rather to generate meaningful knowledge that sheds light on the nature of human disease. Future studies need to investigate the presence of bipotential hepatocyte-derived proliferative ducts in human diseases with the highest disease burden like alcoholic cirrhosis, hepatitis C, and NASH. Cell fractionation technology using cell surface antigens, new *in vitro* assay systems, and single cell genomics techniques are critical tools for testing the generalizability of the *decoy metaplasia hypothesis.*

Perhaps the most interesting question stemming from this work revolves upon the nature of the differentiated cell. The epigenetic mechanisms that underlie the phenotypic conversion of hepatocytes to ductal cells are not known. Why do hepatocyte-derived ductal cells retain a memory of the hepatocyte but cholangiocytes lose the memory of an embryonic hepatoblast? Does the metaplastic change from hepatocyte to ductal cell observed in injury contribute to or protect against hepatocarcinogenesis? Uncovering the mechanisms of the fate conversion in chronic liver injury may help improve the engineering of iPS-derived hepatocyte for cell therapy applications or suggest pharmacologic strategies to manipulate the fate of these cells in patients with end-stage liver failure.

LITERATURE REFERENCES

1. Murphy SL, Xu J, Kochanek KD. National vital statistics reports. National vital statistics reports. 2012;60:1.

2. Schuppan D, Afdhal NH. Liver cirrhosis. Lancet. 2008;371:838–851.

3. Alvarez-Dolado M, Pardal R, Garcia-Verdugo JM, Fike JR, Lee HO, Pfeffer K, et al. Fusion of bone-marrow-derived cells with Purkinje neurons, cardiomyocytes and hepatocytes. Nature. 2003;425:968–973.

4. Bacon BR. Chapter 302. Cirrhosis and its complications. Harrison's Principles of Internal Medicine. 17th ed. San Francisco, CA: McGraw-Hill. 2008;:274–284.

5. D'Amico G, Garcia-Tsao G, Pagliaro L. Natural history and prognostic indicators of survival in cirrhosis: a systematic review of 118 studies. Journal of Hepatology. 2006;44:217–231.

6. Fattovich G, Stroffolini T, Zagni I, Donato F. Hepatocellular carcinoma in cirrhosis: incidence and risk factors. YGAST. 2004;127:S35–50.

7. Fisher RA, Strom SC. Human Hepatocyte Transplantation: Worldwide Results. Transplantation. 2006;82:441–449.

8. Colnot S, Perret C. Liver zonation. 2011;:7–16.

9. Kaestner KH. In the zone: how a hepatocyte knows where it is. Gastroenterology. 2009;137:425–427.

10. Isse K, Lesniak A, Grama K, Maier J, Specht S, Castillo-Rama M, et al. Preexisting epithelial diversity in normal human livers: a tissue-tethered cytometric analysis in portal/periportal epithelial cells. Hepatology. 2013;57:1632–1643.

11. Zong Y, Panikkar A, Xu J, Antoniou A, Raynaud P, Lemaigre FP, et al. Notch signaling controls liver development by regulating biliary differentiation. Development. 2009;136:1727–1739.

12. Dill MT, Tornillo L, Fritzius T, Terracciano L, Semela D, Bettler B, et al. Constitutive Notch2 signaling induces hepatic tumors in mice. Hepatology. 2013;57:1607–1619.

13. Fan B, Malato Y, Calvisi DF, Naqvi S, Razumilava N, Ribback S, et al. Cholangiocarcinomas can originate from hepatocytes in mice. J Clin Invest. 2012;122:2911–2915.

14. Zaret KS. Regulatory phases of early liver development: paradigms of organogenesis. Nature Publishing Group. 2002;3:499–512.

15. Zaret KS, Grompe M. Generation and regeneration of cells of the liver and pancreas. Science. 2008;322:1490–1494.

16. Si-Tayeb K, Lemaigre FP, Duncan SA. Organogenesis and Development of the Liver. DEVCEL. 2010;18:175–189.

17. Laudadio I, Manfroid I, Achouri Y, Schmidt D, Wilson MD, Cordi S, et al. A feedback loop between the liver-enriched transcription factor network and mir-122 controls hepatocyte differentiation. Gastroenterology. 2012;142:119–129.

18. Zong Y, Stanger BZ. Molecular mechanisms of bile duct development. Int. J. Biochem. Cell Biol. 2011;43:257–264.

19. Decaens T, Godard C, de Reyniès A, Rickman DS, Tronche F, Couty J-P, et al. Stabilization of beta-catenin affects mouse embryonic liver growth and hepatoblast fate. Hepatology. 2008;47:247–258.

20. Carpentier R, Suñer RE, Van Hul N, Kopp JL, Beaudry J-B, Cordi S, et al. Embryonic ductal plate cells give rise to cholangiocytes, periportal hepatocytes, and adult liver progenitor cells. Gastroenterology. 2011;141:1432–8– 1438.e1–4.

21. Margall-Ducos G, Celton-Morizur S, Couton D, Brégerie O, Desdouets C. Liver tetraploidization is controlled by a new process of incomplete cytokinesis. J Cell Sci. 2007;120:3633–3639.

22. Wood MJ, Gadd VL, Powell LW, Ramm GA, Clouston AD. Ductular reaction in hereditary hemochromatosis: the link between hepatocyte senescence and fibrosis progression. Hepatology. 2014;59:848–857.

23. Roskams TA, De Vos R, Van Eyken P, Myazaki H, Van Damme B, Desmet V. Hepatic OV-6 expression in human liver disease and rat experiments: evidence for hepatic progenitor cells in man. Journal of Hepatology. 1998;29:455–463.

24. Sancho-Bru P, Altamirano J, Rodrigo-Torres D, Coll M, Millán C, José Lozano J, et al. Liver progenitor cell markers correlate with liver damage and predict short-term mortality in patients with alcoholic hepatitis. Hepatology. 2012;55:1931–1941.

25. Lowes KN, Brennan BA, Yeoh GC, Olynyk JK. Oval Cell Numbers in Human Chronic Liver Diseases Are Directly Related to Disease Severity. American Journal of Pathology. 1999;154:537–541.

26. Demetris AJ, Seaberg EC, Wennerberg A, Ionellie J, Michalopoulos GK. Ductular reaction after submassive necrosis in humans. Special emphasis on analysis of ductular hepatocytes. Am J Pathol. 1996;149:439–448.

27. Roskams TA, Katoonizadeh A, Komuta M. Hepatic Progenitor Cells: An Update. Clinics in Liver Disease. 2010;14:705–718.

28. Hattoum A, Rubin E, Orr A, Michalopoulos GK. Expression of hepatocyte epidermal growth factor receptor, FAS and glypican 3 in EpCAM-positive regenerative clusters of hepatocytes, cholangiocytes, and progenitor cells in human liver failure. Hum Pathol. 2012;:1–7.

29. Yoon S-M, Gerasimidou D, Kuwahara R, Hytiroglou P, Yoo JE, Park YN, et al. Epithelial cell adhesion molecule (EpCAM) marks hepatocytes newly derived from stem/progenitor cells in humans. Hepatology. 2011;53:964–973.

30. Fujita M, Furukawa H, Hattori M, Todo S, Ishida Y, Nagashima K. Sequential observation of liver cell regeneration after massive hepatic necrosis in auxiliary partial orthotopic liver transplantation. Mod. Pathol. 2000;13:152–157.

31. Grisham JW, Porta E. Origin and fate of proliferated hepatic ductal cells in the rate: electron microscopic and autoradiographic studies. Exp. Mol. Pathol. 1964;86:242–261.

32. Fausto N. Liver regeneration and repair: hepatocytes, progenitor cells, and stem cells.

Hepatology. 2004;

33. Duncan AW, Dorrell C, Grompe M. Stem cells and liver regeneration. Gastroenterology. 2009;137:466–481.

34. Itoh T, Miyajima A. Liver regeneration by stem/progenitor cells. Hepatology. 2013;

35. Petersen BE. Bone Marrow as a Potential Source of Hepatic Oval Cells. Science. 1999;284:1168–1170.

36. Lagasse E, Connors H, Al-Dhalimy M, Reitsma M, Dohse M, Osborne L, et al. Purified hematopoietic stem cells can differentiate into hepatocytes in vivo. Nat Med. 2000;6:1229–1234.

37. Alison MR, Poulsom R, Jeffery R, Dhillon AP, Quaglia A, Jacob J, et al. Hepatocytes from non-hepatic adult stem cells. Nature. 2000;406:257.

38. Furuyama K, Kawaguchi Y, Akiyama H, Horiguchi M, Kodama S, Kuhara T, et al. Continuous cell supply from a Sox9-expressing progenitor zone in adult liver, exocrine pancreas and intestine. Nat Genet. 2010;43:34–41.

39. Español-Suñer R, Carpentier R, Van Hul N, Legry V, Achouri Y, Cordi S, et al. Liver Progenitor Cells Yield Functional Hepatocytes in Response to Chronic Liver Injury in Mice. Gastroenterology. 2012;143:1564–1575.e7.

40. Yang L, Jung Y, Omenetti A, Witek RP, Choi S, Vandongen HM, et al. Fate-mapping evidence that hepatic stellate cells are epithelial progenitors in adult mouse livers. Stem Cells. 2008;26:2104–2113.

41. Huch M, Dorrell C, Boj SF, van Es JH, Li VSW, van de Wetering M, et al. In vitro expansion of single Lgr5(+) liver stem cells induced by Wnt-driven regeneration. Nature. 2013;

42. Iverson SV, Comstock KM, Kundert JA, Schmidt EE. Contributions of new hepatocyte lineages to liver growth, maintenance, and regeneration in mice. Hepatology. 2011;54:655–663.

43. Kuwahara R, Kofman AV, Landis CS, Swenson ES, Barendswaard E, Theise ND. The hepatic stem cell niche: identification by label-retaining cell assay. Hepatology. 2008;47:1994–2002.

44. Tarlow BD, Finegold MJ, Grompe M. Clonal tracing of Sox9(+) liver progenitors in mouse oval cell injury. Hepatology. 2014;60:278–289.

45. Malato Y, Naqvi S, Schürmann N, Ng R, Wang B, Zape J, et al. Fate tracing of mature hepatocytes in mouse liver homeostasis and regeneration. J Clin Invest. 2011;121:4850–4860.

46. Michalopoulos GK. Liver Regeneration. Science. 1997;276:60–66.

47. Miyajima A, Tanaka M, Itoh T. Stem/progenitor cells in liver development, homeostasis, regeneration, and reprogramming. Cell Stem Cell. 2014;14:561–574.

48. Zajicek G, Oren R, WEINREB M JR. The streaming liver. Liver. 1985;5:293–300.

49. Fellous TG, Islam S, Tadrous PJ, Elia G, Kocher HM, Bhattacharya S, et al. Locating the stem cell niche and tracing hepatocyte lineages in human liver. Hepatology. 2009;49:1655–1663.

50. Bralet MP, Branchereau S, Brechot C, Ferry N. Cell lineage study in the liver using retroviral mediated gene transfer. Evidence against the streaming of hepatocytes in normal liver. Am J Pathol [Internet]. 1994;144:896–905. Available from: http://www.ncbi.nlm.nih.gov/sites/entrez?Db=pubmed&Cmd=Retrieve&list_uids=8178942&dopt=abstractplus

51. Michalopoulos GK. The liver is a peculiar organ when it comes to stem cells. Am J Pathol. 2014;184:1263–1267.

52. Erker L, Grompe M. Signaling networks in hepatic oval cell activation. Stem Cell Res. 2007;1:90–102.

53. Gordon GJ, Coleman WB, Hixson DC, Grisham JW. Liver regeneration in rats with retrorsine-induced hepatocellular injury proceeds through a novel cellular response. Am J Pathol. 2000;156:607–619.

54. Willenbring H, Sharma AD, Vogel A, Lee AY, Rothfuss A, Wang Z, et al. Loss of p21 Permits Carcinogenesis from Chronically Damaged Liver and Kidney Epithelial Cells despite Unchecked Apoptosis. Cancer Cell. 2008;14:59–67.

55. Petersen BE, Zajac VF, Michalopoulos GK. Bile ductular damage induced by methylene dianiline inhibits oval cell activation. Am J Pathol. 1997;151:905–909.

56. Calado RT, Brudno J, Mehta P, Kovacs JJ, Wu C, Zago MA, et al. Constitutional telomerase mutations are genetic risk factors for cirrhosis. Hepatology. 2011;53:1600–1607.

57. Gong L, Li Y-H, Su Q, Chu X, Zhang W. Clonality of nodular lesions in liver cirrhosis and chromosomal abnormalities in monoclonal nodules of altered hepatocytes. Histopathology. 2010;56:589–599.

58. Yasui H, Hino O, Ohtake K, Machinami R, Kitagawa T. Clonal growth of hepatitis B virus-integrated hepatocytes in cirrhotic liver nodules. Cancer Res. 1992;52:6810–6814.

59. Dorrell C, Erker L, Lanxon-Cookson KM, Abraham SL, Victoroff T, Ro S, et al. Surface markers for the murine oval cell response. Hepatology. 2008;48:1282–1291.

60. Shin S, Walton G, Aoki R, Brondell K, Schug J, Fox A, et al. Foxl1-Cre-marked adult hepatic progenitors have clonogenic and bilineage differentiation potential. Genes Dev. 2011;25:1185–1192.

61. Dorrell C, Erker L, Schug J, Kopp JL, Canaday PS, Fox AJ, et al. Prospective isolation of a bipotential clonogenic liver progenitor cell in adult mice. Genes Dev. 2011;25:1193–1203.

62. Suzuki A, Sekiya S, Onishi M, Oshima N, Kiyonari H, Nakauchi H, et al. Flow cytometric isolation and clonal identification of self-renewing bipotent hepatic progenitor cells in adult mouse liver. Hepatology. 2008;48:1964–1978.

63. Dunn JC, Yarmush ML, Koebe HG, Tompkins RG. Hepatocyte function and extracellular matrix geometry: long-term culture in a sandwich configuration. FASEB J. 1989;3:174–177.

64. Block GD, Locker J, Bowen WC, Petersen BE, Katyal S, Strom SC, et al. Population expansion,

clonal growth, and specific differentiation patterns in primary cultures of hepatocytes induced by HGF/SF, EGF and TGF alpha in a chemically defined (HGM) medium. J Cell Biol. 1996;132:1133–1149.

65. Sone M, Nishikawa Y, Nagahama Y, Kumagai E, Doi Y, Omori Y, et al. Recovery of mature hepatocytic phenotype following bile ductular transdifferentiation of rat hepatocytes in vitro. Am J Pathol. 2012;181:2094–2104.

66. Chen Y, Wong PP, Sjeklocha L, Steer CJ, Sahin MB. Mature hepatocytes exhibit unexpected plasticity by direct dedifferentiation into liver progenitor cells in culture. Hepatology. 2012;55:563–574.

67. Tanimizu N, Nishikawa Y, Ichinohe N, Akiyama H, Mitaka T. Sry HMG Box Protein 9-positive (Sox9+) Epithelial Cell Adhesion Molecule-negative (EpCAM-) Biphenotypic Cells Derived from Hepatocytes Are Involved in Mouse Liver Regeneration. J. Biol. Chem. 2014;289:7589–7598.

68. Snippert HJ, Clevers H. Tracking adult stem cells. EMBO Rep. 2011;12:113–122.

69. Desai TJ, Brownfield DG, Krasnow MA. Alveolar progenitor and stem cells in lung development, renewal and cancer. Nature. 2014;507:190–194.

70. Van Keymeulen A, Rocha AS, Ousset M, Beck B, Bouvencourt G, Rock J, et al. Distinct stem cells contribute to mammary gland development and maintenance. Nature. 2011;479:189–193.

71. Si-Tayeb K, Noto FK, Nagaoka M, Li J, Battle MA, Duris C, et al. Highly efficient generation of human hepatocyte-like cells from induced pluripotent stem cells. Hepatology. 2010;51:297–305.

72. Du Y, Wang J, Jia J, Song N, Xiang C, Xu J, et al. Human hepatocytes with drug metabolic function induced from fibroblasts by lineage reprogramming. Cell Stem Cell. 2014;14:394–403.

73. Grompe M. Principles of therapeutic liver repopulation. Journal of inherited metabolic disease. 2006;29:421–425.

74. Spangrude G, Heimfeld S, Weissman IL. Purification and characterization of mouse hematopoietic stem cells. Science. 1988;241:58–62.

75. Rountree CB, Barsky L, Ge S, Zhu J, Senadheera S, Crooks GM. A CD133-expressing murine liver oval cell population with bilineage potential. Stem Cells. 2007;25:2419–2429.

76. Okabe M, Tsukahara Y, Tanaka M, Suzuki K, Saito S, Kamiya Y, et al. Potential hepatic stem cells reside in EpCAM+ cells of normal and injured mouse liver. Development. 2009;136:1951–1960.

77. Overturf K, Al-Dhalimy M, Tanguay R, Brantly M, Ou CN, Finegold M, et al. Hepatocytes corrected by gene therapy are selected in vivo in a murine model of hereditary tyrosinaemia type I. Nat Genet. 1996;12:266–273.

78. Wallace BM, Wallace H. Participation of grafted nerves in amphibian limb regeneration. J Embryol Exp Morphol. 1973;29:559–570.

79. Kragl M, Knapp D, Nacu E, Khattak S, Maden M, Epperlein HH, et al. Cells keep a memory of their tissue origin during axolotl limb regeneration. Nature. 2009;460:60–65.

80. Turner R, Lozoya O, Wang Y, Cardinale V, Gaudio E, Alpini G, et al. Human hepatic stem cell and maturational liver lineage biology. Hepatology. 2011;53:1035–1045.

81. Kushida T, Inaba M, Hisha H, Ichioka N, Esumi T, Ogawa R, et al. Intra-bone marrow injection of allogeneic bone marrow cells: a powerful new strategy for treatment of intractable autoimmune diseases in MRL/lpr mice. Blood. 2001;97:3292–3299.

82. Szilvassy SJ, Humphries RK, Lansdorp PM, Eaves AC, Eaves CJ. Quantitative assay for totipotent reconstituting hematopoietic stem cells by a competitive repopulation strategy. Proc Natl Acad Sci USA. 1990;87:8736–8740.

83. Wang X, Foster M, Al-Dhalimy M, Lagasse E, Finegold M, Grompe M. The origin and liver repopulating capacity of murine oval cells. Proc Natl Acad Sci USA. 2003;100 Suppl 1:11881–11888.

84. Cogle CR, Goldman DC, Madlambayan GJ, Leon RP, Masri Al A, Clark HA, et al. Functional integration of acute myeloid leukemia into the vascular niche. Leukemia. 2014;

85. Kam I, Lynch S, Svanas G, Todo S, Polimeno L, Francavilla A, et al. Evidence that host size determines liver size: studies in dogs receiving orthotopic liver transplants. Hepatology. 1987;7:362–366.

86. Rhim JA, Sandgren EP, Palmiter RD. Complete reconstitution of mouse liver with xenogeneic hepatocytes. 1995.

87. Suzuki A, Zheng Y, Kondo R, Kusakabe M, Takada Y, Fukao K, et al. Flow-cytometric separation and enrichment of hepatic progenitor cells in the developing mouse liver. Hepatology [Internet]. 2000;32:1230–1239. Available from: http://eutils.ncbi.nlm.nih.gov/entrez/eutils/elink.fcgi?dbfrom=pubmed&id=11093729&retmode=ref&cmd=prlinks

88. Joseph B, Kumaran V, Berishvili E, Bhargava KK, Palestro CJ, Gupta S. Monocrotaline promotes transplanted cell engraftment and advances liver repopulation in rats via liver conditioning. Hepatology. 2006;44:1411–1420.

89. Zhou X-F, Wang Q, Chu J-X, Liu A-L. Effects of retrorsine on mouse hepatocyte proliferation after liver injury. WJG. 2006;12:1439–1442.

90. Guha C, Sharma A, Gupta S, Alfieri A, Gorla GR. Amelioration of radiation-induced liver damage in partially hepatectomized rats by hepatocyte transplantation. Cancer Res. 1999;

91. Dandri M. Repopulation of mouse liver with human hepatocytes and in vivo infection with hepatitis B virus. Hepatology. 2001;33:981–988.

92. Azuma H, Paulk N, Ranade A, Dorrell C, Al-Dhalimy M, Ellis E, et al. Robust expansion of human hepatocytes in Fah-/-/Rag2-/-/Il2rg-/- mice. Nat Biotechnol. 2007;25:903–910.

93. Huang P, He Z, Ji S, Sun H, Xiang D, Liu C, et al. Induction of functional hepatocyte-like cells from mouse fibroblasts by defined factors. Nature. 2011;:1–6.

94. Sekiya S, Suzuki A. Direct conversion of mouse fibroblasts to hepatocyte-like cells by

defined factors. Nature. 2011;475:390–393.

95. Liu H, Kim Y, Sharkis S, Marchionni L, Jang YY. In Vivo Liver Regeneration Potential of Human Induced Pluripotent Stem Cells from Diverse Origins. Science Translational Medicine. 2011;3:82ra39–82ra39.

96. Yovchev MI, Grozdanov PN, Zhou H, Racherla H, Guha C, Dabeva MD. Identification of adult hepatic progenitor cells capable of repopulating injured rat liver. Hepatology. 2008;47:636–647.

97. Sandhu JS, Petkov PM, Dabeva MD. Stem cell properties and repopulation of the rat liver by fetal liver epithelial progenitor cells. The American Journal of …. 2001;

98. Wang X, Willenbring H, Akkari Y, Torimaru Y, Foster M, Al-Dhalimy M, et al. Cell fusion is the principal source of bone-marrow-derived hepatocytes. Nature. 2003;422:897–901.

99. Dorrell C, Tarlow B, Wang Y, Canaday PS, Haft A. The organoid-initiating cells in mouse pancreas and liver are phenotypically and functionally similar. Stem Cell Res. 2014;

100. Li L, Clevers H. Coexistence of Quiescent and Active Adult Stem Cells in Mammals. Science. 2010;327:542–545.

101. Buczacki SJA, Zecchini HI, Nicholson AM, Russell R, Vermeulen L, Kemp R, et al. Intestinal label-retaining cells are secretory precursors expressing Lgr5. Nature. 2013;495:65–69.

102. Kiel MJ, He S, Ashkenazi R, Gentry SN, Teta M. Haematopoietic stem cells do not asymmetrically segregate chromosomes or retain BrdU. Nature. 2007;

103. Evarts RP, Nagy P, Marsden E, Thorgeirsson SS. A precursor-product relationship exists between oval cells and hepatocytes in rat liver. Carcinogenesis [Internet]. 1987;8:1737–1740. Available from: http://eutils.ncbi.nlm.nih.gov/entrez/eutils/elink.fcgi?dbfrom=pubmed&id=3664968&retmode=ref&cmd=prlinks

104. Jaitin DA, Kenigsberg E, Keren-Shaul H, Elefant N, Paul F, Zaretsky I, et al. Massively parallel single-cell RNA-seq for marker-free decomposition of tissues into cell types. Science. 2014;343:776–779.

105. Kawaguchi Y. Sox9 and programming of liver and pancreatic progenitors. J Clin Invest. 2013;123:1881–1886.

106. Reinert RB, Kantz J, Misfeldt AA, Poffenberger G, Gannon M, Brissova M, et al. Tamoxifen-Induced Cre-loxP Recombination Is Prolonged in Pancreatic Islets of Adult Mice. PLoS ONE. 2012;7:e33529.

107. DeGregorio MW, Coronado E, Osborne CK. Tumor and serum tamoxifen concentrations in the athymic nude mouse. Cancer Chemother. Pharmacol. 1989;23:68–70.

108. Sekiya S, Suzuki A. Hepatocytes, Rather than Cholangiocytes, Can Be the Major Source of Primitive Ductules in the Chronically Injured Mouse Liver. Am J Pathol. 2014;:1–12.

109. Koitabashi N, Bedja D, Zaiman AL, Pinto YM, Zhang M, Gabrielson KL, et al. Avoidance of Transient Cardiomyopathy in Cardiomyocyte-Targeted Tamoxifen-Induced MerCreMer Gene Deletion Models. Circulation Research. 2009;105:12–15.

110. Cole LK, Jacobs RL, Vance DE. Tamoxifen induces triacylglycerol accumulation in the mouse liver by activation of fatty acid synthesis. Hepatology. 2010;52:1258–1265.

111. Snippert HJ, van der Flier LG, Sato T, van Es JH, van den Born M, Kroon-Veenboer C, et al. Intestinal Crypt Homeostasis Results from Neutral Competition between Symmetrically Dividing Lgr5 Stem Cells. Cell. 2010;143:134–144.

112. Yanger K, Zong Y, Maggs LR, Shapira SN, Maddipati R, Aiello NM, et al. Robust cellular reprogramming occurs spontaneously during liver regeneration. Genes Dev. 2013;27:719–724.

113. Michalopoulos GK, Barua L, Bowen WC. Transdifferentiation of rat hepatocytes into biliary cells after bile duct ligation and toxic biliary injury. Hepatology. 2005;41:535–544.

114. Sekiya S, Suzuki A. Intrahepatic cholangiocarcinoma can arise from Notch-mediated conversion of hepatocytes. J Clin Invest. 2012;122:3914–3918.

115. Lora JM, Rowader KE, Soares L, Giancotti F, Zaret KS. Alpha3beta1-integrin as a critical mediator of the hepatic differentiation response to the extracellular matrix. Hepatology. 1998;28:1095–1104.

116. Kim KK, Wei Y, Szekeres C, Kugler MC, Wolters PJ, Hill ML, et al. Epithelial cell alpha3beta1 integrin links beta-catenin and Smad signaling to promote myofibroblast formation and pulmonary fibrosis. J Clin Invest. 2009;119:213–224.

117. Sato T, Vries RG, Snippert HJ, van de Wetering M, Barker N, Stange DE, et al. Single Lgr5 stem cells build crypt-villus structures in vitro without a mesenchymal niche. Nature. 2009;459:262–265.

118. de Lau W, Barker N, Low TY, Koo B-K, Li VSW, Teunissen H, et al. Lgr5 homologues associate with Wnt receptors and mediate R-spondin signalling. Nature. 2011;

119. Fox IJ, Chowdhury JR, Kaufman SS, Goertzen TC, Chowdhury NR, Warkentin PI, et al. Treatment of the Crigler-Najjar syndrome type I with hepatocyte transplantation. N Engl J Med. 1998;338:1422–1426.

120. Turner RA, Wauthier E, Lozoya O, McClelland R, Bowsher JE, Barbier C, et al. Successful transplantation of human hepatic stem cells with restricted localization to liver using hyaluronan grafts. Hepatology. 2013;57:775–784.

121. Overturf K, Al-Dhalimy M, Ou CN, Finegold M, Grompe M. Serial transplantation reveals the stem-cell-like regenerative potential of adult mouse hepatocytes. Am J Pathol. 1997;151:1273–1280.

122. Farber E. Similarities in the sequence of early histological changes induced in the liver of the rat by ethionine, 2-acetylamino-fluorene, and 3'-methyl-4-dimethylaminoazobenzene. Cancer Res. 1956;16:142–148.

123. Sell S. Comparison of liver progenitor cells in human atypical ductular reactions with those seen in experimental models of liver injury. Hepatology. 1998;27:317–331.

124. Sell S. Is there a liver stem cell? Cancer Res. 1990;50:3811–3815.

125. Evarts RP, Nagy P, Nakatsukasa H, Marsden E, Thorgeirsson SS. In vivo differentiation of rat

liver oval cells into hepatocytes. Cancer Res. 1989;49:1541–1547.

126. Sackett SD, Li Z, Hurtt R, Gao Y, Wells RG, Brondell K, et al. Foxl1 is a marker of bipotential hepatic progenitor cells in mice. Hepatology. 2009;49:920–929.

127. Kopp JL, Dubois CL, Schaffer AE, Hao E, Shih HP, Seymour PA, et al. Sox9+ ductal cells are multipotent progenitors throughout development but do not produce new endocrine cells in the normal or injured adult pancreas. Development. 2011;138:653–665.

128. Muzumdar MD, Tasic B, Miyamichi K, Li L, Luo L. A global double-fluorescent Cre reporter mouse. Genesis. 2007;45:593–605.

129. Hameyer D, Loonstra A, Eshkind L, Schmitt S, Antunes C, Groen A, et al. Toxicity of ligand-dependent Cre recombinases and generation of a conditional Cre deleter mouse allowing mosaic recombination in peripheral tissues. Physiological Genomics. 2007;31:32–41.

130. Pryce BA, Brent AE, Murchison ND, Tabin CJ, Schweitzer R. Generation of transgenic tendon reporters, ScxGFP and ScxAP, using regulatory elements of the scleraxis gene. Dev. Dyn. 2007;236:1677–1682.

131. Boulter L, Govaere O, Bird TG, Radulescu S, Ramachandran P, Pellicoro A, et al. Macrophage-derived Wnt opposes Notch signaling to specify hepatic progenitor cell fate in chronic liver disease. Nat Med. 2012;18:572–579.

132. Miyaoka Y, Ebato K, Kato H, Arakawa S, Shimizu S, Miyajima A. Hypertrophy and unconventional cell division of hepatocytes underlie liver regeneration. Curr. Biol. 2012;22:1166–1175.

133. Takase HM, Itoh T, Ino S, Wang T, Koji T, Akira S, et al. FGF7 is a functional niche signal required for stimulation of adult liver progenitor cells that support liver regeneration. Genes Dev. 2013;27:169–181.

134. Español-Suñer R, Lemaigre FP, Leclercq IA. Reply. Gastroenterology. 2013;145:255–256.

135. Ishikawa T, Factor VM, Marquardt JU, Raggi C, Seo D, Kitade M, et al. Hepatocyte growth factor/c-met signaling is required for stem-cell-mediated liver regeneration in mice. Hepatology. 2012;55:1215–1226.

136. Jeliazkova P, Jörs S, Lee M, Zimber-Strobl U, Ferrer J, Schmid RM, et al. Canonical Notch2 signaling determines biliary cell fates of embryonic hepatoblasts and adult hepatocytes independent of Hes1. Hepatology. 2013;57:2469–2479.

137. Yimlamai D, Christodoulou C, Galli GG, yanger K, Pepe-Mooney B, Gurung B, et al. Hippo pathway activity influences liver cell fate. Cell. 2014;157:1324–1338.

138. Santangelo L, Marchetti A, Cicchini C, Conigliaro A, Conti B, Mancone C, et al. The stable repression of mesenchymal program is required for hepatocyte identity: a novel role for hepatocyte nuclear factor 4α. Hepatology. 2011;53:2063–2074.

139. Grompe M, Al-Dhalimy M, Finegold M, Ou CN, Burlingame T, Kennaway NG, et al. Loss of fumarylacetoacetate hydrolase is responsible for the neonatal hepatic dysfunction phenotype of lethal albino mice. Genes Dev. 1993;7:2298–2307.

140. Robinson MD, McCarthy DJ, Smyth GK. edgeR: a Bioconductor package for differential

expression analysis of digital gene expression data. Bioinformatics. 2010;26:139–140.

141. Wang X, Montini E, Al-Dhalimy M, Lagasse E, Finegold M, Grompe M. Kinetics of Liver Repopulation after Bone Marrow Transplantation. Am J Pathol. 2002;161:565–574.

142. Overturf K, Al-Dhalimy M, Finegold M, Grompe M. The repopulation potential of hepatocyte populations differing in size and prior mitotic expansion. Am J Pathol. 1999;155:2135–2143.

143. Preisegger KH, Factor VM, Fuchsbichler A, Stumptner C, Denk H, Thorgeirsson SS. Atypical ductular proliferation and its inhibition by transforming growth factor beta1 in the 3,5-diethoxycarbonyl-1,4-dihydrocollidine mouse model for chronic alcoholic liver disease. Lab Invest. 1999;79:103–109.

144. Rodrigo-Torres D, Affò S, Coll M, Morales-Ibanez O, Millán C, Blaya D, et al. The biliary epithelium gives rise to liver progenitor cells. Hepatology. 2014;

145. Kalluri R, Weinberg RA. The basics of epithelial-mesenchymal transition. J Clin Invest. 2009;119:1420–1428.

146. Alison MR, Golding M, Sarraf CE, Edwards RJ, Lalani EN. Liver damage in the rat induces hepatocyte stem cells from biliary epithelial cells. YGAST. 1996;110:1182–1190.

147. Fujio K, Evarts RP, Hu Z, Marsden ER, Thorgeirsson SS. Expression of stem cell factor and its receptor, c-kit, during liver regeneration from putative stem cells in adult rat. Lab Invest. 1994;70:511–516.

148. Li W-L, Su J, Yao Y-C, Tao X-R, Yan Y-B, Yu H-Y, et al. Isolation and Characterization of Bipotent Liver Progenitor Cells from Adult Mouse. Stem Cells. 2006;24:322–332.

149. Gleiberman AS, Encinas JM, Mignone JL, Michurina T, Rosenfeld MG, Enikolopov G. Expression of nestin-green fluorescent protein transgene marks oval cells in the adult liver. Dev. Dyn. 2005;234:413–421.

150. Mosnier J-F, Kandel C, Cazals-Hatem D, Bou-Hanna C, Gournay J, Jarry A, et al. N-cadherin serves as diagnostic biomarker in intrahepatic and perihilar cholangiocarcinomas. Mod. Pathol. 2009;22:182–190.

151. Zhou H, Rogler LE, Teperman L, Morgan G, Rogler CE. Identification of hepatocytic and bile ductular cell lineages and candidate stem cells in bipolar ductular reactions in cirrhotic human liver. Hepatology. 2007;45:716–724.

152. Roskams TA, van den Oord JJ, De Vos R, Desmet VJ. Neuroendocrine features of reactive bile ductules in cholestatic liver disease. Am J Pathol. 1990;137:1019–1025.

153. Michelotti GA, Xie G, Swiderska M, Choi SS, Karaca G, Krüger L, et al. Smoothened is a master regulator of adult liver repair. J Clin Invest. 2013;

154. Bin Li, Zheng Y-W, Sano Y, Taniguchi H. Evidence for Mesenchymal–Epithelial Transition Associated with Mouse Hepatic Stem Cell Differentiation. PLoS ONE. 2011;6:e17092.

155. Shafritz DA, Oertel M, Menthena A, Nierhoff D, Dabeva MD. Liver stem cells and prospects for liver reconstitution by transplanted cells. Hepatology. 2006;43:S89–98.

156. Slack J. Metaplasia and somatic cell reprogramming. J Pathol. 2009;217:161–168.

157. Elmore LW, Sirica AE. Sequential appearance of intestinal mucosal cell types in the right and caudate liver lobes of furan-treated rats. Hepatology. 1992;16:1220–1226.

158. Kuo F-Y, Swanson PE, Yeh MM. Pancreatic acinar tissue in liver explants: a morphologic and immunohistochemical study. The American Journal of Surgical Pathology. 2009;33:66–71.

159. Sánchez Alvarado A, Yamanaka S. Rethinking Differentiation: Stem Cells, Regeneration, and Plasticity. Cell. 2014;157:110–119.

160. Friedman SL. Mechanisms of Hepatic Fibrogenesis. Gastroenterology. 2008;134:1655–1669.

161. Ellis AJ, Hughes RD, Wendon JA, Dunne J, Langley PG, Kelly JH, et al. Pilot-controlled trial of the extracorporeal liver assist device in acute liver failure. Hepatology. 1996;24:1446–1451.

162. Demetriou AA, Brown RS, Busuttil RW, Fair J, McGuire BM, Rosenthal P, et al. Prospective, randomized, multicenter, controlled trial of a bioartificial liver in treating acute liver failure. Ann. Surg. 2004;239:660–7– discussion 667–70.

163. Lebrec D, Thabut D, Oberti F, Perarnau JM, Condat B, Barraud H, et al. Pentoxifylline Does Not Decrease Short-term Mortality but Does Reduce Complications in Patients With Advanced Cirrhosis. YGAST. 2010;138:1755–1762.e2.

164. Schuppan D, Kim YO. Evolving therapies for liver fibrosis. J Clin Invest. 2013;123:1887–1901.

165. Patsenker E, Popov Y, Stickel F, Jonczyk A, Goodman SL, Schuppan D. Inhibition of integrin alphavbeta6 on cholangiocytes blocks transforming growth factor-beta activation and retards biliary fibrosis progression. Gastroenterology. 2008;135:660–670.

166. Syn W-K, Jung Y, Omenetti A, Abdelmalek M, Guy CD, Yang L, et al. Hedgehog-Mediated Epithelial-to-Mesenchymal Transition and Fibrogenic Repair in Nonalcoholic Fatty Liver Disease. Gastroenterology. 2009;137:1478–1488.e8.

167. Morell CM, Strazzabosco M. Notch signaling and new therapeutic options in liver disease. Journal of Hepatology. 2014;:1–6.

168. Chen Y, Zheng S, Qi D, Zheng S, Guo J, Zhang S, et al. Inhibition of Notch signaling by a γ-secretase inhibitor attenuates hepatic fibrosis in rats. PLoS ONE. 2012;7:e46512.

169. Reebye V, Sætrom P, Mintz PJ, Huang K-W, Swiderski P, Peng L, et al. Novel RNA oligonucleotide improves liver function and inhibits liver carcinogenesis in vivo. Hepatology. 2014;59:216–227.

170. Yoshida Y, Tokusashi Y, Lee GH, Ogawa K. Intrahepatic transplantation of normal hepatocytes prevents Wilson's disease in Long-Evans cinnamon rats. YGAST. 1996;111:1654–1660.

171. Zhou H, Dong X, Kabarriti R, Chen Y, Avsar Y, Wang X, et al. Single liver lobe repopulation with wildtype hepatocytes using regional hepatic irradiation cures jaundice in Gunn rats. PLoS ONE. 2012;7:e46775.

172. Takebe T, Sekine K, Enomura M, Koike H, Kimura M, Ogaeri T, et al. Vascularized and functional human liver from an iPSC-derived organ bud transplant. Nature. 2013;:1–5.

173. Hoppo T, Komori J, Manohar R, Stolz DB, Lagasse E. Rescue of lethal hepatic failure by hepatized lymph nodes in mice. Gastroenterology. 2011;140:656–666.e2.

174. Liu L, Yannam GR, Nishikawa T, Yamamoto T, Basma H, Ito R, et al. The microenvironment in hepatocyte regeneration and function in rats with advanced cirrhosis. Hepatology. 2012;55:1529–1539.

175. Wang M-J, Chen F, Li J-X, Liu C-C, Zhang H-B, Xia Y, et al. Reversal of hepatocyte senescence after continuous in vivocell proliferation. Hepatology. 2014;60:349–361.

APPENDIX

Funding Sources

The work performed here was made possible through the generous financial support of the following sources:

National Institutes of Health: National Institutes of Diabetes and Digestive and Kidney Disease (NIDDK)

F30-DK095514-03 to Branden D. Tarlow

RO1-DK051592-17 to Markus Grompe

P30-DK056338-11 to Milton J. Finegold

N.L. Tartar Trust Fellowship (2012) to Branden D. Tarlow

T32-GM071338 Training Grant, OHSU Program in Molecular and Cellular Biology (PMCB)

T32-GM067549 Training Grant, OHSU Medical Scientist Training Program

OHSU School of Medicine, Dean's Office (MD/PhD Program)

Copyright permissions

The following figures were reused or adapted from publications with permission of the publisher. The figure, license number, publisher, and journal are listed below:

Figure 1-1: License number 3441640487953, Elsevier, Journal of Hepatology. Figure 1-2: License number 3441550363390, Elsevier, Gastroenterology. Table 1-1. License number 3441550700625, Elsevier, Developmental Cell. Figure 1-3: License number 3441550884320, John Wiley & Sons, Hepatology. Figure 1-4: License numbers 3441551475841, Elsevier, Clinics in Liver Disease; 3441560185368, Elsevier, Human Pathology. Figure 2-1: License 3442190108697, John Wiley and Sons, Hepatology. Chapter 4: License number 3441560503082, John Wiley and Sons, Hepatology.

Conflict of Interest Statement

For a portion of this graduate thesis work, I held a significant equity interest and stock options from Genentech, Inc that were declared, pursuant to Oregon Health & Sciences University Conflict of Interest disclosure policy, when my role as a researcher began in 2009 and continued through December 2010.

From 2011 – 2014, I had no conflicts of interest to declare, pursuant to OHSU policy. I designed and performed one set of experiments in 2013-2014 using a Genentech drug used over a 6-month period; however, no financial relationship existed at the time of those studies.

Markus Grompe contributed to the design, interpretation, and writing of Chapter 4 and 5. Both of these chapters used technology commercialized by Yecuris, Inc. Dr. Grompe is a founder of Yecuris and holds stock in the company. He also receives royalties on antibodies marketed by Novus, Inc which were used in Chapters 3, 4, and 5 of the thesis.

Biographical information

Education:

2008 – Oregon Health & Science University, Portland, Oregon
Doctor of Medicine (M.D.) candidate, expected graduation 2016.

2010 – 2014 Oregon Health & Science University, Portland, Oregon
Doctor of Philosophy (Ph.D.), Department of Cell, Developmental & Cancer Biology. Dissertation defense July 31, 2014.
Research mentor: Markus Grompe, M.D.
Thesis title: Cellular plasticity in liver injury: on the origin and mechanisms of liver regeneration

2000 – 2004 Stanford University, Palo Alto, California
Bachelor of Science (B.S) in Biological Sciences, with honors
Senior thesis mentor: Robert M. Sapolsky, Ph.D. Dept. of Biological Sciences
Thesis title: Glucocorticoids and inflammation regulate hippocampal neurogenesis through distinct mechanisms

1996 – 2000 Lakeridge High School, Lake Oswego, Oregon

Research Experience:

2009 – 2014 Graduate Student, Oregon Health & Sciences University, Portland, OR
Oregon Stem Cell Center & Department of Pediatrics, Mentor: Markus Grompe M.D.

2004 – 2008 Research Associate I/II, Genentech, Inc, South San Francisco, CA
Department of Pathology. Mentor: Hartmut Koeppen, M.D., Ph.D.

2002– 2004 Undergraduate Research Assistant, Stanford University
Department of Biological Sciences. Mentor: Robert Sapolsky, Ph.D.

1999 Research Assistant, Oregon Health Sciences University, Portland, OR.
Dept of Biochemistry & Mol. Biology. Mentor: James Hare, Ph.D.

Personal / interests:

Wife: Kathleen; Children: Ramona, age 5; Benjamin, age 2.
Interests: Family outdoor activities, Gardening, Beer/Cider Brewing, Running

Scientific Presentations

Peer-Reviewed Publications

(Includes submitted manuscripts)

Li B, **Tarlow B**, Dorrell C, Haft A, Finegold MJ, Grompe M. Isolation and identification of clonogenic liver ductal cells in adult human." *In preparation.*

Tarlow BD, Pelz C, Naugler W, Wakefield L, Wilson E, Finegold MJ, Grompe M. Bipotential adult liver progenitors are derived from chronically injured mature hepatocytes. *Cell Stem Cell*, in revision. Submitted June 23, 2014.

Dorrell C, **Tarlow BD**, Wang Y, Canaday P, Haft A, Schug J, Streeter P, Finegold M, Grompe M. The organoid-initiating cells in mouse pancreas and liver are phenotypically and functionally similar. *Stem Cell Research.* 2014 Jul 27; Doi: 10.1016/j.scr.2014.07.006.

Tarlow BD, Finegold MJ, Grompe M. Clonal tracing of Sox9+ liver progenitors in mouse oval cell injury. Hepatology. 2014 Feb 22. Doi: 10.1002/hep.27084. PMID: 24700457.

Wen YH, Koeppen H, Garcia R, Chiriboga L, **Tarlow BD**, Peters BA, Eigenbrot C, Yee H, Steiner G, Greco MA. Epidermal growth factor receptor in osteosarcoma: expression and mutational analysis. Hum Pathol. 2007 Aug; 38(8):1184-91. PMID: 17509661

Conference Abstracts

National & International Conferences: selected abstracts and talks

Tarlow B, Pelz C, Naugler W, Wakefield L, Finegold, Grompe M. "Bipotential adult liver progenitor cells are derived from chronically injured mature hepatocytes." Selected short talk. FASEB Liver Biology: Fundamental mechanisms and translational applications. Keystone, Colorado, July 7, 2014.

Tarlow B, Pelz C, Haft A, Wakefield L, Finegold M, Grompe M. "Hepatocyte metaplasia is a source of oval cell heterogeneity in mice." Selected poster, 2014 International Society for Stem Cell Research Conference (ISSCR). Vancouver, B.C. Canada, June 18, 2014.

Tarlow B, Naugler W, Wakefield L, Pelz C, Wilson EM, Grompe M. "Human hepatocytes are oval cell precursors." Selected poster, 2014 American Society for Clinical Investigation (ACSI) Annual Meeting and American Physician Scientist Association (APSA) Joint Meeting. Chicago, IL, April 25, 2014.

Tarlow B, Finegold MJ, Grompe M. "Hepatocyte-driven regeneration is sufficient for adaptation to chronic injury." Selected poster, 2013 International Society for Stem Cell Research Conference (ISSCR). Boston, MA, Japan, June 12, 2013.

Tarlow B, Dorrell C, Canaday P, Huch M, Grompe M. "Isolation and characterization of primary human liver progenitor cells." Selected poster, 2012 International Society for Stem Cell Research Conference (ISSCR). Yokohama, Japan, June 14, 2012.

Tarlow BD, Strickland L, Koeppen K et al. "Global Gene Expression profiling of microdissected tumor endothelial cells." Selected Oral Presentation. US Canadian Academy of Pathology (USCAP) Feb 2006, Atlanta, GA.

Tarlow BD, Strickland L, Koeppen K et al. "Laser capture microdissection and bioinformatics profiling to identify tumour vascular markers." Selected Oral Presentation. Pathological Society of Great Britain & Ireland, July 5, 2006. Manchester, United Kingdom.

Local Conference Presentations

Tarlow BD, Finegold MJ, Grompe M. "Hepatocytes are the major source of regenerating hepatocytes in mouse oval cell injury ." Research Week, Oregon Health & Sciences University, May 5, 2014, Portland, OR.

Tarlow BD, Naugler W, Orloff S, Grompe M. "Establishing patient-specific xenograft models of chronic liver disease from needle core biopsies." Research Week, Oregon Health & Sciences University, May 18, 2013, Portland, OR. **Poster Award.**

Tarlow BD, Loi J, Naimark M, Young A, Patel P, Searns J, Thornburg K, Gillingham M. "Effect of a High Fructose Diet on Postprandial Fat Oxidation." OHSU Student Research Forum, May 15, 2009, Portland, OR. **Oral Presentation Award.**

Tarlow B, Liang Y, Davis D, Peale F, Koeppen H. "Lentiviral RNAi screen to identify endothelial-specific regulators of angiogenesis." 2008 Genentech Research Conference, Pacific Grove, California. May 11, 2008.

Tarlow B, Sanders L, Knezevic D, McNeal A, Chalasani S, Frantz G, and Koeppen H. "Identification of CCDC3, ADAMTS4, and PCDH17 in tumor-associated vasculature." 2006 Genentech Research Conference, Pacific Grove, California. September 26, 2006.

Tarlow B, Strickland L, Jubb A, Modrusan Z, Wu T, and Koeppen H. "Identification of tumor vascular markers in colorectal tissues by laser capture microdissection." 2006 Genentech Research Conference, Pacific Grove, California. May 20, 2005.